5-1997

The Greenbrier and Hayesville Faults in Central-Western North Carolina

Camilo Montes
University of Tennessee - Knoxville

To the Graduate Council:

I am submitting herewith a thesis written by Camilo Montes entitled "The Greenbrier and Hayesville Faults in Central-Western North Carolina." I have examined the final electronic copy of this thesis for form and content and recommend that it be accepted in partial fulfillment of the requirements for the degree of Master of Science, with a major in Geology.

Robert D. Hatcher, Major Professor

We have read this thesis and recommend its acceptance:

Harry Y. McSween, William M. Dunne

Accepted for the Council:
Dixie L. Thompson

Vice Provost and Dean of the Graduate School

(Original signatures are on file with official student records.)

To the Graduate Council:

I am submitting herewith a thesis written by Camilo Montes entitled "The Greenbrier and Hayesville faults in central-western North Carolina" I have examined the final copy of this thesis for form and content and recommend that it be accepted in partial fulfillment of the requirements for the degree of Master of Science, with a major in Geology.

Robert D. Hatcher Jr., Major Professor

We have read this thesis and recommend its acceptance:

Harry Y. McSween

William M. Dunne

Accepted for the Council:

Associate Vice Chancellor and
Dean of The Graduate School

THE GREENBRIER AND HAYESVILLE FAULTS IN CENTRAL-WESTERN NORTH CAROLINA

A Thesis
Presented for the
Master of Science Degree
The University of Tennessee, Knoxville

Camilo Montes
May, 1997

This thesis is dedicated in memory of

Fabio Chaparro

professor, mentor, and friend

ACKNOWLEDGEMENTS

I would like to express my gratitude to all the people who helped me in the course of this work. My advisor's revisions improved and shaped up this manuscript, and discussions in the field with him made me understand Appalachian geology. Valuable comments by my committee members Dr. William M. Dunne and Harry Y. McSween were are thanked. This work also benefited from discussions with Dr. William Thomas from the University of Kentucky; Mark Carter, Leonard Wiener, and Carl Merschat from the North Carolina Geological Survey, and Prof. Kauko Laajoki from the University of Oulu, Finland. I would also like to thank Donald Geddes and Steve Martin who helped me with rather important tasks when doing field work in the Appalachians: driving a car and speaking English. The motherly care of Nancy Meadows is greatly appreciated. Sarita's support, infinite patience, and hiking skills were fundamental during this work.

This work was funded by the University of Tennessee Science Alliance Center of Excellence Distinguished Scientist Stipend, by the Geological Society of America research grant 5664-95, and by the Swingle Fellowship offered by the Department of Geological Sciences of the University of Tennessee, Knoxville.

ABSTRACT

Detailed mapping in the easternmost western Blue Ridge of central-western North Carolina revealed that the premetamorphic Greenbrier fault separates the Snowbird Group from Great Smoky Group, and the Hayesville fault separates eastern Blue Ridge assemblages from the Ocoee Supergroup units and western Blue Ridge basement. The faulted nature of the Snowbird-Great Smoky Groups contact suggests that the Great Smoky Group may have been transported northwestward farther than previously thought along the Greenbrier fault, and permitted the reinterpretation of changes in Snowbird Group stratigraphy within the footwall of Greenbrier fault previously associated with lateral facies changes later telescoped by Paleozoic thrusts. Those changes can be explained now as the result of active normal faulting during the time of accumulation of the Snowbird Group. Compositional changes in the Snowbird Group suggest that Snowbird Group strata pinchout to the SE represents a distal downlap with a northwestern clastic provenance, and with an original depositional dip to the southeast. Thus, the granitic rocks beneath the Ocoee Supergroup in the eastern edge of the Western Blue Ridge did not contribute significantly to the sedimentary budget of the Late Proterozoic rifted margin of Laurentia. The concept of a sediment trap and a sediment-starved basin can be derived from asymmetrical rifting models that predict the sequential abandonment of cratonward rift basins as the upper mantle is elevated, and normal faults have to sequentially migrate basinward. The deformation history after the end of the Late Proterozoic rifting includes three periods of deformation. The oldest period of deformation is early Taconic (Penobscottian?), recorded by the premetamorphic emplacement of the Greenbrier and Hayesville thrust sheets; the Greenbrier fault transported Great Smoky Group rocks northwestward over Snowbird Group and basement rocks; the Hayesville fault carried eastern Blue Ridge assemblages over

the Greenbrier thrust sheet, and produced mylonite zones within the Middle Proterozoic basement orthogneiss. The tectonostratigraphic package was metamorphosed to sillimanite grade during the Taconic orogeny. NNE-trending, steeply SW-dipping faults and related flexural folds folded early structures during the Alleghanian orogeny; favorably oriented segments of premetamorphic growth and thrust faults were reactivated during this deformation.

TABLE OF CONTENTS

LIST OF PLATES

LIST OF FIGURES

CHAPTER I
INTRODUCTION

Two major crustal-scale structures, the Greenbrier and Hayesville faults, project into the Blue Ridge of central western North Carolina. Both faults have been defined and studied in other areas, but in this part of the Blue Ridge little is known about their geometry, style, and relationship to one another and to the basement-cover contact. Moreover, detailed field mapping conducted during the 1950s (Hadley and Goldsmith, 1963) did not reveal any major fault in this part of the Blue Ridge. Advances in the knowledge of the regional structure and stratigraphy of the Blue Ridge, and conceptually in earth sciences in general, justify the need for a reevaluation of these boundaries in the study area.

This work summarizes in two independent papers the results of a two-year field investigation in the vicinity of Dellwood, North Carolina. Chapter II focuses on the stratigraphy of the Ocoee Supergroup, while Chapter III characterizes the Greenbrier and Hayesville faults in this part of the Blue Ridge. This study achieved a greater resolution of the trace of Greenbrier and Hayesville faults, the sequence of events, and the stratigraphy of the Ocoee Supergroup. A better understanding of the deformational history and geometric configuration of the Greenbrier and Hayesville faults will help document the initial architecture and destruction of the early Paleozoic Laurentian margin in the southern Appalachian orogen.

LOCATION

The study area is located on the southeastern flank of the Great Smoky Mountains National Park (Fig. 1.1). It is easily accessible by Interstate 40, the Blue Ridge Parkway, U.S. 276, and U.S. 19. A dense network of high-quality secondary roads is present because of intense development and tourism between the Great Smoky Mountains National Park and the Blue Ridge Parkway. This rugged mountain area of North

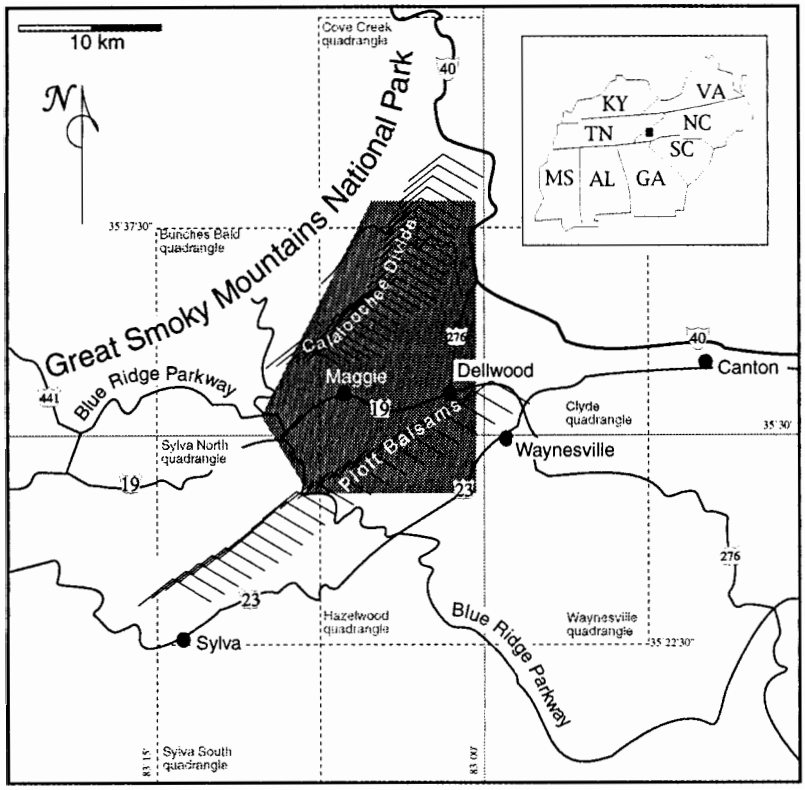

Figure 1.1. Location and access of the area mapped (gray area).

Carolina is dominated by the ENE-WSW Plott Balsams range (1,800 m), traversed only by the Blue Ridge Parkway; and by the NE-SW trending Cataloochee divide (1,500 m), which is the eastern boundary of the Great Smoky Mountains National Park and is accessible by a network of hiking trails.

REGIONAL SETTING

This area was chosen because of the presence of a high quality 1:24,000 geologic map by Hadley and Goldsmith (1963), detailed mapping by Quinn (1991), and reconnaissance maps by Edelman (unpublished). The map by Hadley and Goldsmith (1963) reveals a "hook" outcrop pattern (Fig. 1.2) where both eastern and western Blue Ridge affinity sequences are repeated, thus providing a critical area to examine the relationships between the Ocoee Supergroup and eastern Blue Ridge-affinity sequences. In an effort to determine the geometry of the Greenbrier and Hayesville

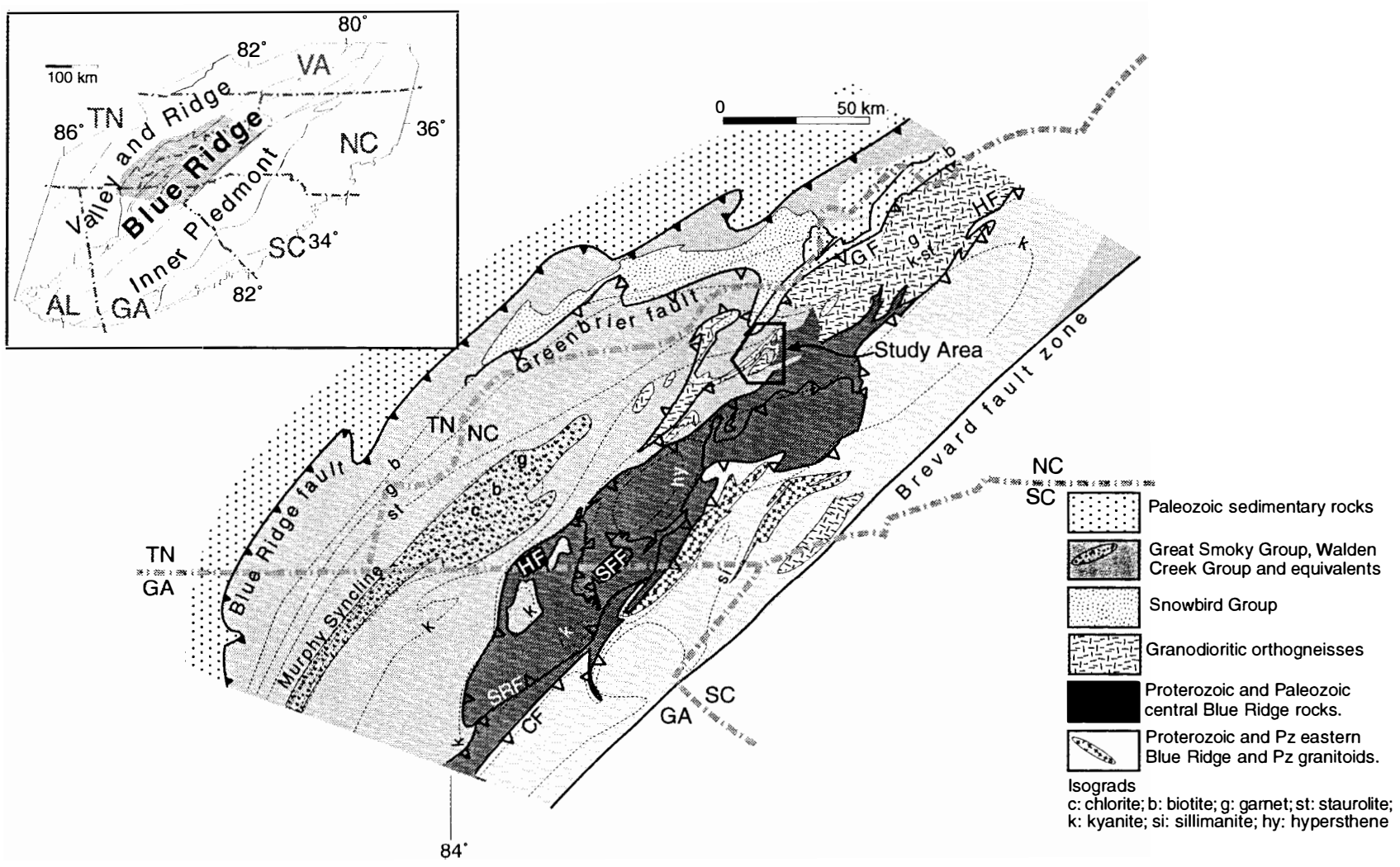

Figure 1.2. Geologic setting of the study area. Modified from North Carolina Geological Survey (1985); Hatcher et al., (1991); and Carter et al., (1995). SRF: Soque River fault; CF: Chatahoochee fault; SFF: shope Fork fault; HF: Hayesville fault; GF: Greenbrier fault. Open teeth: premetamorphic faults, filled teeth postmetamorphic faults.

faults in the Blue Ridge of central-western North Carolina, 1:24,000 mapping was completed in the Dellwood, Sylva North, Hazelwood, Cove Creek, and Bunches Bald quadrangles during winter 1994 and spring and summer 1995. Detailed mapping focused on resolving the structural fabric and stratigraphic sequence within the Ocoee Supergroup, and the contacts with the ortho- and paragneiss, because this was not addressed during earlier work. Over 1,100 data stations were collected mostly within Ocoee Supergroup units, and compiled along with data from earlier studies (Hadley and Goldsmith, 1963; Edelman, unpublished) into geologic and tectonic maps that resolve the structure and stratigraphy of the medium- to high-grade Ocoee Supergroup, and the eastern Blue Ridge ortho- and paragneiss assemblages. The structural style observed in the compiled map was verified using outcrop, hand specimens, and thin sections. A composite stratigraphic succession within the Ocoee was recognized, and several new relationships among these units have been resolved.

The sequence of events was deciphered using cross-cutting relationships with respect to metamorphic peak fabrics. Since the age of this metamorphic event seems to be Middle Ordovician (440-460 Ma. $^{40}Ar/^{39}Ar$, Connelly and Dallmeyer, 1993; 466 Ma. U-Pb, Quinn and Wright, 1993; 495 Ma. ion probe dating, Miller et al., in press) premetamorphic fabrics are likely to correspond to early Taconic deformation (Penobscottian?), and retrograde postmetamorphic fabrics of deformation can be correlated to the Alleghanian orogeny.

THE GREENBRIER AND HAYESVILLE FAULTS

The two major structures recognized during this mapping project, the Greenbrier and Hayesville faults, separate domains with different stratigraphy, slightly different metamorphic histories, and contrasting deformations. Along-strike correlation with mapped segments of these faults is postulated here based on the nature of the stratigraphic packages these structures separate, and on the timing of deformation. The dissimilar tecto-stratigraphic histories recorded in the domains separated by

these structures are addressed in this study in terms of a complex interaction among the stratigraphy of a rift basin, relics of early deformation, fabrics of peak metamorphism, and finally the overprint of postmetamorphic deformation.

Greenbrier fault

The Greenbrier fault was originally mapped in the western Blue Ridge as a thrust separating the Snowbird Group in the footwall from the Great Smoky Group in the hanging wall in most areas (King et al., 1958). The Greenbrier fault does not offset isograds, or affects regional foliation, and therefore is a premetamorphic fault (King et. al, 1958). Garnet-biotite geothermometry across the fault was used to constrain its premetamorphic age (Milton, 1983) because in most places this fault separates rock units unlikely to record metamorphic reactions (Snowbird Group). According to Hadley and Goldsmith, (1963), and Keller, (1980), this fault was preceded by folding both in the hanging wall and in the footwall (in the Copeland Creek anticline and in the Waterville syncline). On the other hand, Connelly and Woodward, (1992), explain these east and northeast-trending structures as folding of a footwall ramp. Mylonites have been reported along the trace of Greenbrier fault (Connelly and Woodward, 1992), but the main criterion for recognition is the contrast between the fine-grained rocks from the top of the Snowbird Group, and the coarser-grained conglomerate and sandstone of the Thunderhead Sandstone (Hadley and Goldsmith, 1963).

East of the Great Smoky Mountains in the vicinity of Dellwood, North Carolina, the contact between the Great Smoky and Snowbird Groups was mapped conformable (Hadley and Goldsmith, 1963), and the trace of the Greenbrier fault was mapped as a NNE-trending, steeply dipping fault separating polydeformed orthogneisses from Ocoee Supergroup rocks (figure 3 in King et al., 1958; Plates 1 and 2 in Hadley and Goldsmith, 1963). The change from a bedding-parallel, folded thrust fault separating the Snowbird from the Great Smoky Groups in the western Blue Ridge, to an essentially vertical, NNE-trending fault cutting through granodioritic basement in the

easternmost western Blue Ridge has been used in subsequent models (DeWindt, 1975, Rast and Kohles, 1985; Woodward et al., 1991; Connelly and Woodward, 1992) to approximately locate the ramp where the Greenbrier fault climbed from the basement to follow the Snowbird-Great Smoky contact to the northwest. The location of this ramp in western North Carolina implies that contrasting Snowbird Group near-shore deposits, now next to each other, were originally separated by a distance equal to the net slip along the Greenbrier fault (King et al., 1958; Hadley and Goldsmith, 1963; DeWindt, 1975). About 24 km of displacement has been estimated for this fault by assuming a constant rate of northwestward thickening of the Snowbird Group beneath the Greenbrier fault (Hadley and Goldsmith, 1963). Similarly, the reconstruction of thrust sheet geometries based on the geometry of hanging wall and footwall to strata yielded a minimum displacement of 23 km (Woodward et al., 1991, and Connelly and Woodward, 1992).

Hayesville fault

The Hayesville fault is defined by the contrast between North American Grenville basement and cover to the west from oceanic-affinity assemblages to the east, and is thought to represent the Taconic suture in the southern Appalachians (Rankin, 1975; Hatcher, 1978, 1989). The trace of the suture marking this contrast (Hayesville fault), however, has not been clearly defined in central-western North Carolina (North Carolina Geological Survey, 1985). In this part of the Blue Ridge the contrast between oceanic- to continental-affinity sequences occurs in and near the Dellwood quadrangle, originally mapped at 1:24,000 scale by Hadley and Goldsmith (1963). Their map showed the easternmost exposures of the Ocoee Supergroup unconformably resting on Precambrian ortho- and paragneisses. While the orthogneisses clearly correlate to western Blue Ridge Middle Proterozoic basement (Rankin et al., 1989), the affinity of the paragneisses is still equivocal. These paragneisses were correlated by Hadley and Goldsmith (1963) with the Carolina Gneiss of Keith (1904), and were assigned a Precambrian age on the basis of field relationships. More recent geologic maps (Quinn, 1991), regional correlations across

the Blue Ridge (Hatcher, 1978; Hatcher et al., 1979), and U/Pb geochronology (Quinn and Wright, 1993) suggest that the paragneisses contain Middle Proterozoic 1.1 Ga old Grenville rocks, as well as Late Proterozoic to early Paleozoic cover rocks of the Tallulah Falls and Otto Formations originally described by Hatcher (1971) in Georgia and thought to be correlative with the Ashe, Alligator Back and Catoctin Formations to the north. It is still unclear whether the Late Proterozoic ages are representative of the entire assemblage, or if they reflect windows exposing Grenville basement in a mostly Late Proterozoic to early Paleozoic cover sequence. In addition, these paragneisses contain the westernmost exposures of mappable bodies of amphibolite and ultramafic rocks in the Blue Ridge (Hess, 1955; Hatcher, 1978; Misra and Keller, 1978; Misra and McSween, 1984).

CHAPTER II
REEVALUATION OF THE EASTERNMOST FACIES OF THE OCOEE SUPERGROUP IN CENTRAL-WESTERN NORTH CAROLINA

ABSTRACT

Detailed geologic mapping in the easternmost exposures of the latest Proterozoic Ocoee Supergroup in western North Carolina suggests that the relationship of Snowbird strata to the nonconformity below is a distal downlap with a clastic provenance located to the north and west, and with an original depositional dip to the southeast. These findings indicate that the granitic rocks immediately beneath the Ocoee Supergroup on the eastern flank of the western Blue Ridge did not contribute significantly to the sediment budget of the Late Proterozoic rifted margin of Laurentia. Rapid thickness changes in the sandy facies of the Snowbird Group delineate an extensional structure active during the time of accumulation of arkosic Longarm Quartzite; northwest of this structure subsidence kept pace with accumulation so that great thicknesses accumulated in shallow water; to the southeast the sediment availability was severely limited as the extensional structure acted as a sediment trap, and only a thin quartz-rich remnant of quartzite facies of the Longarm Quartzite accumulated. The concept of a sediment trap and a sediment starved basin can be derived from asymmetrical rifting models that predict the sequential abandonment of cratonward rift basins as the upper mantle is elevated, and normal faults have to sequentially migrate basinward. The northwestern provenance of the turbiditic Thunderhead Sandstone was reconfirmed, and the contact between the Great Smoky Group and the Snowbird Group was characterized as the Greenbrier fault.

INTRODUCTION

This paper focuses on the lithostratigraphy of part of the latest Proterozoic Ocoee Supergroup (King et al., 1958) in the Blue Ridge of western North Carolina. The stratigraphy of this clastic sequence on the easternmost flank of the western Blue Ridge has often been overlooked, as an eastward-increasing metamorphic gradient was assumed to erase most sedimentary features and stratigraphic relationships. Detailed field mapping (Fig. 2.1), however, proved the existence of these features at middle amphibolite facies. This preservation has permitted subdivision of the Snowbird and Great Smoky Groups previously undifferentiated in the 1:24,000 geologic map of Dellwood (Hadley and Goldsmith, 1963) and surrounding quadrangles.

Detailed mapping, along with basic stratigraphic principles presented herein document the northwest provenance of the sediments making up the Longarm Quartzite; and are used to postulate the distal downlap relationship of the Snowbird sandy sequences to the nonconformity below, contrary to what earlier workers maintained (King et al., 1958; Hadley and Goldsmith, 1963; Hadley, 1970; DeWindt, 1975; Rast and Kohles, 1986). Speculation regarding the paleogeography, mode of filling, and sediment budget of the basin(s) in which the Ocoee Supergroup was deposited are based on stratigraphic-sedimentologic character, map distribution of units and facies, and the nature of contacts observed in the field.

SNOWBIRD GROUP LITHOSTRATIGRAPHY

The lithostratigraphic schemes for the Ocoee Supergroup (Fig. 2.2) erected by King et al. (1958), Hadley and Goldsmith (1963), and Hadley (1970), interpreted the southeastward thinning of the Snowbird Group as a lower boundary proximal onlap (cf. Schoch, 1989) of a sequence transgressive toward the southern margin of the basin (Fig. 2.3), and with sediment provenance to the southeast. This hypothesis

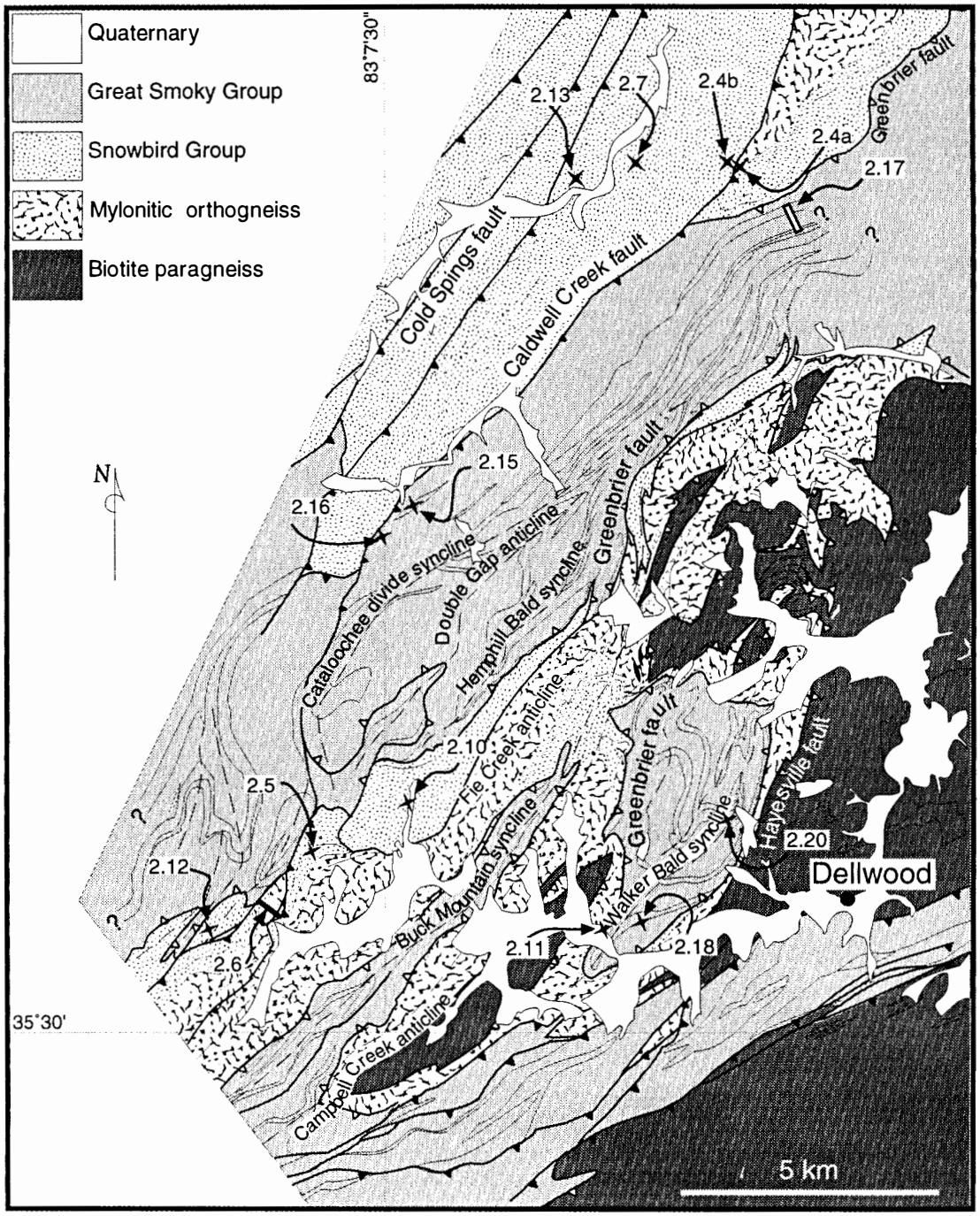

Figure 2.1. Simplified geologic map of the area studied. The general location of figures mentioned in the text is indicated by the figure number (2.4, 2.7, etc.). The refolded trace of the premetamorphic Greenbrier, and Hayesville faults is shown with open teeth, and the trace of postmetamorphic faults is shown with solid teeth. Note the distribution of three outcrop belts of the Snowbird Group: a belt northwest of Caldwell Creek fault, a thin belt around the outline of the southeasternmost trace of Greenbrier fault, and SW-NE belt in between the first two.

a)

AGE	North and below Greenbrier fault	South and above Greenbrier fault	
Early Cambrian	Chilhowee Group	Murphy belt rocks	Natahala slate and higher units
		conformable?	
Late Proterozoic	Ocoee Supergroup: Walden Creek Group	Ocoee Supergroup: Great Smoky Group	Unnamed higher strata (Ammons Formation, Dean Formation)
	Ocoee Supergroup: Unclassified formations	Ocoee Supergroup: Great Smoky Group	Anakeesta Formation Thunderhead Sandstone Elkmont Sandstone
	Ocoee Supergroup: Snowbird Group	Ocoee Supergroup: Snowbird Group	Roaring Fork Sandstone Longarm Quartzite Wading Branch Formation
		Nonconformity	
Middle Proterozoic	Ortho- and paragneiss basement	Ortho- and paragneiss basement	

b)

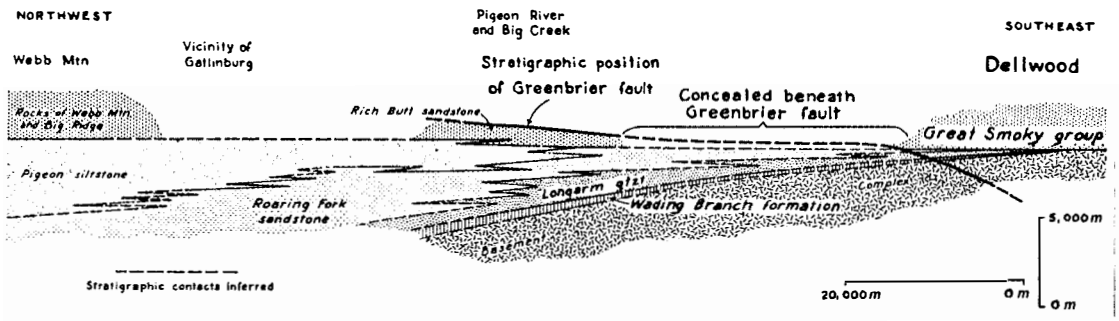

Figure 2.2. Stratigraphy of the Ocoee Supergroup.
(a) Stratigraphic nomenclature of the Ocoee Supergroup, shaded area indicates the stratigraphic package involved in this study. Modified from King *et al.*, (1958), and Carter *et al.*, (1995).
(b) Restored stratigraphic section of the Ocoee Supergroup across the eastern Great Smoky Mountains, showing the relationship of proximal onlap of Snowbird Group units to the granitic basement underneath (reproduced from King et al., 1958).

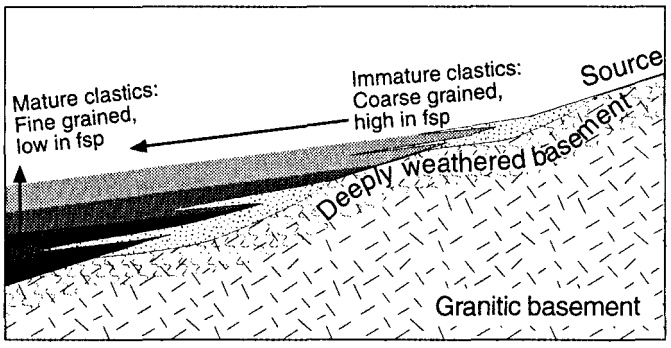

Figure 2.3. Proximal onlap concept (*cf.* Schoch, 1989). Sandstone facies (grey scale) onlapping a deeply altered granitic basement and reworked regolith (dotted pattern). Note that if the deeply altered basement is the source for the sandstone, the contact between the onlapping sanstone and the reworked regolith should be gradational. Fsp feldspar.

was based on the dominance of coarser sandstone to the south (King et al., 1958), and on paleocurrent indicators (DeWindt, 1975; Hadley, 1970, Hadley and Goldsmith, 1963) that record a southeast to northwest flow direction in the sandstones of the Snowbird Group. The reliability of paleocurrent indicators was challenged by Rast and Kohles (1986), because of the overprint of heterogeneous deformation, and because neither the original data nor the methodology to subtract the deformation were ever published. Moreover, it is now clear that proper interpretation of paleocurrent indicators, particularly in near-shore environments, may be impossible (Davis, 1992) unless there is a previous clear-cut understanding of the genetic significance of the structures in which those paleocurrents were measured. These kinds of studies have not been conducted in most of the Ocoee Supergroup, although Keller (1980) presented a detailed description of sedimentary structures in the Snowbird Group near Hot Springs, Tennessee. To better understand the provenance of the sediments in the Snowbird Group a different approach is attempted and discussed herein that includes description of stratigraphic sections, compilation of interpreted depositional environments, and mapping the distribution of feldspar content relative to quartz and mica.

Most stratigraphic observations were made in exposures in the Great Smoky Mountains National Park along the road to Cataloochee, hiking trails, and tributary

creeks draining the northwestern flank of the Cataloochee Divide into Caldwell Creek. This region, the northwestern third of the study area, is better for stratigraphic observations of the Ocoee Supergroup because the deformation is less intense, and exposures offer a better opportunity to observe stratigraphic relations and sedimentary structures. Stratigraphic thicknesses were estimated indirectly by measuring apparent thicknesses, and then calculating the approximate thickness using the average dip and strike, thus providing the level of precision and accuracy needed for the objectives of this work. Composite stratigraphic sections were assembled from individual outcrops elsewhere, in places where tectonic disruption was too intense to preserve complete sections. In order to measure changes in sandstone composition across the area mapped, and compare earlier modes by Hadley and Goldsmith (1963), and Quinn (1991), point counting was performed (assuming original composition is preserved) on seventeen sandstone and pelite samples from the Longarm Quartzite and Thunderhead Sandstone (Appendix A).

Wading Branch Formation

Wading Branch Formation is a commonly thin and discontinuous unit that nonconformably overlies Middle Proterozoic quartz-dioritic orthogneiss. The Wading Brach Formation is less than 100 m thick, and consists of highly variable facies of impure, poorly sorted, sandy black siltstone (Fig. 2.4a), coarse-grained, quartz-rich metaconglomerate (Fig. 2.5), and impure, medium grained, often conglomeratic metasandstone (Fig. 2.6). This unit is well exposed at garnet grade along the road to Cataloocheee in the Great Smoky Mountains National Park, and at kyanite grade south of the Blue Ridge Parkway southwest of Maggie Valley. The relative proportions of quartz and feldspar place the psammitic rocks from this unit within the subarkose to muddy subarkosic field in a Q-F-M diagram (Hadley and Goldsmith, 1963). The Wading Branch Formation gradually thins to the southeast, where it is less than 20 m thick, underlying in sharp stratigraphic contact the Longarm Quartzite.

Figure 2.4. Wading Branch Formation and Longarm Quartzite.
(a) Well exposed anticline of granitic basement nonconformably overlain by Wading Branch Formation and Longarm Quartzite at garnet grade in the northwestern outcrop belt. Unit 1 nonconformably rests on fine-grained, biotite-rich granitic rocks; it is a gray, internally cross-bedded, granule size quartz and feldspar sandy conglomerate. Unit 2- black, internally massive, impure, quartz-conglomeratic siltstone, often cross bedded, or laminated; small randomly oriented biotite porphyroblasts are present. Unit 3- light and gray colored coarse-grained, massive, impure quartzite, and black, sandy massive siltstone and conglomerate (dotted pattern). Unit 4- black metasiltstone and biotite schist containing numerous sheared milky quartz veins. Unit 5- internally massive fine-grained, gray, mica-rich quartzite. Unit 6- coarse-grained, feldspar-rich, light-colored, and internally cross-bedded quartzite. Units 3, 5 and 6 belong to the base of the Longarm Quartzite.
(b) Bedding geometry of a exposure near the top of the Longarm Quartzite in the northwestern outcrop belt. It is a 55 m thick section characteristically more resistant to erosion made up of: Unit 1- light-colored, fine-grained feldspathic quartzite rich in heavy minerals; bedding is wedge shaped and internally layered. Unit 2- light-colored, very fine-grained, muscovite-rich quartzite; it is finely laminated with parallel beds 1 cm thick; the abundance of mica produces a greasy feeling on foliation surfaces; minor muscovite-chlorite schist layers are also present. Unit 3- light-colored, very fine-grained feldspathic quartzite; beds are parallel and 0.5 to 1 m thick. Unit 4- very fine-grained, white, occasionally conglomeratic (mostly feldspar clasts) feldspathic quartzite, bedding is 0.5 to 1 m thick in plane-parallel sets internally cross bedded; this unit contains minor interbeds of muscovite-chlorite schist. Unit 5- light-colored, medium-grained, conglomeratic, cross bedded, feldspathic quartzite, with 10 to 50 cm thick beds. Unit 6- white, very fine-grained, muscovite-rich quartzite; it is cross bedded and internally laminated. Unit 7- thick, monotonous, light-colored, coarse-grained, conglomeratic, feldspathic quartzite; beds are planar, parallel, and range from 25 to 50 cm thick, with abundant heavy minerals defining internal cross beds. Minor muscovite-chlorite schist layers are present.

a)

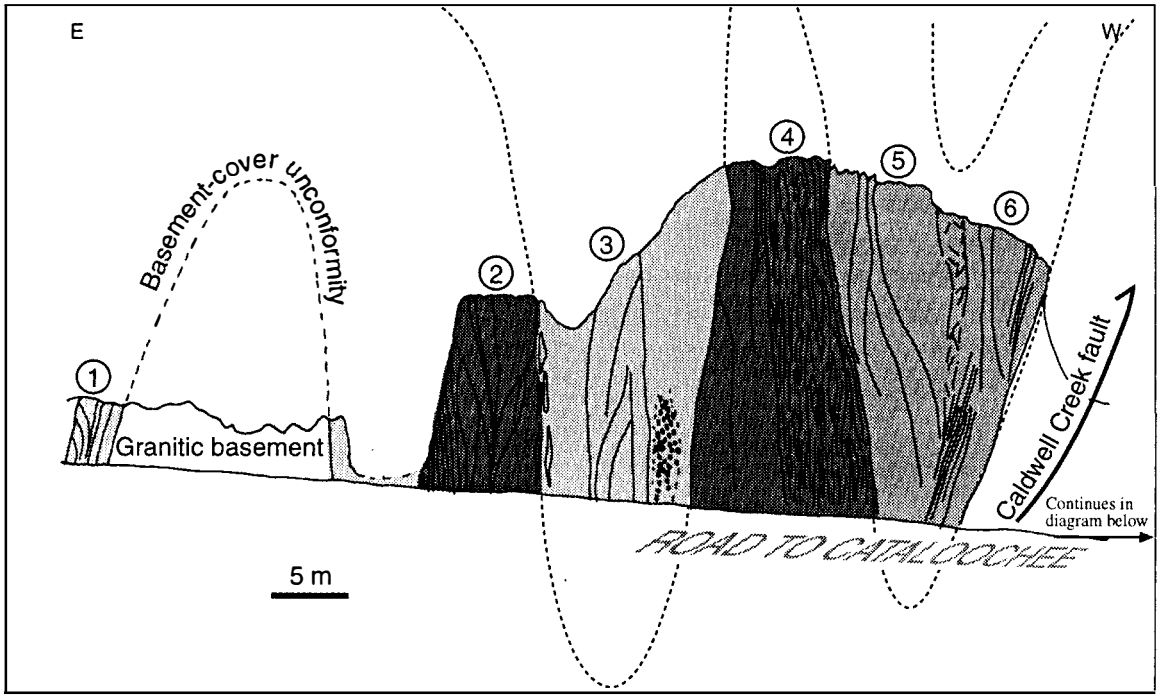
E
W
Basement-cover unconformity
Granitic basement
1
2
3
4
5
6
Caldwell Creek fault
Continues in diagram below
ROAD TO CATALOOCHEE
5 m

b)

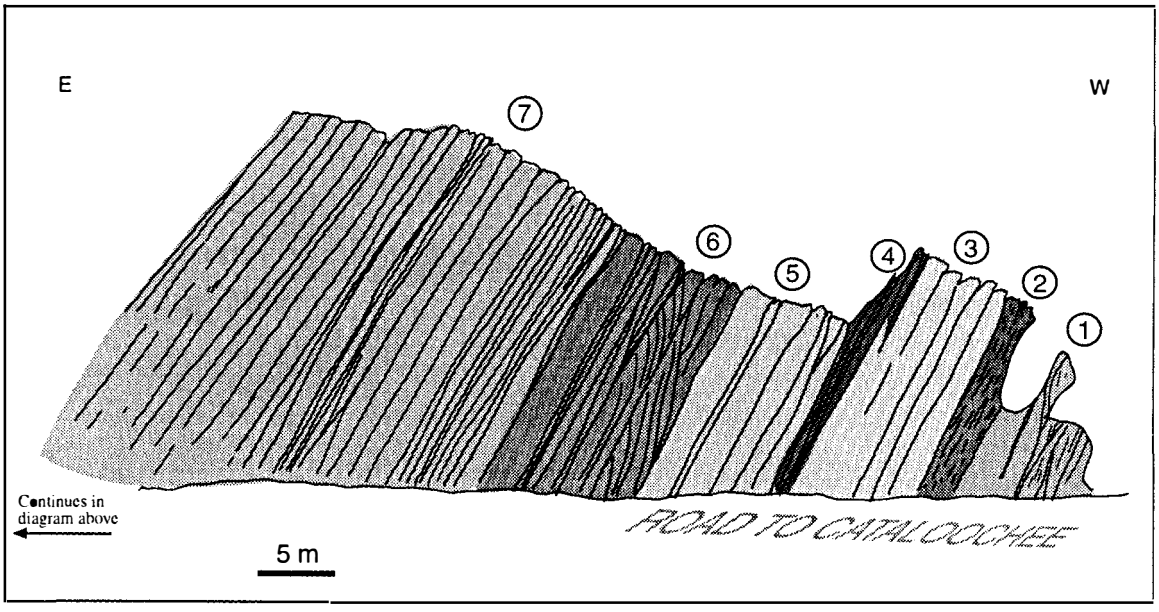
E
W
7
6
5
4
3
2
1
Continues in diagram above
ROAD TO CATALOOCHEE
5 m

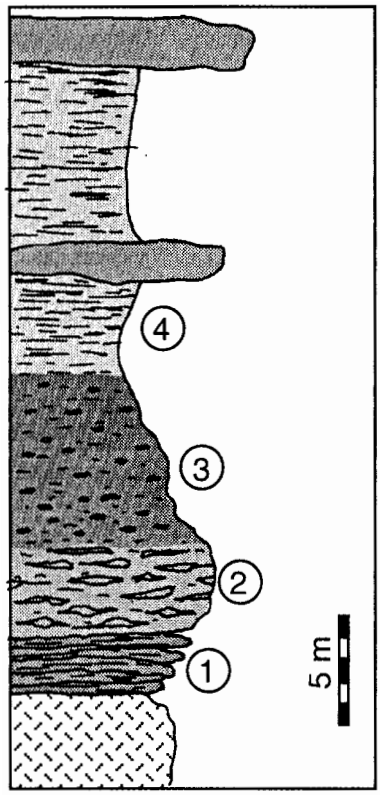

Figure 2.5. Wading Branch Formation column. Typical column of Wading Branch Formation at kyanite grade; Bunches Bald quadrangle west of Indian Creek; 83°8'28" W, 35°31'36" N. Unit 1- very coarse-grained garnet muscovite schist nonconformably resting atop granitic basement. Unit 2- very coarse feldspar-garnet muscovite gneissic metaconglomerate grading into: Unit 3- finer-grained metasandstone of the same composition, and: Unit 4- very coarse-grained garnet muscovite schist. The contact of this 20-m thick sequence with the Longarm Quartzite is sharp.

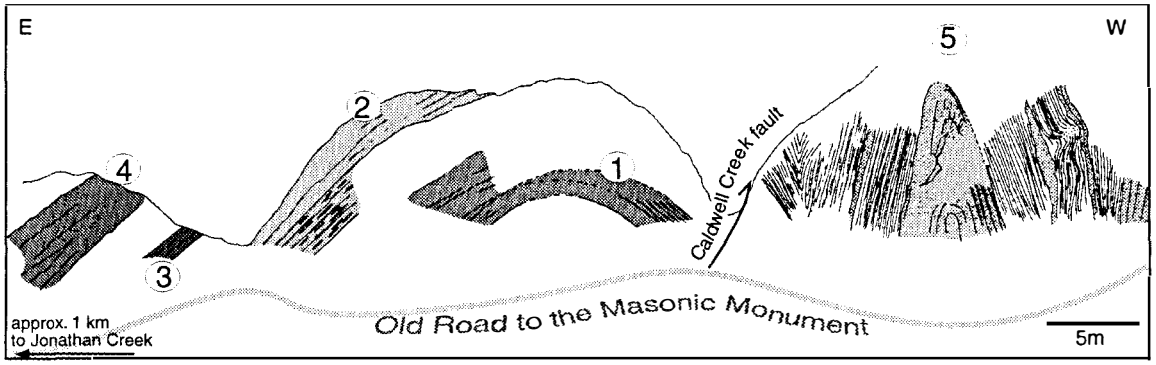

Figure 2.6. Wading Branch Formation section. External geometry of psammitic and pelitic kyanite grade Wading Branch Formation, the location is shown in the figure. Unit 1- biotite, quartz-feldspathic, layered and augen basement orthogneiss. Unit 2- very coarse-grained muscovite-garnet schist belonging to the Wading Branch Formation. Unit 3- biotite-rich metagraywacke that separates the muscovite-garnet schist (unit 3) from the Longarm Quartzite (unit 4), which is made up of white, cross-bedded, conglomeratic arkosic quartzite. Unit 5 immediately below Caldwell Creek fault is a dark, fine-grained, muscovite-biotite metasandstone and sandy schist with conglomerate layers at the base of the sandstone layers belonging to the Wading Branch Formation.

Longarm Quartzite

The Longarm Quartzite is the most distinctive unit within the Snowbird Group because it is composed mostly of light-colored feldspathic quartzite. Toward the northwest of the study area the Longarm Quartzite consists of approximately 1,000 m-thick, coarse- to medium-grained sandstone (Fig. 2.4b, and 2.7). These deposits are characteristically arkosic to subarkosic, in 25 to 50 cm thick internally cross-bedded (Fig. 2.8) parallel beds, commonly containing soft-sediment slump folds (Fig. 2.9). A rather dramatic decrease in thickness occurs southeastward across Caldwell Creek fault (Chapter III) to a 50 to 200 m-thick unit of light-colored, often gray, fine-grained, biotite-rich subarkose with some pelite interlayers, and with conglomerate layers towards the base (Fig. 2.10). This contrast is well exposed approximately 1 km northwest of Cove Creek Gap along the road to Cataloochee. This 50 to 200 m-thick unit gradually thins to the southeast where it pinches out as a very fine-grained, muscovite-rich, pelitic quartzite to quartzite (Fig. 2.11) east and southeast of Maggie Valley, near Johnson Gap, and north of Middle Top. The top of the Longarm Quartzite, although seldom exposed, is more pelitic and finer grained as it grades upward and intertongues with the Roaring Fork Sandstone near Middle Top and to the southwest of the area mapped (Fig. 2.12). Assuming that the mica content in the sandstones represents the metamorphosed clays in the sandstone, the composition of the Longarm Quartzite northwest of Moody Top falls inside the subarkose field when plotted in a Q-F-M diagram. Modal analyses (Appendix A) show that samples 25.1.5, 3.5.4b, and 25.1.9 contain 15 to 25 percent feldspar; 2 to 5 percent is K-feldspar, the remainder is plagioclase in the range of An_{10} to An_{20}. Feldspar grains are angular, well sorted, and generally larger than quartz, reaching up to granule size. To the southeast of the study area feldspar content is consistently less than 5 percent (Fig. 2.11; samples 15.4.13, 26.7.8, 25.4.9, and 6.2.6 from Appendix A).

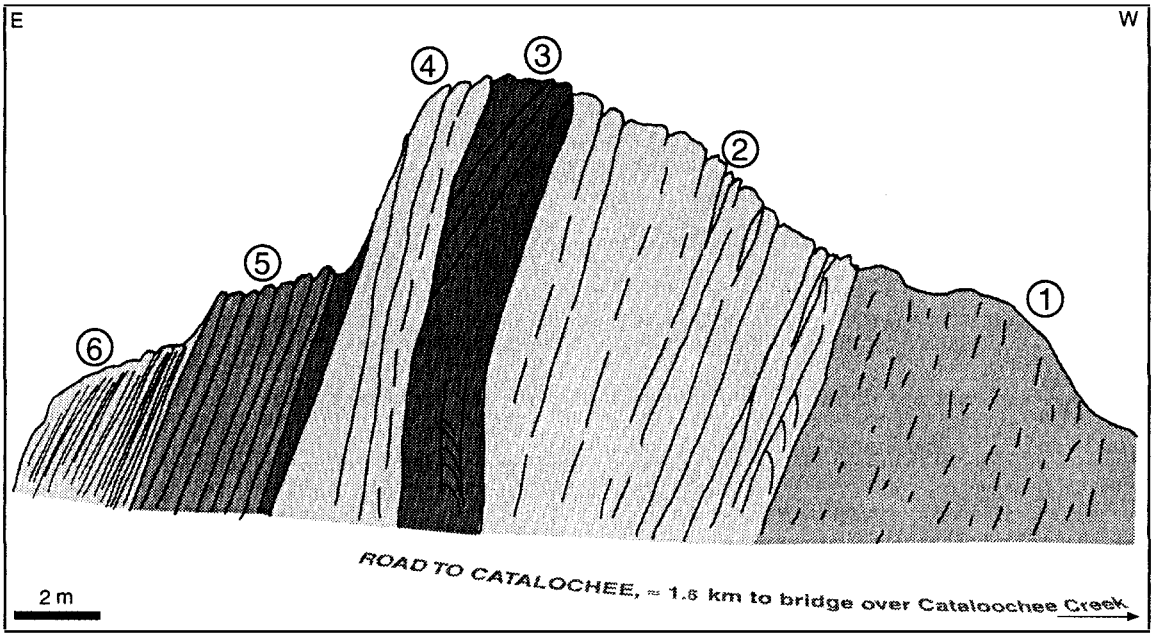

Figure 2.7. Longarm Quartzite road exposure. Bedding geometry near the middle of the Longarm Quartzite in the northwestern outcrop belt (location indicated in the figure). Note the homogeneity from the top (Fig. 2.4b) to the middle of the unit. Unit 1- 20 m thick sequence containing massive, very fine-grained, layered, dark quartzite, and fine-grained, gray quartzite interbedded with black siltstone containing blue quartz pebbles. Unit 2- very coarse-grained, light-colored, feldspathic quartzite rich in heavy minerals in plane-parallel bedded, internally cross-bedded strata. Unit 3- massive, locally cross-bedded, black siltstone. Unit 4- wedge-shaped, fine-grained, gray quartzite, and very fine-grained light-colored, 1 cm wedge-laminated feldspathic quartzite. Unit 5- coarse-grained, light-colored quartzite in internally cross bedded sets of 25 cm thick parallel beds interlayered with dark siltstone. Unit 6- very coarse-grained, light-colored, 1 cm laminated quartzite.

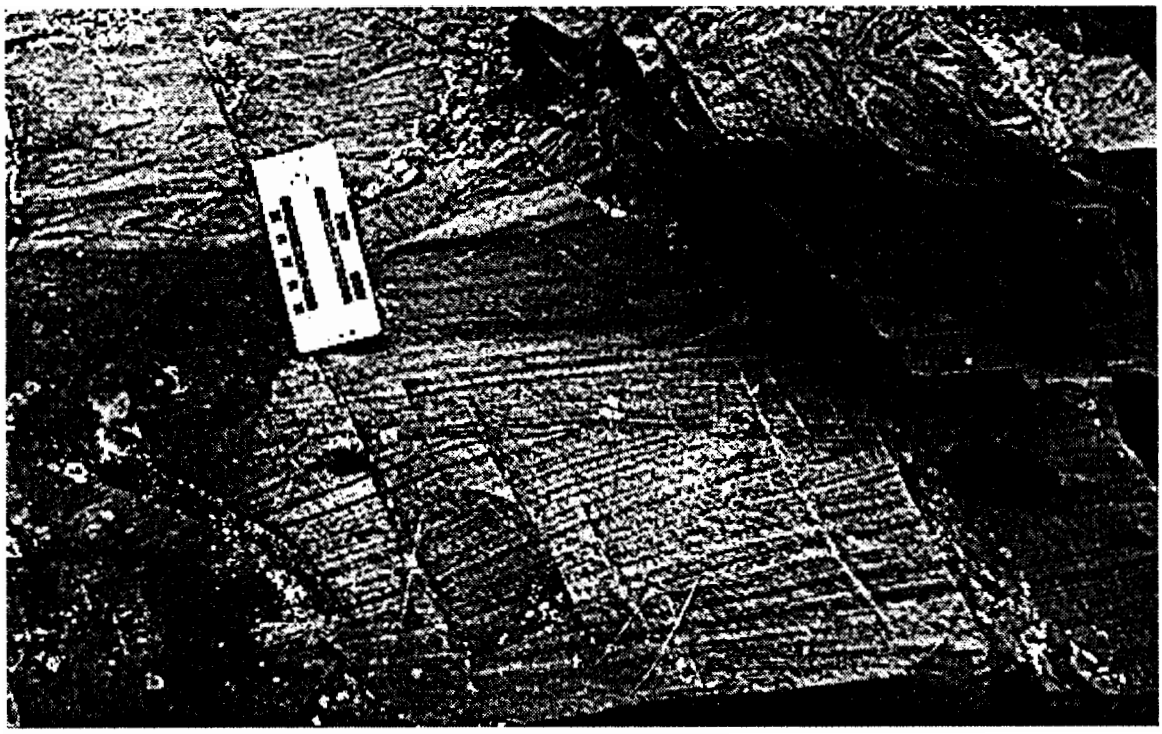

Figure 2.8. Cross-bedding in Longarm Quartzite. Plane-parallel bedded, internally cross-bedded sandstone in the Longarm Quartzite, northwestern outcrop belt. Cross beds are defined by heavy minerals. Road to Cataloochee, approximately 300 m northeast of the bridge over the Cataloochee Creek, Cove Creek Gap quadrangle.

Figure 2.9. Soft-sediment slump folding in the Longarm Quartzite. Northwestern outcrop belt, road to Cataloochee, approximately 300 m northeast of the bridge over the Cataloochee Creek, Cove Creek Gap quadrangle.

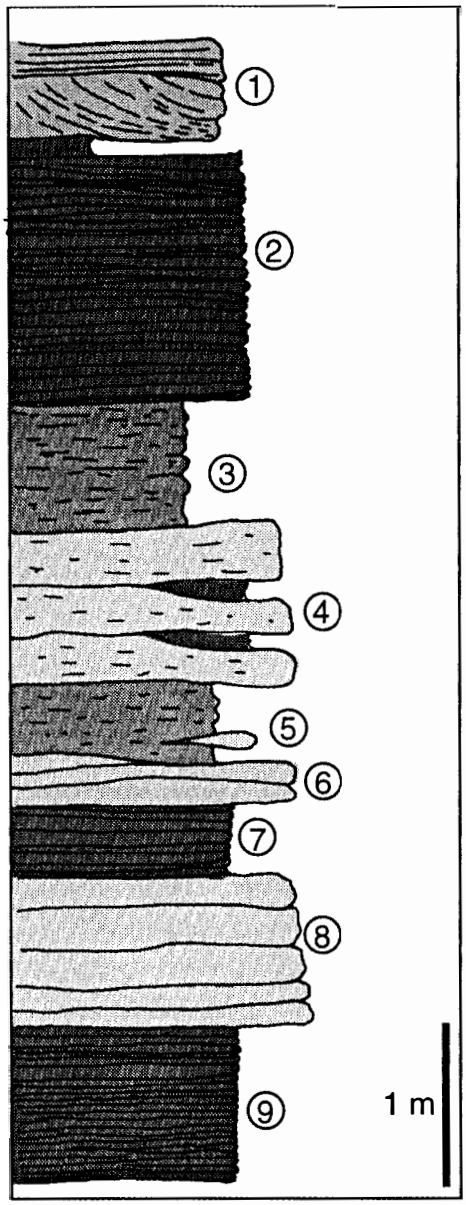

Figure 2.10. Fine-grained facies of the Longarm Quartzite. Located approximately 1.6 km south of Little Bald Knob; 83°7'18" W, 35°32'14" N. Unit 1- light-colored, fine-grained, cross-bedded, muscovite-rich, metasandstone. Units 2, 7 and 9- light-colored, medium- to coarse-grained, muscovite biotite, metasandstone interlayered with dark metasiltstone. Units 3 and 5- light-colored, very fine-grained, very finely laminated feldspathic quartzite. Units 4 and 8- light-colored, medium-grained, clean quartzite. Unit 6- light-colored, fine-grained, biotite-rich quartzite.

a)

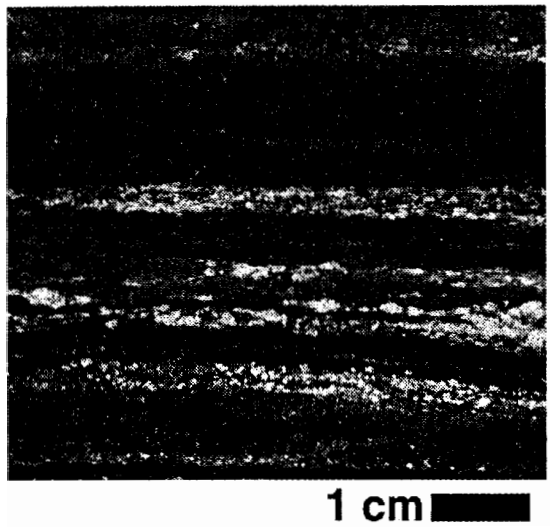

b)

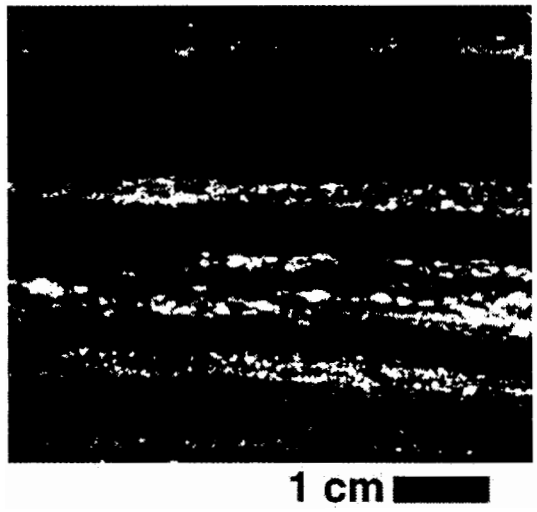

Figure 2.11. Pelitic quartzite in the Longarm Quartzite.
(a) Sawed sample from the thin southeasternmost exposures of the Longarm Quartzite. The reflected-light scanning technique highlights the opaque feldspar-rich layers (white), whereas quartz-muscovite layers appear dark because quartz transmits light; bar equals 1 cm. Located approximately 1 km ENE of Olivet Church, in Maggie Valley; 83°4'49" W, 35°31'12" N.
(b) In order to measure percentages, this image was converted to high contrast using an Adobe Photoshop 3.0™ threshold filter. 120,864 pixels yielded a 94.17 percent in the black channel (quartz + muscovite), and a 5.83 percent in the white channel (feldspar). These results were confirmed by point counting (n = 3517) a thin section of sample 6.2.6 (see Appendix A for details).

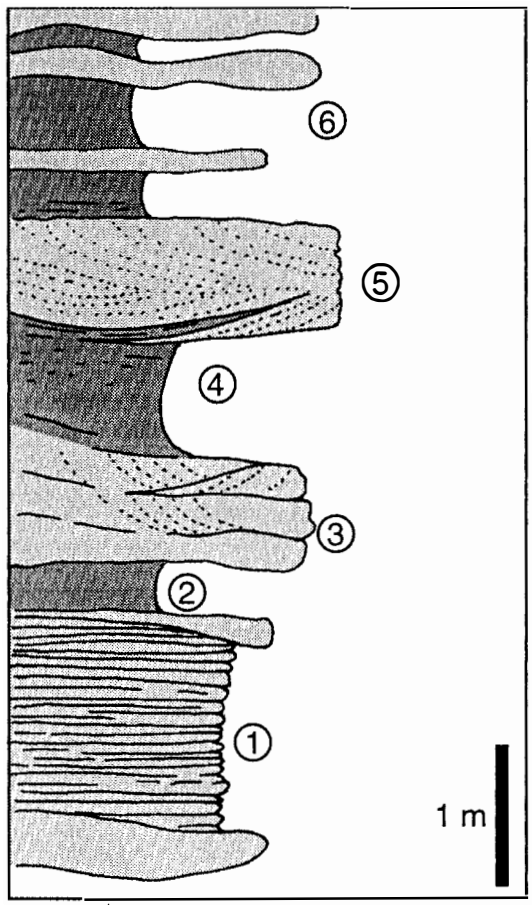

Figure 2.12. Pelitic facies of the top of the Longarm Quartzite. Located approximately 2 km north of Soco Gap, 83°9'48" W, 35°30'51" N. Unit 1- fine-grained, finely laminated, biotite metasandstone. Unit 2- biotite-muscovite schist. Units 3 and 5- fine-grained, light-colored, cross-bedded quartzite with biotite. Units 4 and 6- very sandy, arkosic, muscovite-biotite schist. This section from the top of the Longarm Quartzite is very similar to Roaring Fork Sandstone, which is generally a biotite-rich, arkosic metasandstone, regularly interbedded with mica schists in 5 to 20 m thick packages with the entire unit at least 150 m thick.

Stratigraphic relationships

Although generally affected by several phases of deformation (Chapter III), the geometry and nature of the contacts between units in the Snowbird Group provide important clues regarding the mode of clastic accumulation. The sharp and conformable basal contact of the Longarm Quartzite with the Wading Branch Formation (Hadley and Goldsmith, 1963, p. 31; Keller, 1980, p. 49) is well exposed in the road to Cataloochee (Fig. 2.13), and south of Wycle Fork; or it is nonconformable on granitic basement, which is well exposed south of Moody Top. This nonconformable relationship is modified by faulting along the southeastern flank of the Cataloochee Divide, perhaps resulting from a rheological contrast between the granitic basement and the Longarm Quartzite sandstones. The contact between Roaring Fork Sandstone and the Longarm Quartzite is consistently transitional over stratigraphic distances of 20 to 40 m. Lithologic types characteristic of both units intertongue in the transitional zone between these two units: light-colored quartzite, 2 to 20 m thick intercalation of pelitic beds, and dark, finely layered, medium-grained arkose and subarkose. In addition, the top of the Longarm Quartzite becomes

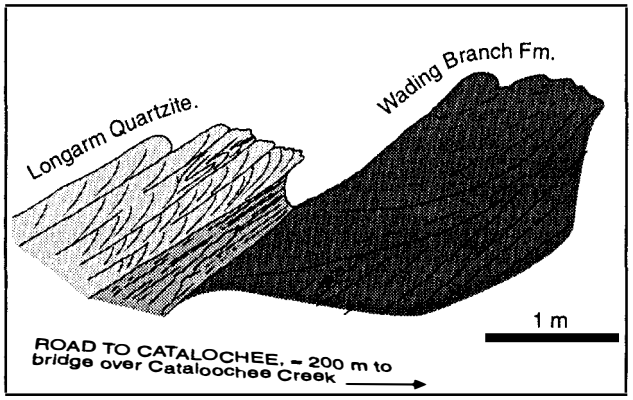

Figure 2.13. Wading Branch Formation-Longarm Quartzite contact. Sharp contact at the base of the Longarm Quartzite in the northwestern outcrop belt. The base of the Longarm Quartzite is exposed as a sharp contact between mostly black siltstone with minor very fine-grained quartzite (Wading Branch Formation), and coarse-grained, white quartzite with abundant heavy minerals and soft-sediment slump folds. The same sharp contact can be observed in Figs. 2.4a and 2.6.

more pelitic to the south and east, resembling facies more characteristic of Roaring Fork Sandstone.

GREAT SMOKY GROUP LITHOSTRATIGRAPHY

The Ocoee Supergroup consists of two sequences separated by the Greenbrier fault (King et al., 1958); those sequences have traditionally been divided into those north and below the Greenbrier fault, and those south and above it (King et al. 1958; DeWindt 1975; Rast and Kohles 1986). Geologic maps from central-western North Carolina (Hadley and Goldsmith, 1963; Hadley and Nelson, 1971; North Carolina Geological Survey, 1985; Keller, 1986; Carter, unpublished) depict the Snowbird and Great Smoky Groups in stratigraphic contact. My work, however, demonstrates that the Greenbrier fault does separate Snowbird from the Great Smoky Group in the easternmost part of the western Blue Ridge (Chapter III). The faulted nature of this contact raises the possibility that the Great Smoky Group is an eastern distal facies of the Snowbird Group deposited farther east, and then thrust to the northwest along the Greenbrier fault. Despite the characteristically thick and repetitive nature of the lithologic types in the Great Smoky Group throughout the western Blue Ridge, the Great Smoky Group was subdivided in the area mapped into upper Elkmont Sandstone, Thunderhead Sandstone, Anakeesta Formation, and possibly the base of the Ammons Formation.

Elkmont Sandstone

Hadley and Goldsmith (1963) recognized a pelitic unit overlying the Snowbird Group southeast of the Great Smoky Mountains and assigned it to the base of the Thunderhead Sandstone, because they found no specific reason to correlate it with the Elkmont Sandstone. My detailed mapping, however, shows that a separate unit, which I correlate to the Elkmont Sandstone (Fig. 2.14), is conformably underneath the Thunderhead Sandstone. The base of this unit is faulted along the Caldwell Creek and Greenbrier faults, and because of the absence of sandstone characteristic

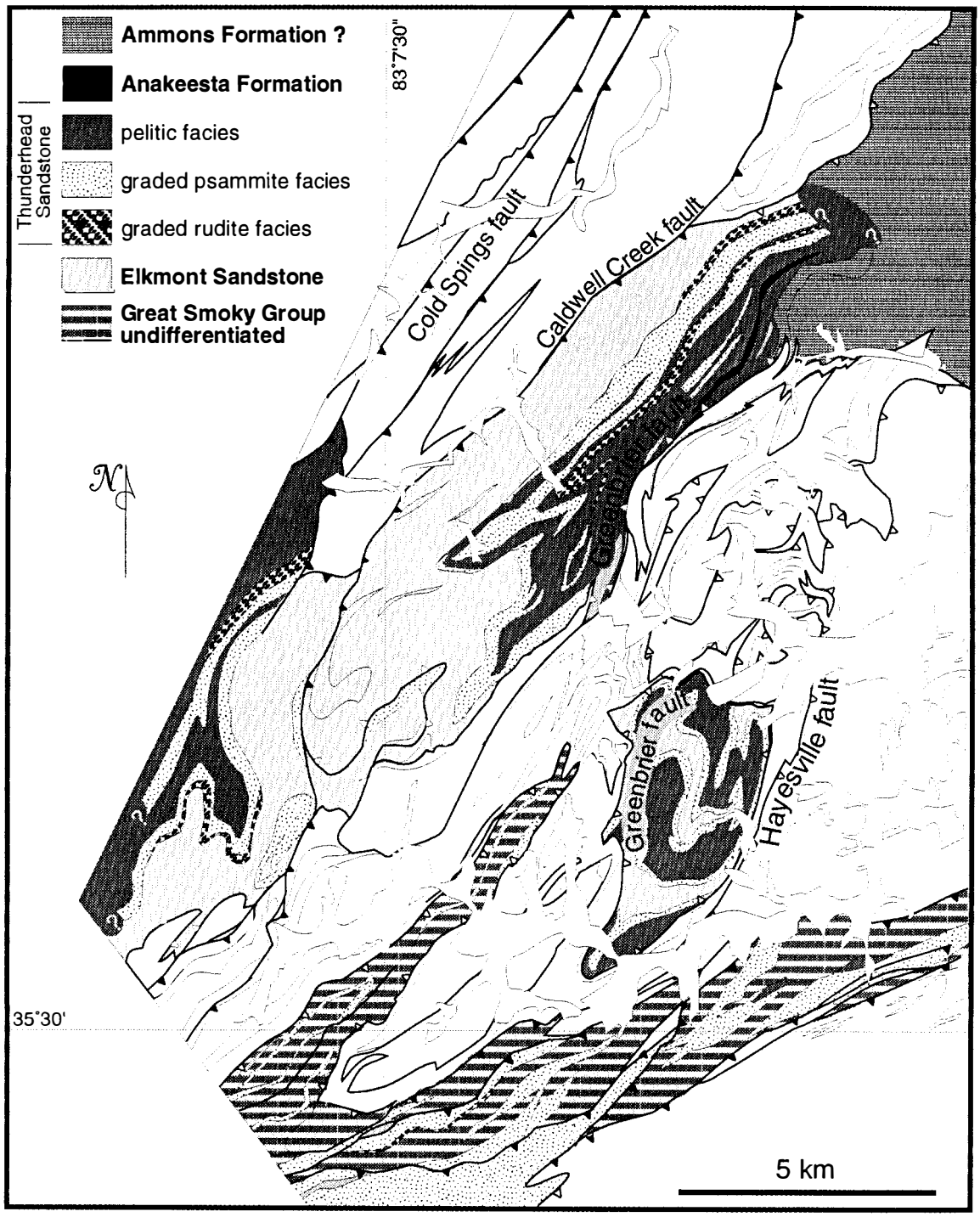

Figure 2.14. Geologic map for the Great Smoky Group. Simplified geologic map (from Plate I) showing the facies distribution within the Thunderhead Sandstone and Elkmont Sandstone. Note the predominance of graded rudite to the north and west in the Thunderhead Sandstone. See Figure 2.1 for explanation of contacts.

of the lower parts of this unit (Hadley and Goldsmith, 1963). I assume that in the area studied only the pelitic upper part (450 to 1050 m) of this unit is present.

The upper part of the Elkmont Sandstone is a monotonous, dark-colored, pelitic and psammitic unit, which because of its composition, records metamorphic grade better than any other unit in the study area (Chapter III). Modal analyses of thin sections (Appendix A) of this unit show that pelites comprise 50 to 55 percent of the unit and the silt-size, quartz-feldspar-rich sediments comprise 45 to 50 percent. This unit is usually a pelitic black, massive, and monotonous metasiltstone. The overall monotony of this unit is occasionally broken by 1- to 3- m thick graded beds of sandstone with granule-size conglomerate at the base (Fig. 2.15). Lenticular and parallel-laminated calcsilicate (Fig. 2.16) is common. This unit is better exposed to the northwest of the study area in the Cove Creek Gap, where it is a dark, massive metasiltstone, and along creek beds draining the northwestern flank of the Cataloochee Divide, where the mostly dark metasiltstone sequence is more often interrupted by 1- to 3- m thick graded sandstone-conglomerate beds.

Thunderhead Sandstone

The Thunderhead Sandstone is an approximately 1200-m thick sequence of graded, fining-upward metaconglomerate-metasandstone-schist (Figs. 2.17 and 2.18). The contact with the underlying Elkmont Sandstone is transitional over a stratigraphic distance of 10 to 20 m. The Thunderhead Sandstone is better exposed to the northwest of the study area on both flanks of the Cataloochee Divide, where both, the base and the top are exposed, and the stratigraphic sequence is not disrupted by major faults. In outcrop scale the Thunderhead Sandstone is made up of 1- to 10 m thick intercalations of graded granule-size conglomerate beds grading upward into fine-grained metasandstone (Figs. 2.17 and 2.19). Graded conglomerate beds toward the base of the unit contain abundant quartz and feldspar clasts along with less abundant black siltstone clasts. Toward the top of the unit, the conglomerate-sandstone sequence gradually becomes a graded, medium-grained, massive

Figure 2.15. Graded sandstone in the Elkmont Sandstone.
(a) Coarse-grained bed interrupting the monotony of the mostly pelitic upper part of the Elkmont Sandstone. Note the sharp contact at the base of unit 1 versus the transitional contact toward unit 3. Unit 1- medium- to very fine-grained graded metasandstone and quartzite with granule-size conglomerate at the base. Unit 2- dark, very fine-grained, garnet-rich metasandstone that grade into light-brown, sandy, garnet-rich metasiltstone. Unit 3- dark, mica-rich, garnet, biotite metasiltstone. Caldwell Creek east of Big Fork Ridge; 83°7'27" W, 35°35'1" N.
(b) Fining-upward, overturned bed of graded sandstone in the Elkmont Sandstone. Note the granule-size conglomerate at its stratigraphic base (in the box). These sandstone beds grade upward into variably recrystallized black phyllite and metasiltstone. Same location as above.

a)

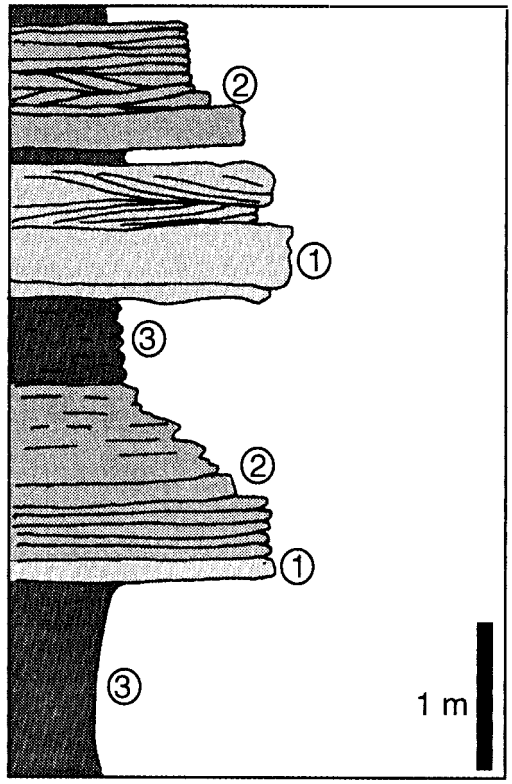

b)

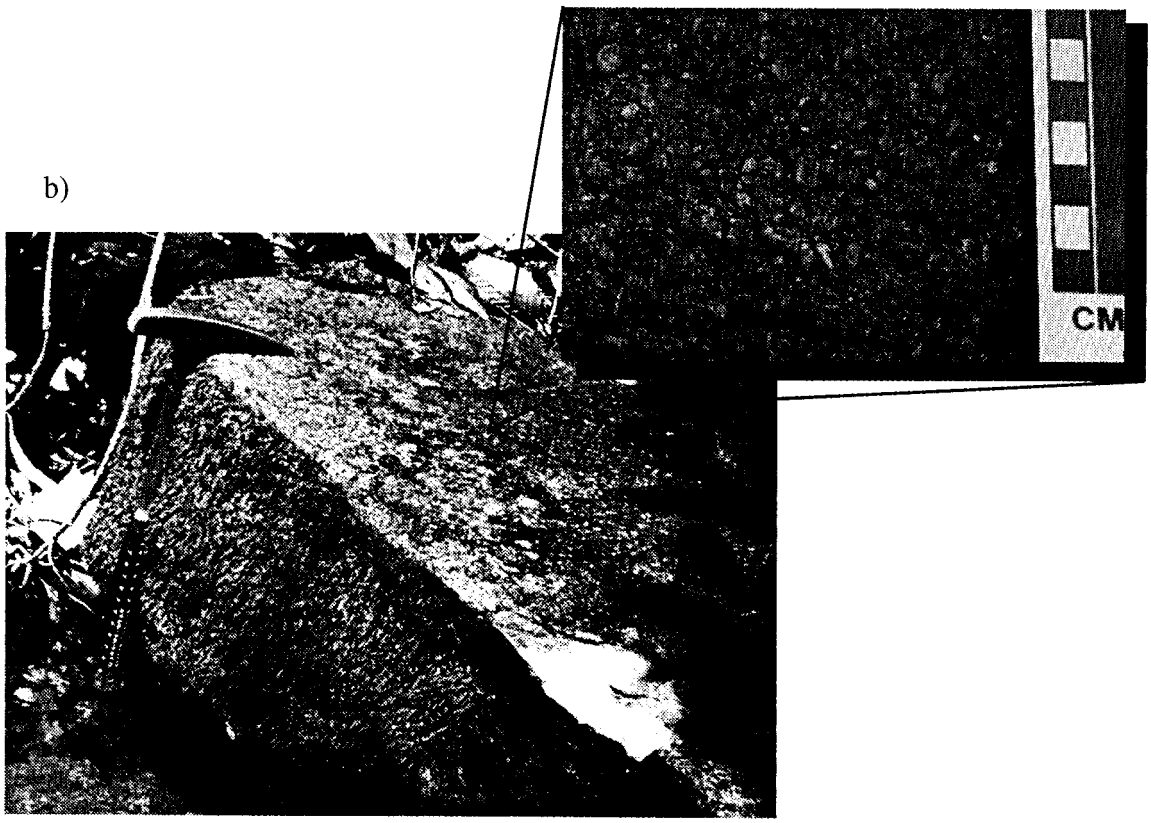

Figure 2.16. Calcsilicate in the Elkmont Sandstone. Interlayered calcsilicate (more resistant) and garnet schist near the top of the Elkmont Sandstone. Caldwell Fork, 350 m upstream from its confluence with Straight Creek, Dellwood quadrangle; 83°7'3" W, 35°34'27" N.

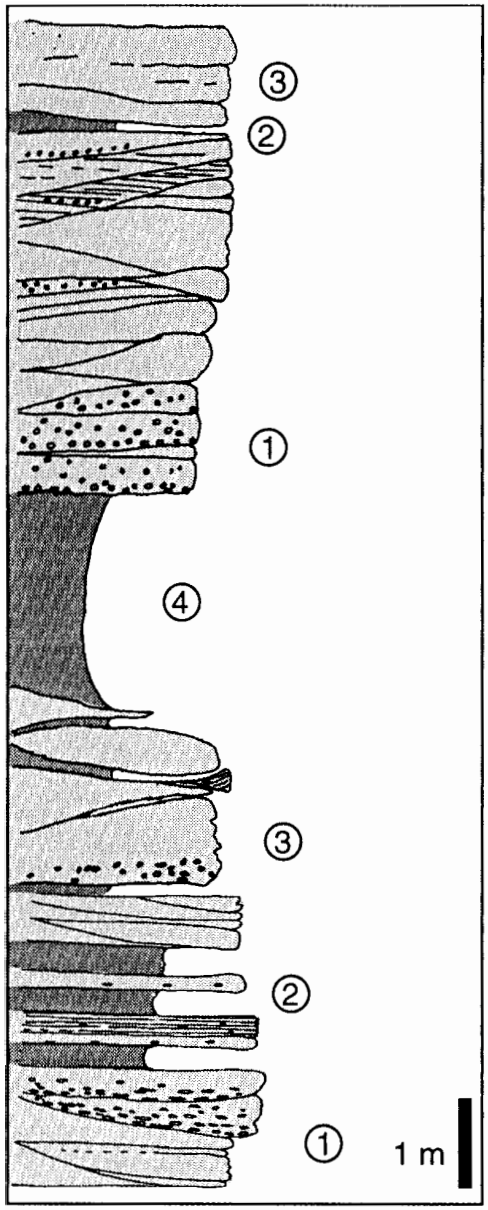

Figure 2.17. Stratigraphic section at the base of the Thunderhead Sandstone. It shows the lowermost part of the fining-upward turbiditic sequence. Unit 1- one-meter thick, cross-bedded, dark, biotite-muscovite, graded metaconglomerate interbedded with dark, fine- to medium-grained, metasandstone. Units 2 and 3- thin bedded, dark metasandstone with occasional granule-size conglomeratic layers. Unit 4- sandy mica schists. Located on the road to Cataloochee near the Great Smoky Mountains National Park boundary; 83°2'50" W, 35°37'49" N.

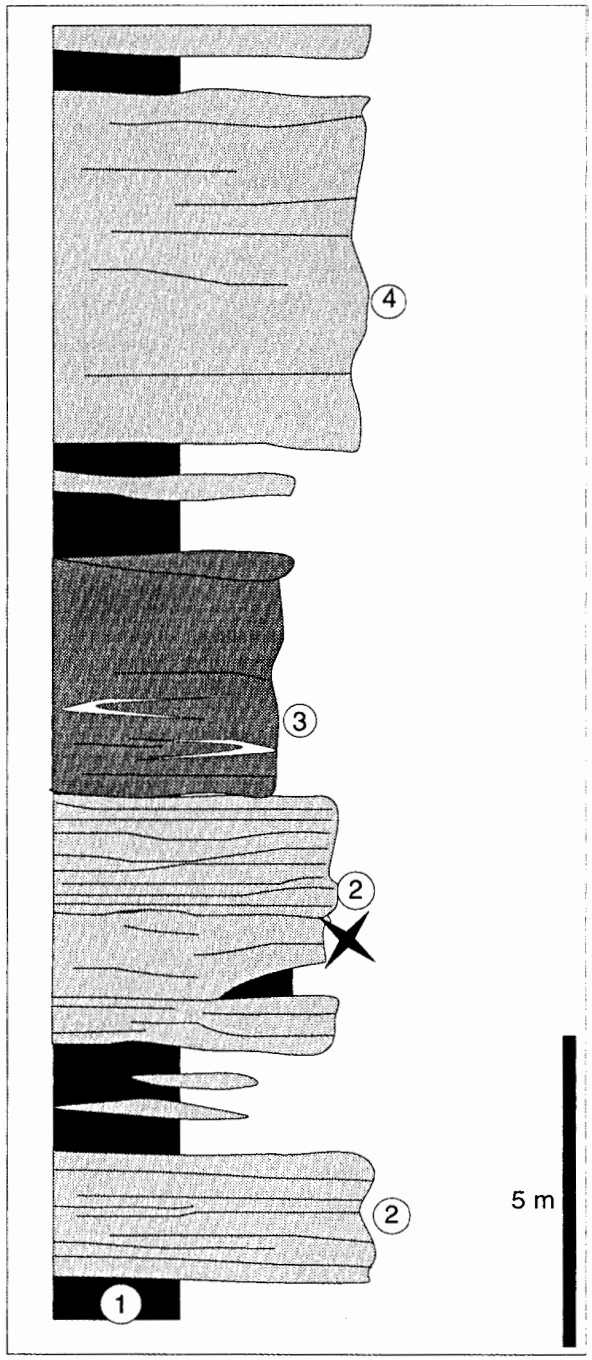

Figure 2.18. Finer-grained facies at the base of the Thunderhead Sandstone. Located approximately 1 km ESE of Olivet Church, Maggie Valley; 83°4'54" W, 35°30'56 N. This is a sequence made up mostly of medium-grained, layered, biotite-muscovite metasandstone, interlayered with biotite-garnet schist. Unit 1- massive biotite-garnet schist. Unit 2- medium-grained biotite metasandstone (Sample inidcated with a star, sample 6.2.1a in Appendix A). Unit 3- very fine-grained biotite-garnet metasandstone with intercalated biotite schist beds. Note the intrafolial folds preserved in this unit. Unit 4- massive, coarse-grained biotite metasandstone.

a)

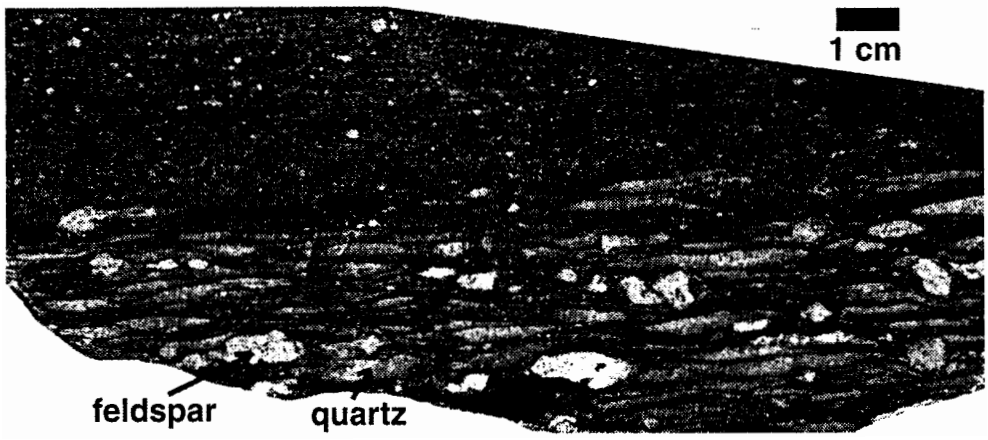

b)

Figure 2.19. Graded bed in the Thunderhead Sandstone.
(a) Base of a graded conglomerate bed near the base of the Thunderhead Sandstone in the northwestern corner of the study area. Located along the Cataloochee Divide hiking trail; 83°4'24" W, 35°36'8" N. The scanner reflected light, and the differential flattening highlights the compositional differences. White and stubby: feldspar; elongated and gray: quartz.
(b) In order to measure feldspar percentages, this image was converted to high contrast using an Adobe Photoshop 3.0™ threshold filter. 536,655 pixels yielded a 95.8 percent in the black channel (quartz clasts, plus dark sandy matrix), and a 4.12 percent in the white channel (feldspar clasts).

metasandstone (Fig. 2.20) that changes upwards to fine-grained, laminated metasandstone, and higher in the sequence to a pelitic schist. The contacts at the base of the coarse-grained units are always sharp with finer-grained units (Fig. 2.21). Thunderhead and Elkmont Sandstones can be easily distinguished even at high metamorphic grade, because of the contrasting bed-scale homogeneity of Elkmont Sandstone versus the small-scale intercalation of graded ruditic-psammitic-pelitic facies in the Thunderhead Sandstone. To the southeast of the study area, along the north flank of the Eaglenest Ridge, the Thunderhead Sandstone seems to become a more homogeneous, finer-grained unit, where the sandstone beds do not show graded bedding as often as to the northwest, and where the change from sandstone to pelite is not clearly transitional. This greater homogeneity, however, may be due to increasing metamorphic grade (up to sillimanite) erasing some of the fine sedimentary structures in the sandstones. On top of the pelitic Thunderhead Sandstone is the Anakeesta Formation. In the area studied, however, this unit is a characteristically thin (about 20 m thick) discontinuous graphitic schist.

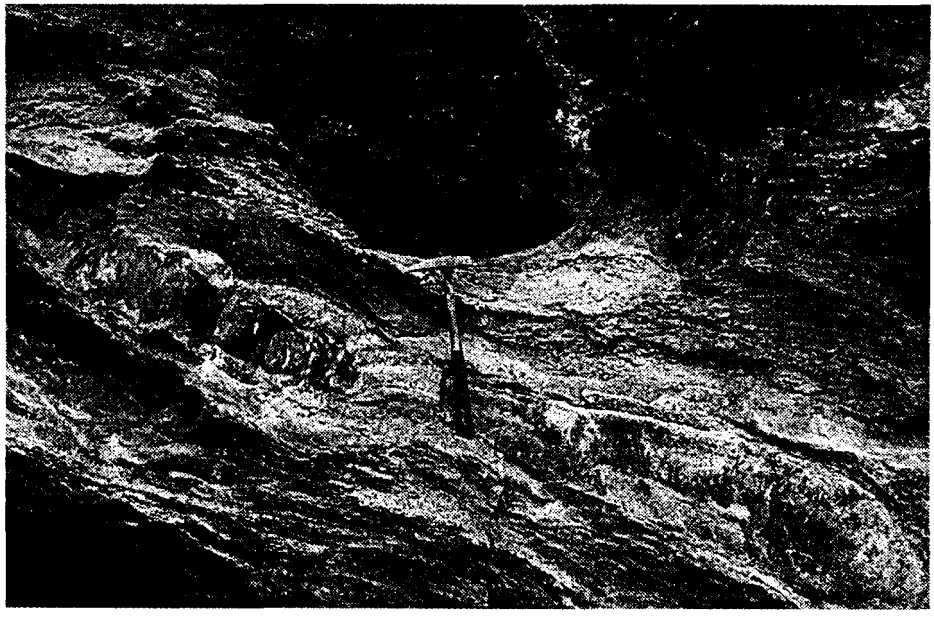

Figure 2.20. Boudined pelitic-psammitic interlayers in Thunderhead Sandstone. Road to Leatherwood Top; 83°3'42" W, 35°32'14" N.

Figure 2.21. Pebbles at the base of a sandy bed in turbiditic deposits of the Thunderhead Sandstone. The characteristically sharp basal contact with schist at the base of these beds very often produces overhangs where hogback-shaped pebbles extend into the surface by weathering and erosion of the schist bed beneath. 83°4'60" W, 35°34'29" N.

Modal analyses (Appendix A) on thin sections of Thunderhead Sandstone reveal that the sandstones generally contain from 23 to 35 percent of feldspar (An_{20} to An_{30}), and from 48 to 58 percent of quartz; the pelitic facies of this unit are comprised by about 60 percent or slightly more of pelitic minerals, under 40 percent sand-size, and silt-size quartz and feldspar, although some pelites may contain as much as 88 percent pelitic minerals. These modes agree with previous modes by Hadley and Goldsmith (1963), and Quinn (1991).

OCOEE SUPERGROUP: NORTHWESTERN PROVENANCE

Stratigraphic relationships, depositional environments, sandstone composition, and changes in thickness and facies across the study area are discussed below to decipher the mode of accumulation of the Ocoee Supergroup in the area mapped, with emphasis in the sandstones of the Longarm Quartzite and the Thunderhead Sandstone because these two units provide the most complete record of stratigraphic elements. Previous

hypothesis by King et al. (1958), DeWindt (1975), and Rast and Kohles (1986) regarding the mode of accumulation of the Ocoee Supergroup are also discussed in the light of the new observations made in this work.

Snowbird Group paleoenvironments

The impure, poorly sorted nature of the Wading Branch Formation may indicate continental accumulation, perhaps in quiet coastal lagoons intermittently affected by currents bringing coarser clastics into an otherwise pelitic sequence (Keller, 1980). The absence of granitic fragments and the scarcity of feldspar with respect to quartz are evidence of very slow erosion, deep weathering, and reworking of a granitic basement before filling the discontinuous depressions (Hadley and Goldsmith, 1963). Above the Wading Branch Formation, the abundant sedimentary structures in the Longarm Quartzite, such as cross-bedding and soft-sediment slump folds, represent an important break in the sedimentologic style of the Snowbird Group. They record strong currents in braided fluvial systems (Keller, 1980) to fluvio-deltaic environments (DeWindt, 1975) that produced a cleaner, more homogeneous, coarser-grained, and continuous unit than the poorly sorted, impure, non-marine Wading Branch Formation (Fig. 2.22). The high feldspar content in the Longarm Quartzite is an indication of rapid mechanical disintegration of the source rock with virtually no chemical decomposition (Hadley and Goldsmith, 1963; Hadley, 1970) that requires significant relief in the source area during deposition (Keller, 1980).

The contrasting depositional styles between the Wading Branch Formation (slow, deep weathering of the granitic basement beneath) and the Longarm Quartzite (rapid mechanical disintegration of a granitic basement) clearly indicate that the same source area could not have supplied the sediments needed for the accumulation of both units. The clastics coming from a deeply weathered basement could not have provided fresh feldspar for the arkosic facies of the Longarm Quartzite. In the same manner, a rapidly eroding granitic basement could not have preserved a reworked regolith like the Wading Branch Formation. Therefore, the granitic basement beneath

Figure 2.22. Snowbird lithostratigraphy. Simplified composite stratigraphic columns of the Snowbird Group from three regions in the study area (note that the vertical scale changes for every column).
(a) Northwestern outcrop belt of the Longarm Quartzite characterized by very thick, arkosic sandstone, containing abundant sedimentary structures.
(b) Central outcrop belt of the Longarm Quartzite characterized by subarkosic and thinner deposits. Cross bedding is still present.
(c) Southeastern outcrop belt of the Longarm Quartzite, consists of a very thin pelitic quartzite.
(d) Variation in composition from NW to SE; data points obtained by point counting thin sections (see appendix A).

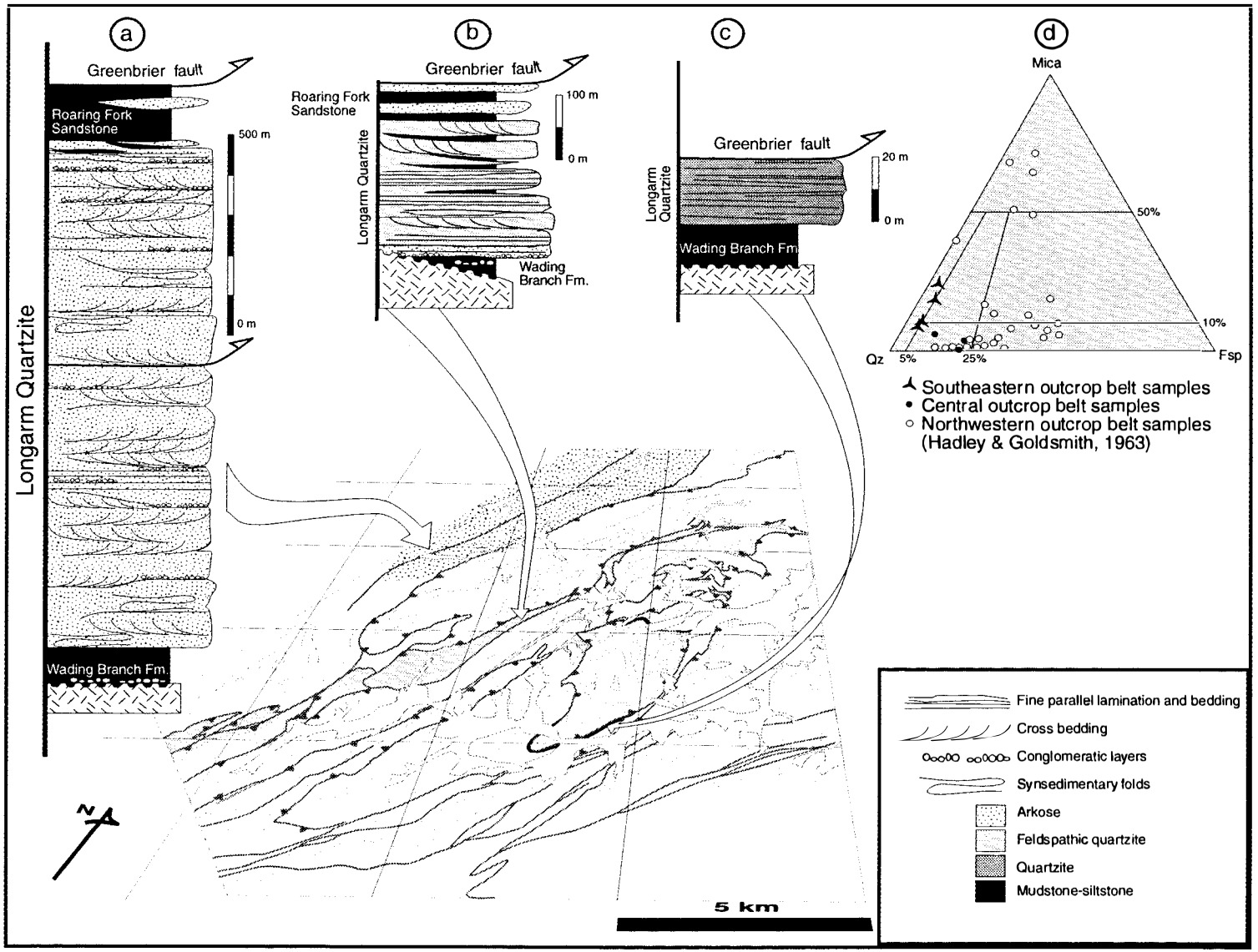
a
b
c
d
Greenbrier fault
Roaring Fork Sandstone
500 m
0 m
Longarm Quartzite
Wading Branch Fm.
100 m
20 m
Mica
50%
10%
Qz
5%
25%
Fsp
Southeastern outcrop belt samples
Central outcrop belt samples
Northwestern outcrop belt samples
(Hadley & Goldsmith, 1963)
N
5 km
Fine parallel lamination and bedding
Cross bedding
Conglomeratic layers
Synsedimentary folds
Arkose
Feldspathic quartzite
Quartzite
Mudstone-siltstone

the southeastern edge of the western Blue Ridge did not supply clastic sediments for the Longarm Quartzite because a deeply altered granitic basement has difficulty yielding fresh feldspar in sufficient amount to form the thick arkosic facies of the Longarm Quartzite to the northwest (Fig. 2.22a).

Longarm Quartzite sandstone composition

Point counting on samples from the Longarm Quartzite across the study area shows that thin fine-grained ortho-quartzite facies dominates to the southeast with more than 95 percent quartz and micas (Fig. 2.22c), whereas the coarser-grained, subarkosic (25 to 10 percent feldspar; Fig. 2.22b), to arkosic (25 to 50 percent feldspar; Fig. 2.22a) facies is located to the north and west. These observed compositional changes are evidence for northwestern provenance, as the less mature arkosic facies is located to the northwest, and the more mature quartzitic facies is found to the southeast. Thus, the ratio of feldspar to quartz (Fig. 2.22d), as a measure of maturity (Folk, 1974; Dickinson, 1984), suggests that the southeasternmost exposures of the Longarm Quartzite also represent the more distal facies of this unit.

Snowbird Group stratigraphic relationships: A distal downlap

The sharp contact between the Longarm Quartzite and the Wading Branch Formation indicates that the transition from one environment characterized by quiet coastal lagoons intermittently affected by currents (Wading Branch Formation), to another characterized by strong currents in braided fluvial to fluvio-deltaic systems (Longarm Quartzite) was abrupt. This change perhaps records rapid influx of sand, and burial of the basement and the Wading Branch Formation. A sharp contact between these two units rules out the possibility suggested by King et al. (1958) that the Snowbird Group onlapped the granitic basement and the reworked regolith, because in that scenario the Wading Branch Formation pelites would intertongue with the Longarm Quartzite. This would require the basement and the reworked regolith to be the primary source for the clastic material making up the Longarm Quartzite (Figs. 2.2

and 2.3). In contrast, if Longarm Quartzite facies migrated from northwest to southeast and buried a deeply weathered granitic basement the contact between the sands and the reworked basement regolith could be sharp (Fig. 2.23). In addition, the high quartz-to-feldspar ratio to the southeast supports this hypothesis and suggests that the relationship of the Longarm Quartzite to the basement below is a distal downlap, because the more distal facies (orthoquartzite and pelitic quartzite) is located to the southeast (Fig. 2.22c), and the more proximal facies (arkose) is located toward the northwest (Fig. 2.22a). If the Longarm Quartzite facies onlapped the granitic basement as suggested by King et al. (1958), the southeasternmost Longarm Quartzite facies would be more feldspar-rich than equivalent facies to the northwest, because they would be closer to the source (Folk, 1974).

Longarm Quartzite thickness changes: Evidence for a synrift fault

The original structural geometry of a depositional basin can be inferred from stratigraphic contrasts that delineate paleogeographic domains. The boundaries of

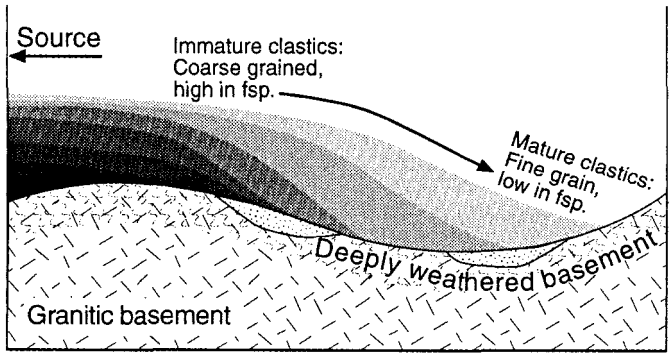

Figure 2.23. Distal downlap concept (*cf.* Schoch, 1989). Sandstone (grey scale) downlapping deeply altered granitic basement and reworked regolith below. Note that in a distal downlap relationship the contact at the base of the sandstone is sharp. The distal sandstone facies should consist of fine-grained quartzite, whereas the proximal facies should consist of coarse-grained feldspathic sandstone. Fsp- feldspar.

these domains in turn can be linked to fault systems active during deposition of stratigraphic units. This approach has been used to locate the axial zone of Late Proterozoic rifting in the central Appalachians (Wehr and Glover, 1985), and to palinspastically reconstruct the southeastern rifted margin of Laurentia (Thomas, 1991) from the Ouachita to the southern Appalachians in Tennessee. The changes in the stratigraphy of the Longarm Quartzite on both sides of a minor postmetamorphic fault in the study area may reflect one such fault that was later inverted.

The presence of a growth fault active during the deposition of the Longarm Quartzite is suggested in Fig. 2.24 because of the impressive thickness changes, over short horizontal distances, observed in the Longarm Quartzite in the area mapped (Fig. 2.22). This possibility was not contemplated by earlier workers primarily because the trace of the Greenbrier fault, as mapped by Hadley and Goldsmith (1963), separated this impressive stratigraphic contrast (Figs. 2.24, and 2.2b) along the Caldwell Creek between Cataloochee Divide and the Big Fork Ridge in the Great Smoky Mountains National Park (Plate I). My mapping, however, indicates that the trace of the premetamorphic Greenbrier fault still follows the contact between the Snowbird and Great Smoky Groups southeast of the Great Smoky Mountains, and that the fault mapped along Caldwell Creek by Hadley and Goldsmith, (1963) instead of Greenbrier fault, is a postmetamorphic fault with small displacement (Chapter III). Therefore, both the thick arkosic facies and the thin quartzite facies of the Longarm Quartzite lie side by side in the footwall of the Greenbrier fault. Since the thickness contrast in the Longarm Quartzite is separated by a postmetamorphic fault with small displacement (Chapter III), it may be better explained by normal faulting active at the time of deposition of the Longarm Quartzite (Wiener and Merschat, personal communication). Direct evidence for a growth fault, however, is missing because of reactivation during the Alleghanian orogeny, the same way as suitably oriented segments of Paleozoic thrust faults were inverted (Hatcher et al., 1989).

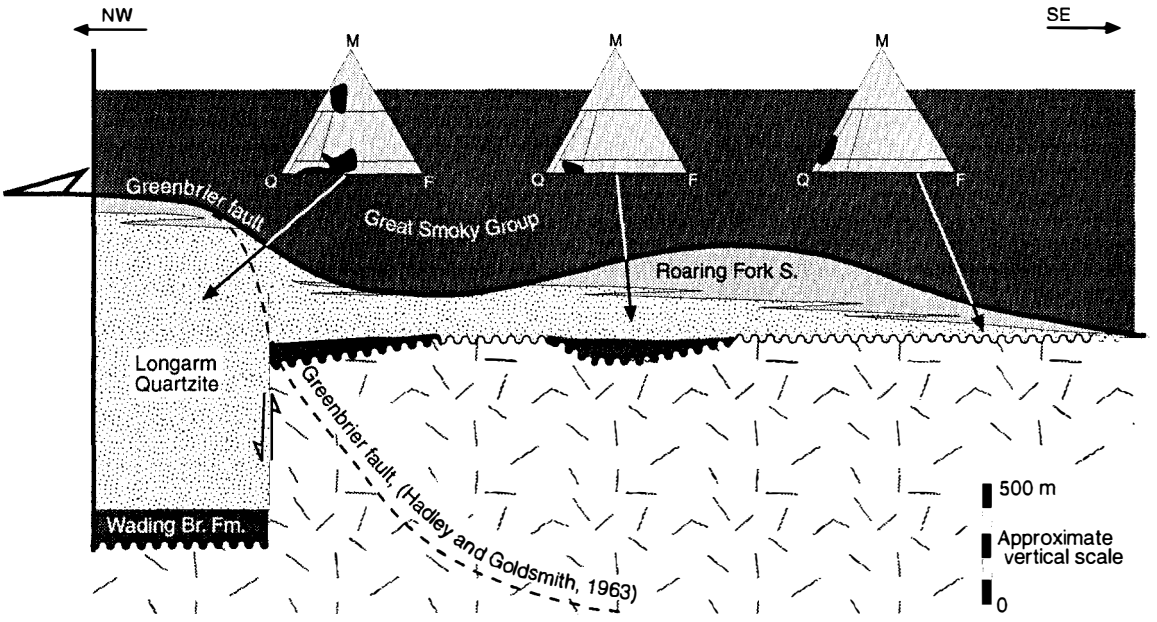

Figure 2.24 Reconstruction of the stratigraphic relationships among the Snowbird Group units in the area studied. The Longarm Quartzite distal downlap relationship to the basement and the Wading Branch Formation is suggested by the sharp contact between the Longarm Quartzite and the Wading Branch Formation, and by changes in Longarm Quartzite sandstone composition(note the variation in sandstone composition in the Q-F-M diagrams). The abrupt thickness change in the Longarm Quartzite suggests that a growth fault was active during the accumulation of this unit. The trace of the Greenbrier fault as mapped by Hadley and Goldsmith (1963) is indicated by dashes (compare with Fig. 2.2b).

A number of geologists have suggested the presence of synrift faults in the western Blue Ridge during deposition of the Late Proterozoic Ocoee Supergroup (Rodgers, 1972; Rankin, 1975; DeWindt, 1975; Hatcher, 1978, 1987; Keller et. al., 1983; Rast and Kohles, 1986). These fault-bounded basins are the relict of the Late Proterozoic (Odom and Fullgar, 1984) opening of the Iapetus ocean. Basement faults with probable vertical separation in excess of 10 km (Thomas, 1991) moved before the accumulation of the Lower Cambrian Chilhowee Group. Diverse approaches have been employed to locate these growth faults, including the search for extensional mylonitic fabrics in the Blue Ridge (Simpson and Kalaghan, 1989).

Thunderhead Sandstone: Northwest provenance

A northwestern provenance for the turbidites of the Thunderhead Sandstone was suggested (Hadley and Goldsmith, 1963) because of the abundance of boulder conglomerate to the northwest, and the lack thereof to the southeast of the Great Smoky Mountains. The same distribution was reconfirmed during my mapping (Figs. 2.25, and 2.14); the sediment size, however, changes from pebble to the northwest to fine sand to the southeast. Graded beds (Figs. 2.19, and 2.21), cross bedding near the base of the unit, and fine parallel lamination near the top are the most characteristic sedimentary structures throughout the Thunderhead Sandstone, and indicate transport by turbidite flows. It has been customary to interpret the

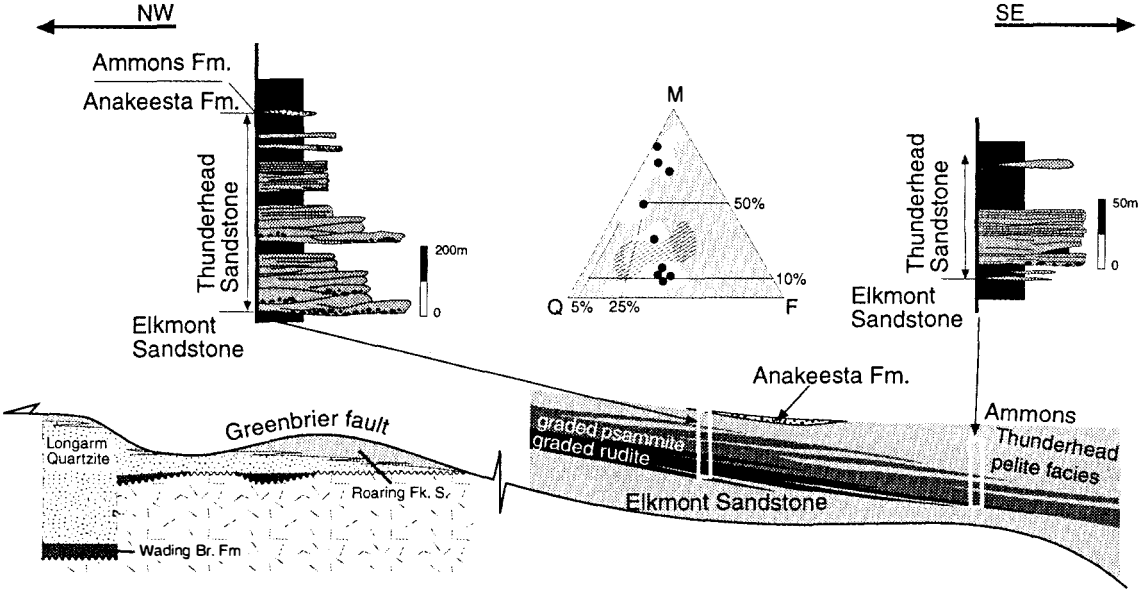

Figure 2.25. Reconstruction of the stratigraphic relationships among the Ocoee Supergroup units in the area studied. The abundance of conglomerate in the graded beds of Thunderhead Sandstone to the northwest indicate northwestern provenance. Fining upward of the Thunderhead Sandstone indicates that it is a retrogradational sequence. Black dots in the Q-F-M diagram indicate the composition of sandstone samples from the Thunderhead Sandstone (see Appendix A); white areas indicate the modal analyses by Hadley and Goldsmith, (1963); dashed area represents modal analyses by Quinn (1991) in the SE part of the study area NW of the Hayesville fault noth of Sylva, North Carolina.

turbidite deposits of the Thunderhead Sandstone as having been deposited in a deep water environment (King et al., 1958; Hadley and Goldsmith, 1963; Hadley, 1970; DeWindt, 1975; Rast and Kohles, 1986). The turbidite facies, however, reflects solely processes of deposition (Shanmugam et al., 1985) and there is still no agreement between modern submarine fans and ancient turbidite deposits (Normark et al., 1993; Lewis and McConchie, 1994). Without further evidence it can only be stated that the Thunderhead Sandstone was transported and accumulated below the wavebase by turbidity currents.

The Thunderhead Sandstone gradually fines upward (Figs. 2.17 and 2.25), indicating that this is a retrogradational (cf. Wagoner, 1995) sequence probably resulting from a progressive deepening of the depositional environment or, alternatively, from a progressively diminishing sediment supply (cf. Davis, 1992). Retrogradational turbiditic sequences are rarely observed in the geologic record (Davis, 1992), perhaps because most turbidite deposits accumulate near the unstable continental slope during sea-level lowstand, resulting in active fan progradation (Stow et al., 1985), therefore, turbiditic sequences usually show grain coarsening upward. On the other hand, during sea-level highstand, retrogradational sequences must onlap the unstable slope environment, thus making its preservation unlikely. In fact, in the event of a sea-level highstand, retrogressive slumping takes place near the mouth of the submarine fan upwards, toward the slope (Normark et al., 1993), and no record of such activity may be preserved.

STARVED BASIN RIFTED MARGIN SEQUENCE

The contrast between the interpretations above made and those of earlier workers in the same area is now discussed considering the regional framework of the Late Proterozoic evolution of the rifted margin of Laurentia, and modern rifting models for continental margins.

The lithostratigraphic schemes erected by King et al. (1958), Hadley and Goldsmith (1963), and Hadley (1970) state that the Snowbird Group provenance was located to the southeast, in a paleogeographic high marking the southeastern boundary of the Ocoee basin (Fig. 2.2.b), and that the source shifted to the north and then northwest by the time of deposition of the Thunderhead Sandstone. Evidence includes paleocurrents, the overall southeastward fining of Snowbird Group sediments, and the presence of tourmaline and zircon in the Great Smoky Group, suggesting the granitic composition of the source area. In contrast, the observations made in this work indicate that the source of the Longarm Quartzite was to the northwest, rather than the southeast, and that the granitic basement immediately beneath the easternmost western Blue Ridge did not supply clastics to the Ocoee basin to the northwest. In addition, a NE-SW trending growth fault may have acted as a barrier to the northwest-southeast flow of sediments across the basin, as implied by the stratigraphic contrasts in the Longarm Quartzite across the study area (Figs. 2.22 and 2.24). The southeastward pinchout of the Longarm Quartzite thus may delineate the zone of maximum downlap (Fig. 2.23) of starved and mature Snowbird Group sandy facies southeast of this growth fault. Northwest of the fault, the thick arkosic Longarm Quartzite was accumulated in shallow water as the hanging wall subsided at the same rate as the sand accumulation took place (cf. Ingersoll and Busby, 1995).

Modern continental rifting models (e.g., Wernicke, 1985; Lister et al., 1986; Lister et al., 1991) applied to the latest Proterozoic evolution of the rifted Laurentian margin (Hatcher and Goldberg, 1991) suggest that the Great Smoky and the Snowbird Groups record the initial rifting stages with texturally and compositionally immature sediments that quickly accumulated in a rapidly subsiding complex rift basin. Filling of the southeastern edge of this basin, as documented above, mainly occurred from northwest to southeast, in shallow-water environments, and was restricted by a NE-SW trending growth fault active during the accumulation of the Longarm Quartzite. The mode of filling, inferred from the stratigraphic observations, and the map relationships discussed above, can be compared with sediment distribution through time as predicted by the rifting sequence in continental rifting models (Fig. 2.26). If

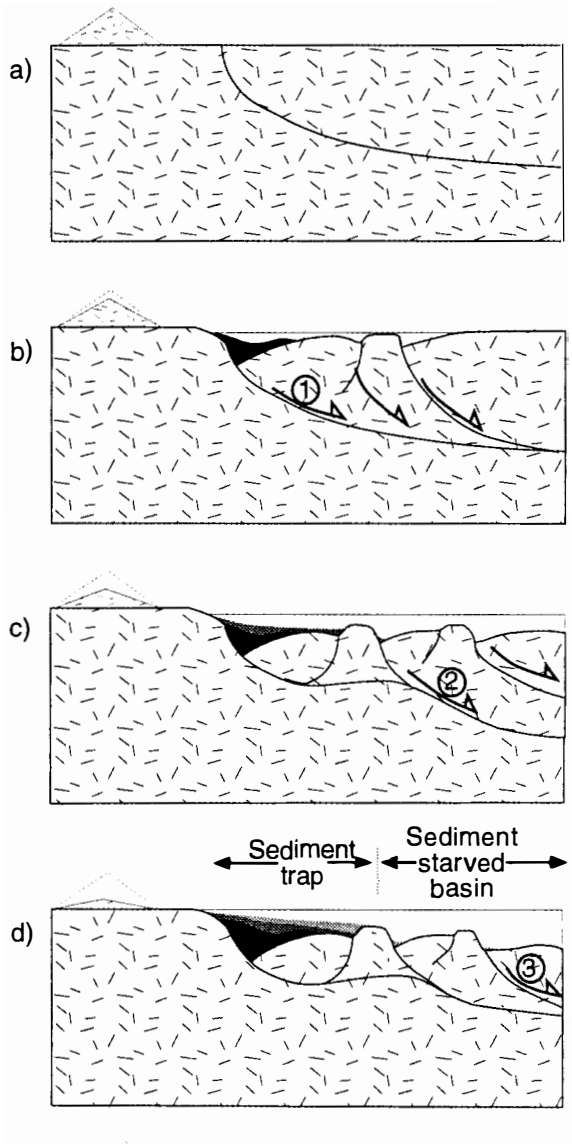

Figure 2.26. Evolution of a lower-plate extended continental margin (Lister *et al.*, 1986; Lister *et al.*, 1991). Sequence of opening (1, 2, 3) of rift basins is dictated by isostatic flexure of the lower crust, forcing the sequential abandonment of basins cratonward (*cf.* Wernicke and Axen, 1988). The effects of this sequence of rifting in the filling mode (*cf.* Leeder, 1995) are superimposed to Lister's *et al.*, (1986, 1991) model to show how some portions of a rift basin can contain huge volumes of rift-related deposits on top of the basement, whereas neighboring portions remain starved and contain virtually no record of the initial opening event. The resulting stratigraphy, remarkably similar to the Snowbird Group in western North Carolina, would be characterized by a thick sequence of coarse-grained, rapidly accumulated clastic sediments separated by normal faults from a thin sequence of mature, fine-grained clastics thinning out to a feather edge basinward, and covered by turbidites of the Great Smoky Group.

the locus of rifting migrates away from the cratonic source area probably related to the uplift of the crust in response to buoyancy forces (Wernicke and Axen, 1988), the sediment supply would be restricted to younger basins that open basinward (Leeder, 1995; Ori, 1989), because much of the sediment derived from the craton would be trapped in the older cratonward sub-basins. This sequential migration of the rift axis would result in a facies distribution where immature sediments quickly fill older basins located closer to the source, leaving almost nothing to fill younger basins located toward the center of the rift basin. The younger basins would have anomalously thin rift-related stratigraphic packages containing mature and finer grained lithologic types. If the early rifting stages of the opening of the Iapetus Ocean operated as modern rifting models predict (Hatcher and Goldberg, 1991), then the facies distribution, mode of filling, provenance, and thickness changes described in the Snowbird Group in the easternmost western Blue Ridge are in agreement.

CONCLUSIONS

1) The relationship of the Longarm Quartzite to the nonconformity below is a distal downlap with a clastic provenance located to the northwest, and with an original depositional dip to the southeast.

2) The granitic rocks immediately beneath the Ocoee Supergroup in the eastern part of the western Blue Ridge did not contribute significantly to the sediment budget of the Late Proterozoic rifted margin of Laurentia.

3) A growth fault, active during the accumulation of the Longarm Quartzite, acted as a sedimentary trap. To the northwest subsidence kept pace with accumulation so that this unit accumulated over 1,000 m of arkose in the absence of a deep basin. To the southeast only a thin sequence of pelitic orthoquartzite accumulated, because most clastics were trapped to the northwest.

4) The Thunderhead Sandstone is a retrogradational turbiditic sequence with northwestern provenance.

CHAPTER III
THE GREENBRIER AND HAYESVILLE FAULTS IN WESTERN NORTH CAROLINA

ABSTRACT

The Blue Ridge of western North Carolina records a long history of deformation beginning with Late Proterozoic rifting that was overprinted by early and late Paleozoic deformation events. The oldest period of deformation is Late Proterozoic rifting of the Laurentian continental margin, and the opening of Iapetus. Early Taconic deformation (Penobscottian?) is recorded by the premetamorphic emplacement of the Greenbrier and Hayesville thrust sheets. The Greenbrier fault transported Great Smoky Group rocks northwestward over Snowbird Group and basement rocks. The Hayesville fault carried eastern Blue Ridge assemblages over the Greenbrier thrust sheet, and produced mylonite zones within the Middle Proterozoic basement orthogneiss. This tectonostratigraphic package was metamorphosed to sillimanite grade during the Taconic orogeny. Tight to isoclinal folds and accompanying dominant foliation formed near the metamorphic peak. NNE-trending, steeply SW-dipping faults and related flexural folds folded older structures during the Alleghanian orogeny. Favorably oriented segments of premetamorphic growth and thrust faults were reactivated during this deformation. New detailed geologic mapping reveals that the premetamorphic Greenbrier fault separates the Snowbird from the Great Smoky Group, and the Hayesville fault separates eastern Blue Ridge assemblages from Ocoee Supergroup units and western Blue Ridge basement. The newly mapped trace of the Greenbrier fault suggests that the Great Smoky Group may have been transported northwestward farther than previously thought.

INTRODUCTION

This chapter describes the deformation fabrics observed along the boundary between the eastern and the western Blue Ridge in western North Carolina, and presents a second-generation compiled map that provides new data regarding the premetamorphic emplacement of the Greenbrier and Hayesville thrust sheets, as well the deformation fabrics and metamorphism that overprint these early structures.

Revisions to high quality, first-generation geologic maps made during the 1940s and '50s and more recent ones are necessary as we improve our knowledge of the stratigraphy and geochronology of the rocks mapped at that time. The 1:24,000 geologic map (Plate I, and Fig. 3.1) presents new detailed mapping, and compilation of earlier geologic maps. This new mapping and compilation produced a more complete picture of the geology of this region because early maps (Hadley and Goldsmith, 1963; Edelman, unpublished) focused on resolving the broader structure and stratigraphy of the Ocoee Supergroup and the basement ortho- and paragneiss units. My mapping, in contrast, has focused on resolving the stratigraphy (Chapter II) and internal structure of the Ocoee Supergroup, permitting a better resolution of the traces of major structures. Southward, the compiled map adjoins Quinn's (1991) detailed mapping of parts of the Sylva North and Sylva South quadrangles. The stratigraphic sequence described in Chapter II helped track key stratigraphic levels across isograds and through complex folds. Tectonic truncation of stratigraphic units or gaps in the established stratigraphic hierarchy provided evidence for cryptic faulting in units of the Ocoee Supergroup. The fabric elements described in this chapter are illustrated with photographs, and with sawed samples collected near critical contacts of the Ocoee Supergroup and the ortho- and paragneisses. Computer-based image-enhancing techniques were used to highlight compositional differences and textures.

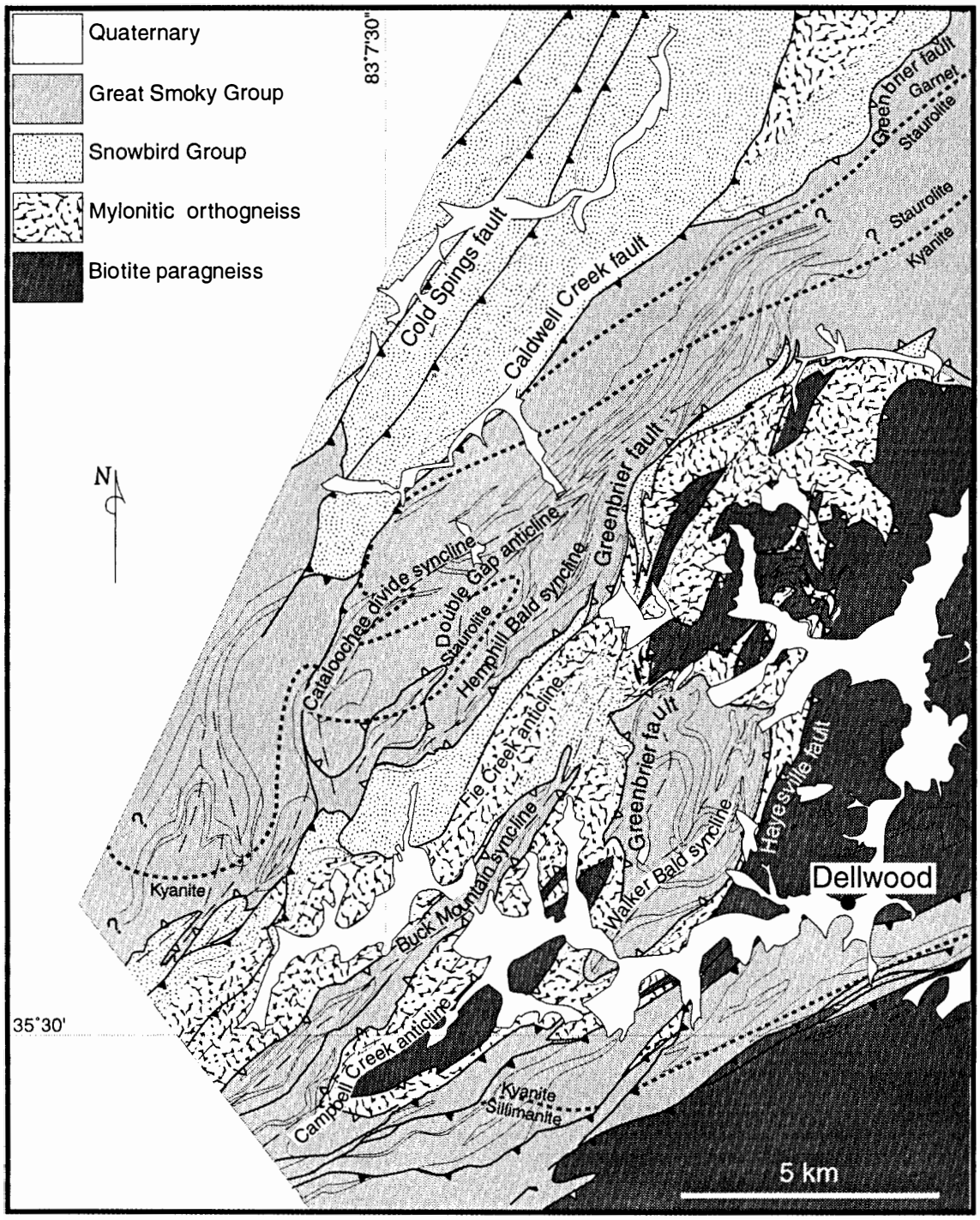

Figure 3.1. Generalized geologic map of the study area. The trace of the Greenbrier fault, as mapped by Hadley and Goldsmith (1963), is reinterpreted in this work as the postmetamorphic Caldwell Creek fault (here defined). This map shows that the Greenbrier fault follows the Snowbird-Great Smoky Group contact (unconformable in Hadley and Goldsmith's map). Filled teeth—postmetamorphic faults; white teeth—premetamorphic faults. Note that the kyanite zone is wider than the staurolite zone, and that the sillimanite isograd is telescoped by postmetamorphic faults.

DEFORMATION FABRICS

The geometry, style, and relative timing of metamorphic and deformation fabrics are described in this section. This description is divided into premetamorphic (D_1), synmetamorphic (D_2), and postmetamorphic (D_3) fabrics, in reference to the early Taconic (Penobscottian?), the Taconic metamorphic peak, and the Alleghanian events respectively. Fabric elements related to these deformation episodes are correlated using corresponding subscripts even though the some boundaries are not clear cut. Crosscutting relationships observed in the field were used to determine the timing of events relative to the metamorphic peak, which in this part of the Appalachians is Ordovician (450 to 480 Ma; Drake et al., 1989, and references therein). Table 3.1 presents the timing, style, and overall orientation of mesoscopic fabric elements in the study area.

Premetamorphic fabrics

Premetamorphic structures (D_1) described here include major faults (the Greenbrier and Hayesville faults), shear zones within the basement, and annealed mylonite fabrics. Most premetamorphic fabric elements are exposed near the Greenbrier and Hayesville faults both in rocks of western- and eastern Blue Ridge affinity. Premetamorphic D_1 fabrics are better exposed in the central region of the area mapped because postmetamorphic folds deformed the Hayesville and Greenbrier faults as well as the kyanite zone, exposing a wide area where those faults (along with their deformation fabrics) are relatively close to the erosion surface.

Premetamorphic faults

Two generations of premetamorphic faults were inferred by studying contrasts in the stratigraphy between this part of western North Carolina and established stratigraphic schemes for the Blue Ridge. A premetamorphic growth fault (Late Proterozoic) was inferred on the basis of compositional, facies, and thickness changes

Table 3.1. Relative timing of deformation of central-western North Carolina and possible regional correlation with regional tectonic events. G = generation; O = orientation.

EVENT		FOLDING			PLANAR FABRICS			LINEAR FABRICS			Faults and fault rocks	Intrusions
G	**Tectonic Setting**	**G**	**Style**	**O**	**G**	**Style**	**O**	**G**	**Style**	**O**		
	Relaxation and cooling after Alleghanian O.											Trondhjemite and pegmatite dikes
D_3	Alleghanian orogeny	F_3	Similar, tight folds and crenulations	NE-trending NW-verging	S_3	Poorly developed crenulation cleavage	15° 70E	L_3	Weak crenulation lineation		Cold Springs, and other reactivated faults. Retrograde mylonites	
D_2	Taconic prograde metamorphic peak	F_2	Isoclinal, intrafolial, and passive flow	NE-trending gently plunging	S_2	Principal foliation, local axial-planar cleavage	Parallel to bedding	L_1	Mineral lineation		Hayesville fault Mylonites.	Pegmatite dikes
D_1	Early Taconic orogeny	?			?						Greenbrier fault	
	Breakup of Gondwana, drift of Laurentia	F_0	Soft-sediment folding		S_0	Bedding in the Ocoee Supergroup and Tallulah Falls Fm.					Growth faults	
	Grenville orogeny											French Broad massif plutons

in the sandstones of the Snowbird Group within the footwall of Greenbrier fault (Chapter II). Paleozoic premetamorphic thrust faults mapped in this part of North Carolina include the Greenbrier and Hayesville faults, and shear zones within the basement orthogneisses.

Greenbrier fault

The trace of the premetamorphic Greenbrier fault was inferred on the basis of stratigraphic truncations of Ocoee Supergroup units, and gaps or repetitions in the stratigraphic sequence described in Chapter II. In contrast to Hadley and Goldsmith's (1963) map of the Dellwood quadrangle, my mapping shows that the Snowbird-Great Smoky Group contact (formerly mapped conformable) is the Greenbrier fault (Fig. 3.1).

The premetamorphic age of the Greenbrier fault is indicated by undisturbed foliation close to the fault despite map-scale truncation of rock units (Plate I). Overprinted isograds could not be used as evidence for a premetamorphic age of this fault because the Greenbrier fault separates rock types (e.g. Longarm Quartzite) unlikely to develop metamorphic assemblages that are useful for mapping isograds. Milton (1983), using garnet-biotite geothermometry confirmed King's et al., (1958) overprinted isograds mapped across Greenbrier fault northwest of the study area.

The trace of Greenbrier fault had not been previously identified in this part of the Blue Ridge because early maps did not separate the units of the Snowbird and Great Smoky Groups, and therefore the stratigraphic truncations could not be recognized. Such truncations are particularly clear on the southeastern flank of Cataloochee Divide near Cove Creek, where the top of the Thunderhead Sandstone (facing southeast) is in contact with the Longarm Quartzite to the east (Plate I). Southward along the southeastern flank of the Cataloochee Divide, the same belt of Longarm Quartzite is progressively in contact with older units: the base of the Thunderhead Sandstone near Hemphill Bald, and the upper part of the Elkmont Sandstone in the

Ivy Hill region. This portion of the Greenbrier thrust sheet is overturned in the southeastern flank of the Cataloochee Divide syncline (Plate II). South of the Ivy Hill region the postmetamorphic Caldwell Creek fault cuts the Greenbrier fault, which then continues south along the top of the Longarm Quartzite. To the east, between Moody Top and the Potato Patch, the upper part of the Elkmont Sandstone rests on top of the Longarm Quartzite and the Roaring Fork Sandstone. These two units, however, disappear in a short distance underneath the Elkmont Sandstone, suggesting this contact is faulted. Further southeast, the upper part of the Elkmont Sandstone lies atop a thin Longarm Quartzite section and in turn basement orthogneiss. Between Little Bald Knob and Whim Knob, along Cataloochee Divide, a splay of the Greenbrier fault duplicates the upper part of the Elkmont Sandstone.

Hayesville fault and shear zones

The transition from cover to basement in this part of the Blue Ridge is marked by a clear change in the structural style from discrete thrust faults which follow weak stratigraphic horizons in the cover sequences (Greenbrier fault along the Ocoee Supergroup), to wider shear zones characterized by mylonitic grain-size reduction in the granodioritic rocks of the French Broad massif basement towards the biotite paragneiss (Tallulah Falls Formation?). The trace of the Hayesville fault was located where a contrast occurs between granodioritic orthogneisses and the biotite-hornblende paragneisses (Tallulah Falls Formation?) in the maps by Hadley and Goldsmith, (1963), Quinn, (1991), and Edelman (unpublished).

As with the Greenbrier fault, overprinted isograds could not be used as primary criterion to constrain the premetamorphic character of Hayesville fault. In this case, however, it was because in the study area this fault lies entirely within the kyanite zone. Annealed mylonitic fabrics along its trace, undisturbed foliation near it, and complex folding (F_2 and F_3) of this contact in the valley of Hemphill Creek seem to confirm a premetamorphic age for this structure. On the other hand, the fabric elements developed along the trace of this structure (mylonites and L-tectonites)

are coaxial and coplanar with the principal foliation and may have developed slightly before the metamorphic peak, and before F_2 (synmetamorphic) folding took place.

Mylonitic grain-size reduction is the main criterion to recognize the Hayesville fault in the area mapped. My mapping in rocks of the French Broad Massif (orthogneiss, Bartholomew and Lewis, 1984) shows that grain size commonly decreases toward the contact with the biotite paragneiss (Hayesville fault in Hemphill Creek valley) or the Ocoee Supergroup. Coarse-grained, often banded megacrystic granodioritic orthogneiss is commonly found away from either the Ocoee Supergroup or the biotite paragneiss; fine-grained mylonitic orthogneiss, on the other hand, forms a belt near the contacts with those units. Transitional textures from the coarse-grained granodioritic orthogneiss, to the mylonitic fine-grained varieties are described next along with the deformation fabrics found along the trace of Hayesville fault.

The southernmost tip of the French Broad massif (Rankin et al., 1989) consists of Middle Proterozoic plutonic rocks in the core of the Ravens Ford anticline, the Bryson City and Ela domes, and in the area mapped. Rankin et al. (1973) grouped these similar orthogneisses and plutonic rocks in the French Broad massif, and proposed that these meta-aluminous plutonic rocks of batholitic dimensions originated at the time of consolidation of continental crust during the Grenville orogeny. Plutonic rocks of the French Broad massif record the effects of pervasive shearing and metamorphism that increase in intensity from northwest to southeast. Metamorphic minerals in these rocks include muscovite, biotite, epidote, and sphene at high metamorphic grade (Rankin et al., 1989) in the vicinity of the study area. Shearing in the plutonic rocks of the French Broad massif produced mylonitic gneiss of different grain size, with feldspar augen derived from originally porphyritic granite. Biotite schist, and other fine-grained rocks, occasionally found interlayered in the orthogneiss, may represent progressively recrystallized phyllonite (Rankin et al., 1989), or other low-temperature, ground down, fault-related rock. An alternative explanation (Bartholomew and Lewis, 1984) is that the schist layers are relicts of country rocks of unknown affinity.

As pointed out by Rankin et al. (1989), the plutonic rocks of the western Blue Ridge can be classified based on the degree of grain-size reduction related to premetamorphic deformation and mylonitization. In the area mapped, Hadley and Goldsmith (1963) recognized three varieties of orthogneiss with slightly different composition and remarkably different textures. From fine- to coarse-grained they are: flaser, augen, and granitoid gneisses. The flaser and augen gneisses are grouped here in a unit called mylonitic augen orthogneiss because they cannot be separated at map scale. The granitoid gneiss (here called granodioritic orthogneiss), was separated at map scale based on its distinctive coarser texture, and poorly developed and discontinuous foliation surfaces. A finer-grained rock type, the mylonitic orthogneiss, is a fine-grained (1 to 3 mm), or finely laminated (1 to 2 mm), biotite-quartz-feldspar gneiss with discontinuous foliation surfaces, an occasionally well-developed linear fabric that lacks coarse banding or large crystals (Fig. 3.2a). The contacts between the different orthogneiss units are gradational, and are commonly intermingled.

The mylonitic augen orthogneiss is a medium-grained gray biotite-quartz-feldspar gneiss of lenticular shaped, 1-6 mm wide, several centimeters long quartz-biotite, and quartz-feldspar folia as well as prominent (up to 5 cm) K-feldspar augen porphyroclasts (Fig. 3.2b); the mylonitic augen orthogneiss and mylonitic orthogneiss have the composition of a granodiorite (Hadley and Goldsmith, 1963). The granodioritic orthogneiss (Fig. 3.2c) is a weakly foliated variety of medium-grained orthogneiss with the composition of quartz-monzonite to granite. This gneiss consists of microcline, quartz, and oligoclase with minor amounts of biotite and muscovite (Hadley and Goldsmith, 1963).

Outcrops of the fine-grained mylonitic orthogneiss commonly define a 100 m or less belt that is well developed along the western flank of the Fie Creek anticline; this fine-grained unit is absent in parts of the Campbell Creek anticline where the granodioritic orthogneiss is in contact with biotite paragneiss (below) and Ocoee

Figure 3.2. Grain-size variation in the orthogneiss.
(a) Granodioritic mylonitic orthogneiss. Note the uniformity in grain size. This rock type has a weakly defined foliation surface and linear fabrics are more frequent. Located approximately 600 m west of Purchase Knob.
(b) Mylonitic augen orthogneiss of quartz-diorite composition. Located approximately 1 km northeast of Olivet Church in Maggie Valley.
(c) Granodioritic orthogneiss. A discontinuous compositional banding is folded by crenulations. Located approximately 1 km north of Moody Top.

(a)

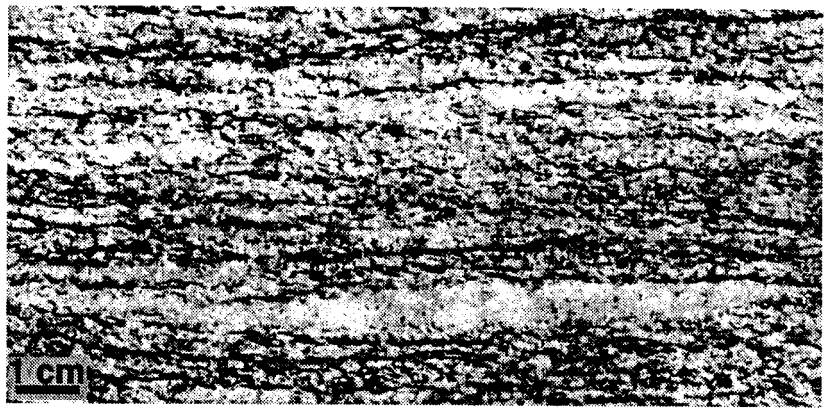

(b)

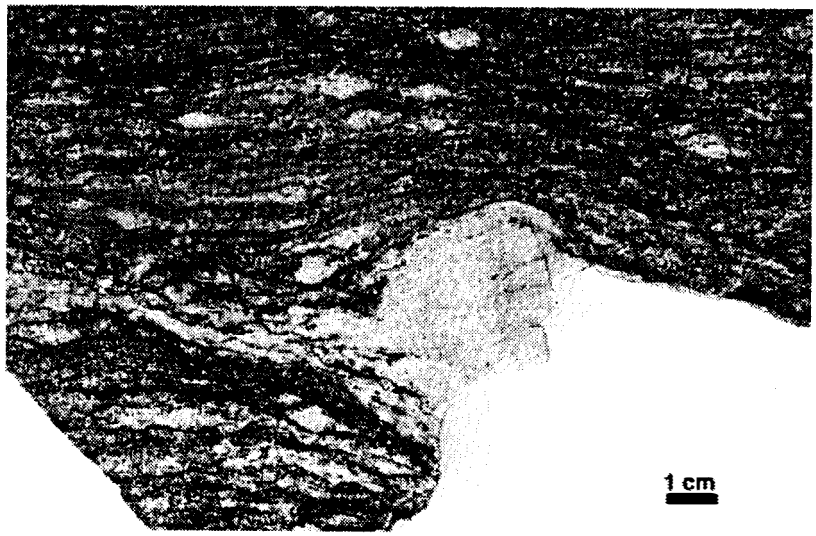

(c)

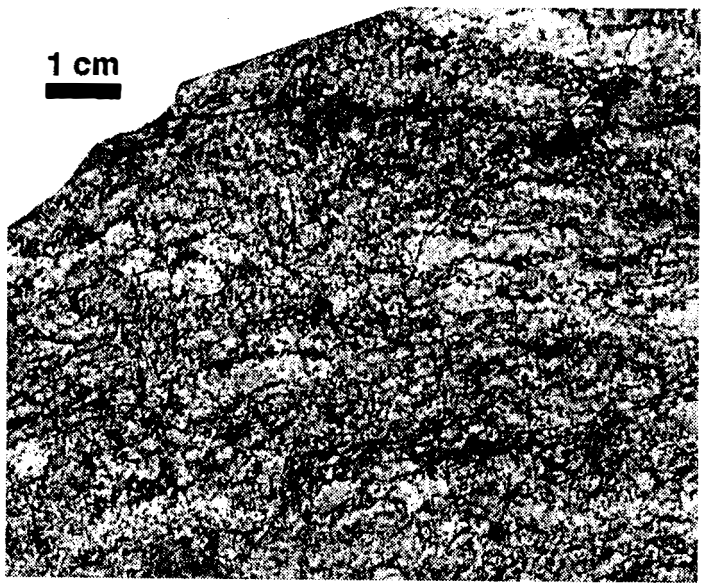

Supergroup (above). This belt is also well developed southwest of Purchase Knob along the contact between the orthogneiss and hornblende-biotite paragneiss. The mylonitic augen orthogneiss is commonly in contact either with the Ocoee Supergroup or the biotite paragneiss elsewhere. Microscopic examination of the rocks along this belt of fine-grained mylonite reveals that the fabric has been annealed.

The folded contact between the orthogneiss (footwall) and the biotite paragneiss (hanging wall) around Ned Branch, south of Purchase Knob is marked by a zone of annealed (Fig. 3.3c) medium-grained, mylonitic augen gneiss (Fig. 3.3a) and finely layered mylonitic gneiss (Fig. 3.3b). This zone of augen mylonitic gneiss is found along this contact in the valley of Hemphill Creek. Mylonite is also found along this contact west of Purchase Knob where hornblende-biotite gneiss (in the hanging wall) is separated by an L-tectonite from fine-grained mylonitic and mylonitic augen orthogneiss (in the footwall) where annealed elongated quartz rods define the lineation (Fig. 3.4). The contact between biotite paragneiss (below) and mylonitic augen orthogneiss (above) is exposed also in the core of the Campbell Creek anticline, but the mylonitic augen gneiss is missing, and mylonitic augen orthogneiss rests atop biotite paragneiss.

Synmetamorphic fabrics

The Ocoee Supergroup was subjected to a progressive, Barrovian type regional metamorphism increasing through a medium-pressure facies series from chlorite grade to the northwest in eastern Tennessee (Fig. 3.5), to sillimanite grade (Carpenter, 1970) and granulite facies to the southeast in western North Carolina (Force, 1976; Absher and McSween, 1985; Eckert et al., 1989). Chlorite is only locally found as a retrograde mineral along postmetamorphic fault zones where metamorphic minerals such as garnet were crushed. An Ordovician age for the prograde metamorphism is constrained by geochronology and also by clastic wedges in the Valley and Ridge foreland deposits (Drake et al., 1989; Miller et al., in press). Synmetamorphic folds (F_2) and transposition of original bedding to parallel foliation surfaces (S_2) took

Figure 3.3. Annealed mylonites along Hayesville fault.
(a) Finely laminated biotite-hornblende mylonitic paragneiss. Located along Ned Branch, approximately 1 km south of Purchase Knob.
(b) Mylonitic augen gneiss along Hayesville fault. Located along Ned Branch, approximately 700 m south of Purchase Knob.
(c) Feldspar porphyroclast with annealed quartz tail in a mylonitic augen gneiss along Hayesville fault. Crossed nicols, the long edge of the photo is 2 mm. same location as above

(a)

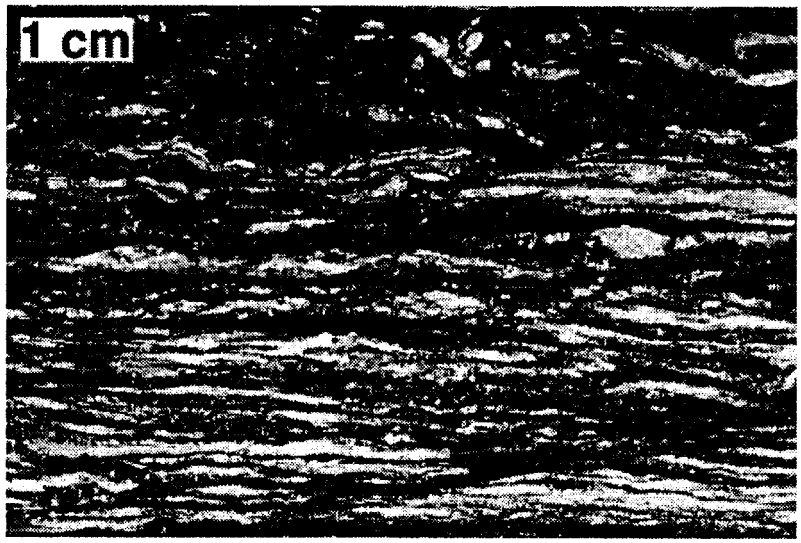

(b)

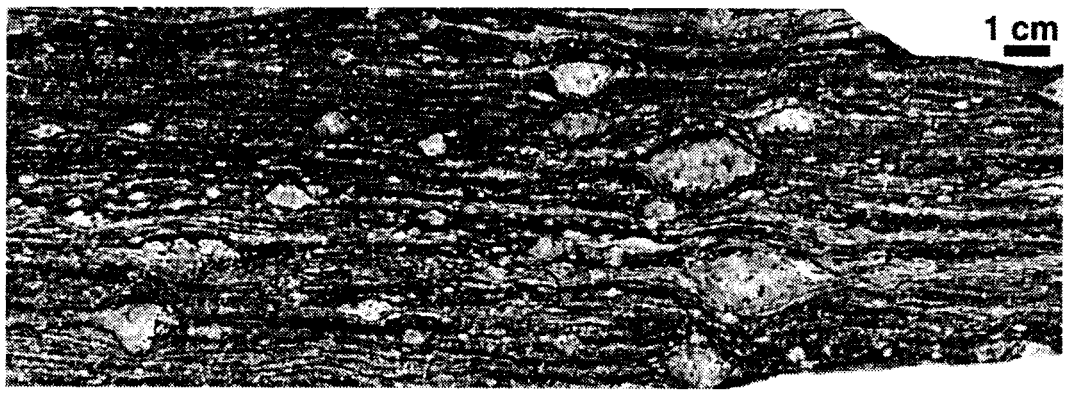

(c)

Figure 3.4. Annealed L-tectonite fabrics.
(a) L-tectonite in an originally felsic gneiss; elongated quartz rods define the linear fabric in this rock. The trend of the mineral lineation in this sample is 199, 55°. Located 2 km east of Double Gap.
(b) Microscopic fabric of the annealed quartz rods from the same sample. Crossed nicols, the long edge of the photo is 4 mm.
(c) Rose diagram of trends of mineral lineation.
(d) Contoured lower-hemisphere equal-area plot of mineral lineation data in the mapped area.
(e) Lower-hemisphere equal-area plot of mineral lineation in the area mapped.

(a)

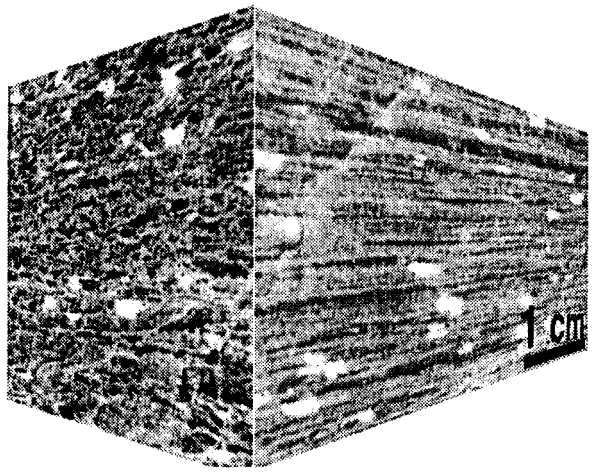

(b)

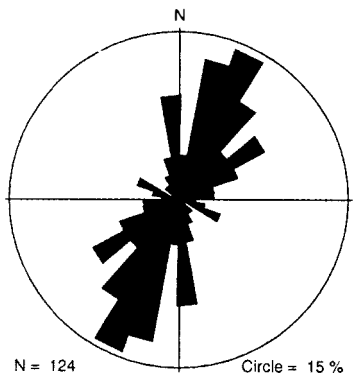

(c)

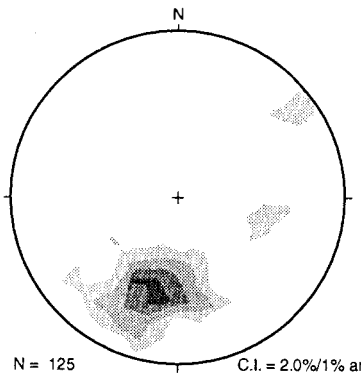

(d)

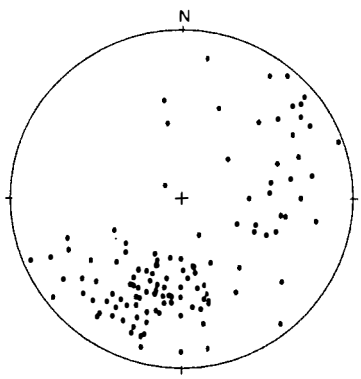

(e)

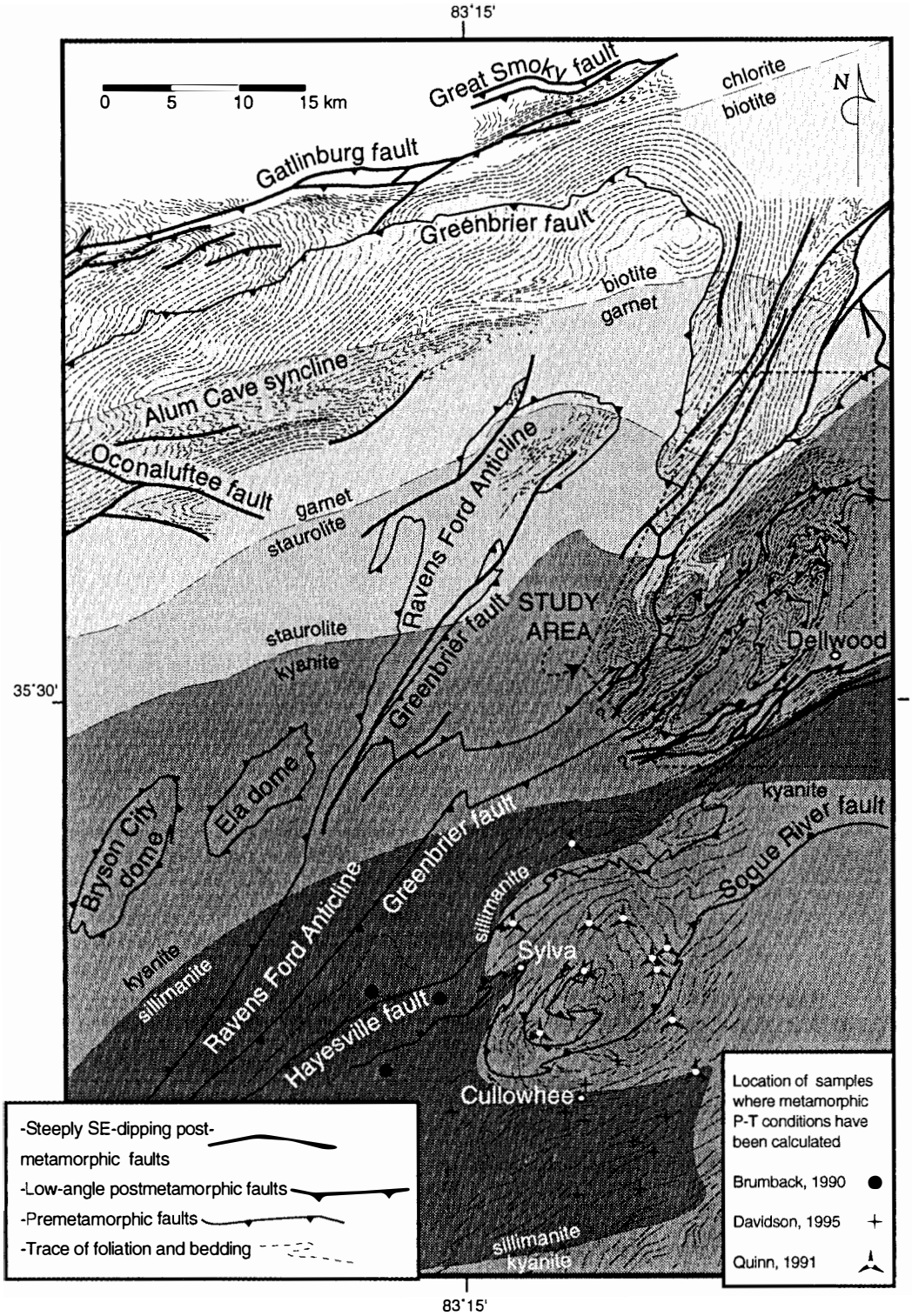

Figure 3.5. Map of the Great Smoky Mountains in East Tennessee and western North Carolina. Shades of gray represent metamorphic zones; note the changes in width of the metamorphic zones. Compiled from Plate 3 in Hadley and Goldsmith (1963), Quinn (1991), Davidson (1995), and this study.

place during metamorphism.

Metamorphic textures

Ocoee Supergroup pelites in the area mapped developed metamorphic index minerals of the garnet, staurolite, kyanite, and sillimanite zones. The Wading Branch Formation, pelitic intercalations of the Roaring Fork Sandstone, the top half of the Elkmont Sandstone, and pelitic intercalations in the Thunderhead Sandstone were useful in tracing metamorphic isograds in the area mapped (Plate I and Fig. 3.1). Feldspathic sandstone, and quartzite, on the other hand, do not contain critical metamorphic assemblages, and at kyanite grade preserve fine sedimentary structures such as lamination.

Primary structures (bedding, graded beds, lamination) and foliation in the Ocoee Supergroup are essentially parallel. With few exceptions (Fig. 3.6) both in the field

Figure 3.6. Relationship between bedding and foliation.
Photomicrograph of a siltstone-schist intercalation in the Elkmont Sandstone showing the transposition of a bedding surface composed of silt-size quartz and feldspar grains (parallel to the long edge of the photo) by the recrystallization of micas along foliation planes (nearly perpendicular to the long edge of the photo). This relationship could only be observed in the northwestern corner of the area mapped where metamorphic grade is staurolite. Located between the Cove Creek Gap and Hazel Top. Crossed nicols, long edge of photomicrograph is 2 mm.

and under the microscope schistosity (defined by aligned biotite and muscovite flakes) is parallel to bedding. The parallelism everywhere between foliation and bedding suggests that all surfaces were rotated to near parallel surfaces by shearing during transposition. The role of shearing in the development of foliation is demonstrated by the parallelism between the foliation and axial surfaces of isoclinal and tight and folds. Preservation of nearly intact stratigraphic sequences, including a finning upward turbiditic sequence in the Thunderhead Sandstone at kyanite and staurolite grade, indicates that shearing took place locally parallel to original bedding surfaces.

Metamorphic minerals such as kyanite and staurolite are parallel to the foliation but the long axes do not define a lineation (Fig. 3.7). Garnets do not show pressure shadows indicating rotation (Fig. 3.8) nor there is any direct evidence of shearing along bedding planes at the time of growth of garnets. Some garnets display cores with abundant inclusions, and rims without inclusions. Further south kyanite was found included in garnet (Quinn, 1991), indicating that garnet growth continued after the metamorphic peak.

Ocoee Supergroup

Metamorphic isograds were traced in the field by mapping the first appearance of index minerals in pelites of the Ocoee Supergroup. With increasing metamorphic grade from northwest (garnet grade) to southeast (sillimanite grade), the appearance of the pelitic upper part of the Elkmont Sandstone exhibits important variations (3.9b) used to trace isograds. Modal analyses of thin sections (Appendix A) of this unit indicate that about 50 to 55 percent of this rock is made up of pelitic minerals, and 45 to 50 percent corresponds to silt-size quartz and feldspar (Fig. 3.9a).

Rocks of the garnet zone occupy the northwestern corner of the study area. The mineral assemblages, however, are only developed in pelites of the Elkmont Sandstone, and the Roaring Fork Sandstone. At garnet grade, the Elkmont Sandstone

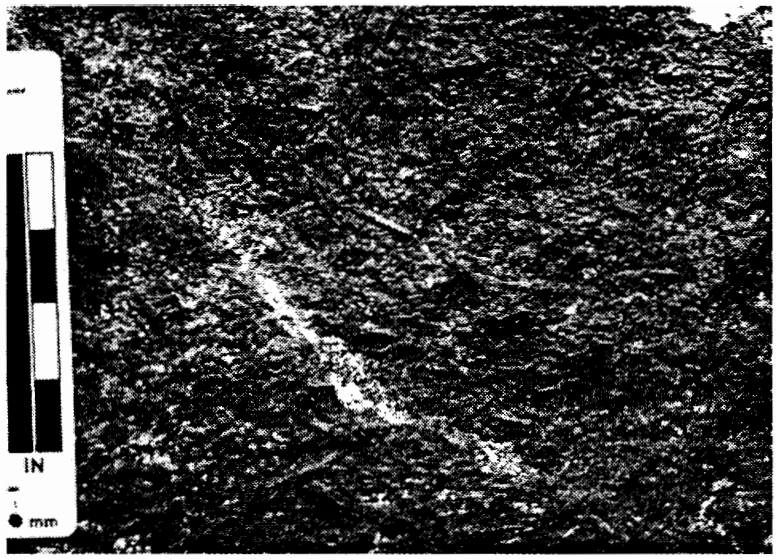

(a)

(b)

Figure 3.7. Alignment of metamorphic minerals parallel to foliation.
(a) Bed surface in the Elkmont Sandstone showing 2-3 cm long kyanite crystals. Located approximately 500 m north of the Eaglenest Ridge in the headwaters of the eastern branch of Tree Cove Creek.
(b) Staurolite schist in Elkmont Sandstone with 1-2 cm long dark staurolite crystals. Penetrating cross twins in staurolite (known as "fairy stone" in North Carolina, Hurlbut, 1971) are common in this rock type. Located approximately 500 m north of Hemphill Bald.

Figure 3.8. Textures of garnet porphyroclasts in the study area.
(a) Garnet porphyroblast in a pelitic bed of the Thunderhead Sandstone. Located approximately 600 m NE of North Eaglenest Mountain. Plane light, long edge of photomicrograph is 4 mm.
(b) Garnet porphyroblast in the Thunderhead Sandstone. Located approximately 2,800 m west of North Eaglenest Mountain. Plane light, long edge of photomicrograph is 4 mm.
(c) Garnet porphyroblast in Elkmont Sandstone. Located approximately 500 m southeast of Moody Top. Plane light, long edge of photomicrograph is 10 mm.
(d) Fragmented garnet porphyroclast from a retrograde mylonite zone. Located along Gaddis Branch approximately 1 km northeast of North Eaglenest Mountain. Plane light, long edge of photomicrograph is 4 mm.

(a)

(b)

(c)

(d)

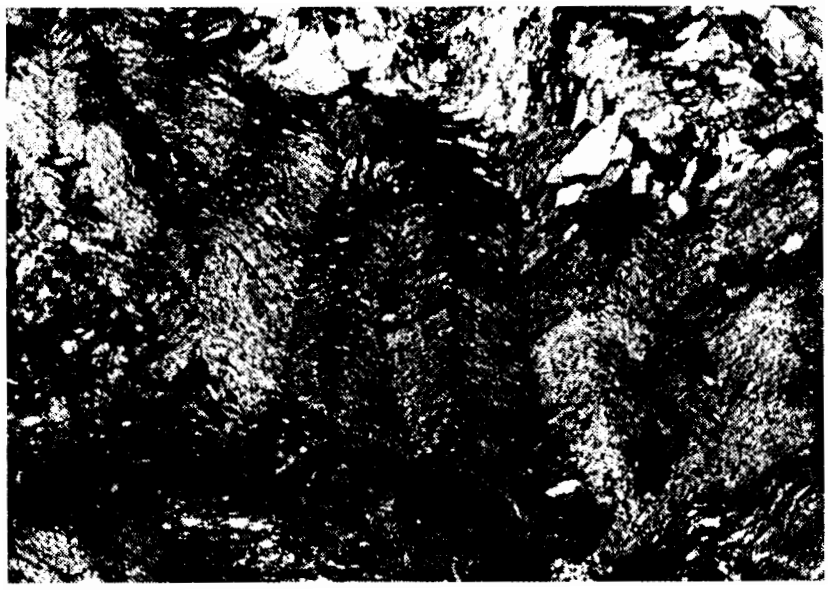

(a)

(b)

Figure 3.9. Metamorphic textures in the Ocoee Supergroup.
(a) Pelitic-rich facies of the Elkmont Sandstone; the size of the quartz-feldspar grains is 0,2 mm; kinked micas defining foliation are mostly muscovite and biotite; kinks are related to D3 deformation. Crossed nicols; the long edge of the photo is 4 mm. Located between Cove Creek Gap and Hazel Top.
(b) Garnet-kyanite schist in the Elkmont Sandstone. G: garnet, M: muscovite, B: biotite, K: kyanite, Qz: quartz. Plane light. The long edge of the photo is 10 mm. Located 500 m SE of Moody Top.

is a dark, massive, garnet-biotite metasiltstone, and dark metasandstone. The only metamorphic minerals visible in hand specimen are small biotite specks and occasional garnets. The typical mineral assemblage in these pelites is biotite, muscovite, quartz, and almandine.

The staurolite isograd is easily mapped in Elkmont Sandstone pelites along the northwestern flank of the Cataloochee Divide syncline, because the first appearance of staurolite is striking with large (up to 5 cm) prismatic staurolite porphyroblasts in a matrix of muscovite, biotite, and garnet. Pelites at this grade are mostly dark gray phyllite to schist where almandine garnets (up to 3 mm) and staurolite crystals often interrupt the foliation surfaces defined by very fine-grained muscovite and biotite. The quartz-feldspar fraction of this rock segregates and recrystallizes into laminae less than 1 mm thick.

The kyanite isograd, folded near the south end of the Cataloochee Divide syncline, Double Gap anticline, and the Hemphill Bald syncline (Fig. 3.1), defines the northwestern boundary of a wide kyanite zone that comprises most of the area mapped. Kyanite commonly coexists with staurolite at the boundary with the staurolite zone. The mineral assemblage in this zone is muscovite, biotite, garnet, kyanite, staurolite, and quartz. The Elkmont Sandstone at kyanite grade contains coarse-grained muscovite and biotite defining foliation surfaces spotted by garnet (up to 3 mm) and kyanite (up to 5 cm) crystals in the more pelitic layers; quartz has segregated into coarser laminae (up to 1 cm thick) paralleling original bedding. The coarse new metamorphic minerals such as kyanite and staurolite (Fig. 3.7), and the segregation of quartz into increasingly thicker laminae, gives the rock the appearance of a coarse-grained metasandstone. Pegmatite bodies concordant with the local foliation further modify the appearance of the rock (Fig. 3.10). The reason for a wide kyanite isograd in the area mapped seems to be first-order postmetamorphic folding in the region from the Cataloochee syncline to the Walker Bald syncline. Postmetamorphic deformation southeast of the Walker Bald syncline was accommodated by a WSW-ENE trending belt of postmetamorphic faults that follow

the northern flank of Eaglenest Mountain Ridge. Along this belt, the sillimanite isograd is telescoped by postmetamorphic faults. Whether or not the sillimanite isograd is telescoped outside the area mapped is unknown because the extent of this belt of faults to the NE and SW of the area mapped has not been mapped.

Textural changes due to metamorphism in pelitic turbidites of the Thunderhead Sandstone are not as marked as the progressive changes in the Elkmont Sandstone pelites because of the lower silica content in the Thunderhead Sandstone pelitic beds. Pelitic facies of the Thunderhead Sandstone contain as much as 88 percent of pelitic minerals, but in general the proportions are 60 percent or more of micas, and under 40 percent of sand-size and silt-size quartz and feldspar (Appendix A). Pelitic beds in the turbidites at kyanite grade are coarse-grained muscovite-biotite schist with small garnets; kyanite crystals rarely exceed 5 mm.

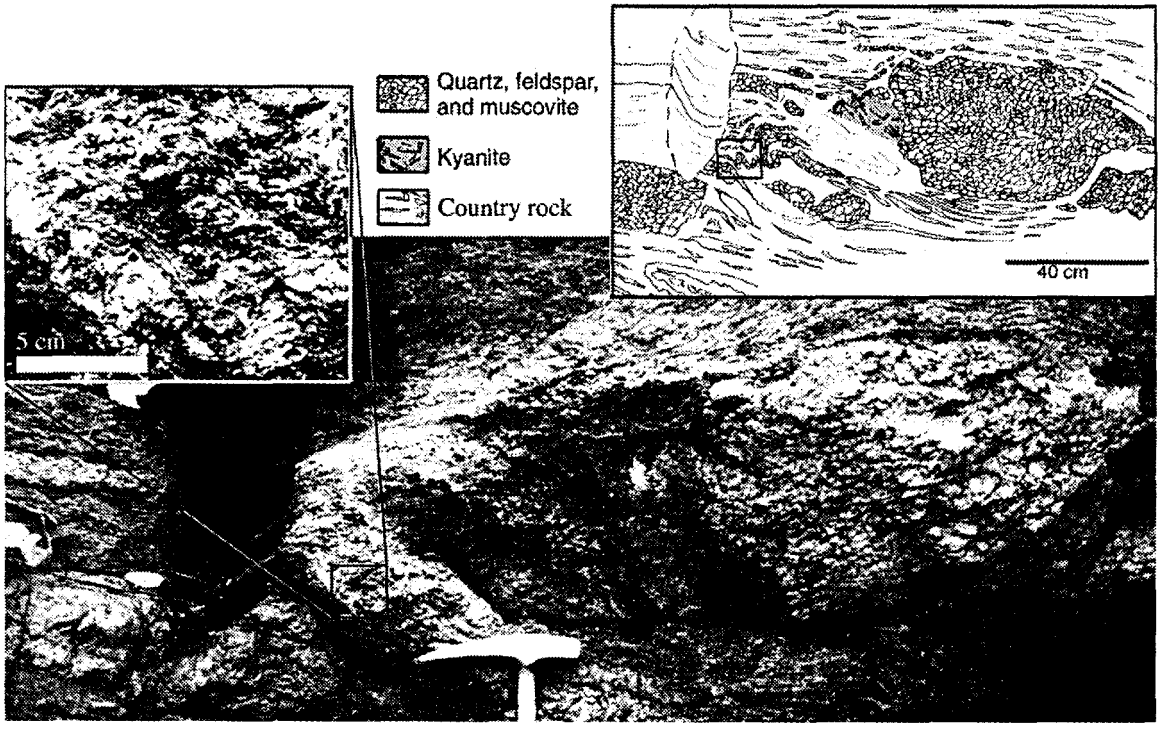

Figure 3.10. Pegmatite in the Thunderhead Sandstone and metagraywacke of the Great Smoky Group at kyanite grade. The sketch in the upper right corner of the diagram shows the foliation surfaces in the metagraywacke and the shape of the deformed pegmatite; the box in the sketch marks the location of the enlarged photo in the upper left corner of the diagram.

Tallulah Falls Formation (?)

Immediately southeast of the study area the garnet + andesine + hornblende assemblage in amphibolites interlayered with the Tallulah Falls Formation indicate amphibolite facies of metamorphism (Quinn, 1991). The northward projection of the Tallulah Falls Formation (Quinn, 1991) into the study area was described by Hadley and Goldsmith (1963) as a biotite paragneiss (they correlated it with the Carolina Gneiss) made up of an assemblage of layered and banded micaceous and hornblende gneiss, mica schist, and amphibolite. It was divided lithologically into micaceous gneiss and hornblende rocks. The micaceous gneisses are made up of biotite gneiss, two-mica gneiss, and mica-quartz-feldspar gneiss. The biotite paragneisses, however, can be found in two different tectonostratigraphic positions: above the granodioritic orthogneisses (Hemphill Creek valley), and below them (Campbell Creek anticline). Neither this work nor previous workers could find criteria to separate these rocks into two different units.

According to Hadley and Goldsmith (1963), the biotite gneiss is interlayered with hornblende gneiss and is composed of quartz, plagioclase (mostly andesine), and olive-colored biotite. The associated two-mica gneiss and schist are composed of subequal amounts of quartz, calcic oligoclase, and reddish biotite, with minor muscovite. The mica-quartz-feldspar gneiss occurs interlayered with the two-mica gneiss, and contains quartz, plagioclase (oligoclase to andesine), K-feldspar, and reddish biotite. The hornblende-bearing rocks consist of hornblende-biotite gneiss, calcsilicate granofels, and amphibolite. The hornblende-biotite gneiss contains plagioclase (andesine), biotite, hornblende, and quartz; the mafic components range from 25-50 percent. The calcsilicate granofels is composed mostly of calcic plagioclase, epidote, hornblende, biotite, and sphene. Amphibolites of uneven grain size, bearing plagioclase (mostly andesine), and quartz are intercalated as bodies of different sizes with both the micaceous and hornblende rocks. Ultramafic rocks described elsewhere in the eastern Blue Ridge south of the study area were not seen

in the area mapped; neither they are reported in Larrabee (1966), nor North Carolina Geological Survey (1985). Ultramafic rocks are mostly dunite and harzburgite with talc, vermiculite, and chlorite + actinolite + talc schist (Quinn, 1991).

P-T conditions

Geothermometric and geobarometric studies have been carried out in rocks of eastern Blue Ridge affinity near Sylva, North Carolina; no P-T estimates, however, have been published for rocks within the area mapped. The location of samples where P-T conditions have been obtained near Sylva is compiled on Fig. 3.5 (Brumback, 1990; Quinn, 1991; and Davidson, 1995). Other studies (Absher and McSween, 1985; Kittleson, 1988; Eckert et al., 1989; Miller et al., in press) carried out further south along the strike near Franklin, North Carolina are also mentioned.

Even though most P-T estimates have been made for eastern Blue Ridge affinity rocks (Fig. 3.11), Quinn (1991) also determined P-T conditions for sillimanite grade rocks of the Great Smoky Group in the footwall of Hayesville fault. Rocks of the Great Smoky Group and the Otto Formation record P-T conditions of 550-650° C and 5.0-6.5 kb during peak metamorphism. P-T conditions calculated for the eastern Blue Ridge affinity rocks (Tallulah Falls Formation) are higher: 675-750° C, and 8.5-9.5 kb. Thermobarometric determinations in pelites of the Otto Formation by Davidson (1995) also indicate that P-T conditions for this unit are lower (530 ± 20° C, and 4 ± 1 kb) than in the pelites of the Tallulah Falls Formation in the Soque River thrust sheet (750 ± 20° C, and 7.3 ± 1 kb). A temperature estimate obtained in the footwall of Hayesville fault using mineral exchange equilibria equations (580° C, Brumback, 1990) is similar to P-T estimates obtained in the hanging wall in the Tallulah Falls Formation (500-650° C, and 5.4 kb). Other mineral exchange equilibria estimates by Brumback (1990) indicate that pressures and temperatures were in the range of 550-600° C and 5.5 kbar in the amphibolite facies, and 670-800° C and 6.5-7.5 kbar in the granulite facies.

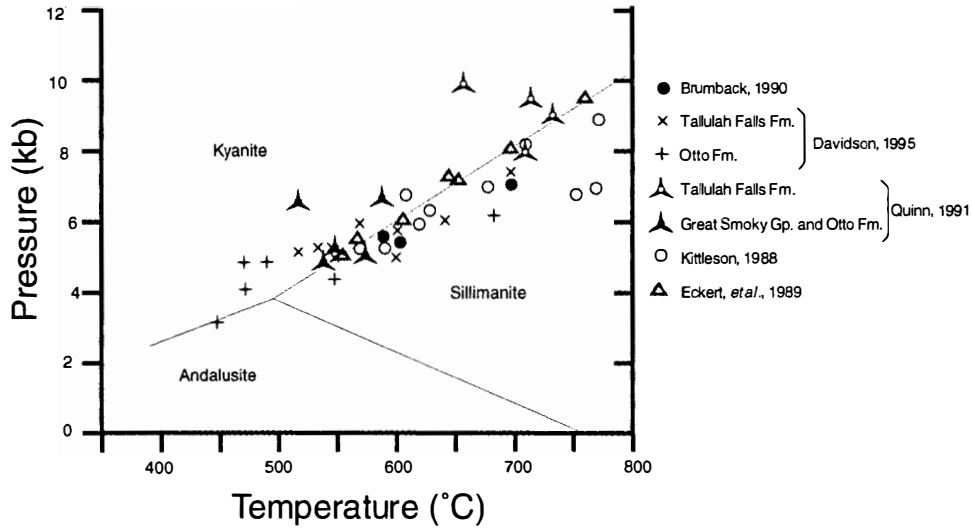

Figure 3.11. P-T metamorphic conditions. Compilation of calculated metamorphic conditions south and southwest of the study area mostly in eastern Blue Ridge assemblages. Samples collected closest to the study area are located in Figure 3.5.

South of the study area, southwest of Franklin, North Carolina, the high-grade Taconic metamorphic core for the southern Appalachians was defined by Force (1976), Hatcher and Butler (1979), and Absher and McSween (1985). Metamorphic assemblages and cation exchange geothermometry-geobarometry in these rocks record a prograde metamorphic event (T = 750-775° C, P = 6.5 - 7.0 kb), followed by isobaric cooling after metamorphic peak conditions. Granulite-facies metamorphic rocks (Eckert et al., 1989) found west of Franklin, North Carolina, record P-T conditions of 585° C, 5.5 kb at the kyanite-sillimanite isograd to 842° C, 9.8 kb in the hornblende-granulite facies in a continuous progression across Hayesville fault. Recent ion probe dating (Miller et al., in press) of these high-grade assemblages yield Taconic ages (495 Ma, U-Pb) for the metamorphic peak.

F_2 Folds

Isoclinal and ptygmatic, disharmonic folds, and tight to isoclinal, flexural-flow folds are commonly found in the study area. These folds are deformed by late F_3 folds and crenulations, and do not fold the dominant foliation. F_2 folds are most commonly found in the southeastern half of the area mapped, east of the eastern flank of the

Cataloochee Divide; in this region tight- to- isoclinal folds are common in the turbidites of the Thunderhead Sandstone (Figs. 3.12, 3.13, and 3.14) between Moody Top and Middle Top north of Maggie Valley, but nearly absent northwest of Cataloochee Divide. These folds are tight to isoclinal cylindrical, plane, flexural-flow folds with thickening of the hinges, and axial surfaces oriented parallel to the foliation.

Noncylindrical, nonplane, ptygmatic disharmonic folds (Figs. 3.15 and 3.16), often isoclinal, are found in 10-cm thick compositional banding in biotite hornblende gneiss north of Hemphill Creek, and east of Purchase Knob. F_2 folds more often verge N and NW; the orientation of axes and axial surfaces, however, has been modified by postmetamorphic folding. In two locations it was possible to determine that isoclinal fold axial surfaces are approximately parallel to the trace of the Greenbrier fault, and to foliation. Facing directions in the graded conglomerate-sandstone beds of the Thunderhead Sandstone were used to map the folded isoclinal folds (Plates I, and II). NNE verging sheath folds (Fig. 3.17) were also observed in the area mapped and may be the expression of larger scale sheath folds (Plate II, section D-D').

Postmetamorphic fabrics

Intrusions

Near horizontal, and gently dipping unfilled joints (Fig. 3.18) cut all the rock types in the area mapped, except the late pegmatite and trondhjemite bodies. A few trondhjemite dikes were observed in the north side of Eaglenest Ridge cutting sillimanite grade Great Smoky Group rocks. The dikes are approximately 2 m-thick tabular bodies, striking E-W, and dipping steeply south; not enough dikes were measured, however, to statistically represent their orientation. The most prominent feature of these bodies is that they are undeformed. Pegmatite bodies are more widespread, and in contrast with the trondhjemite dikes, the pegmatites are both undeformed, cutting postmetamorphic retrograde mylonitic rocks (Fig 3.18c), and

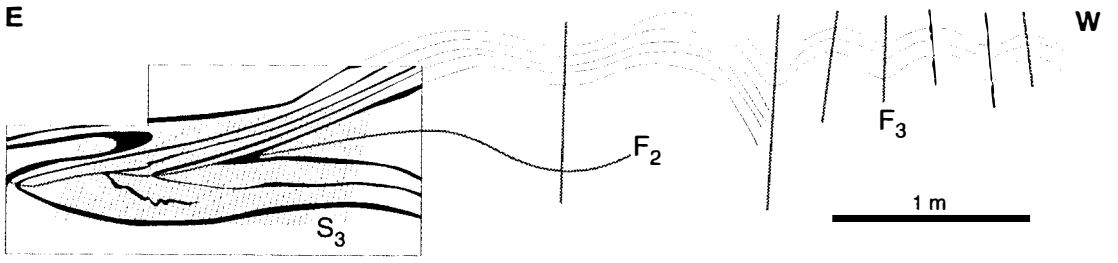

Figure 3.12. Polydeformed sandstone-schist intercalation in Thunderhead Sandstone. Photo of an F_2 isoclinal fold deformed by second-order, F_3 open folds (in the sketch), and third order crenulations (S_3 in the enlarged box). Located near Leatherwood Top.

Figure 3.13. Isoclinal F_2 folding in the Great Smoky Group. Sandstone-schist intercalation immediately above Greenbrier fault, approximately 300 m east of Ghost Town amusement park. In this region the Greenbrier fault separates mylonitic orthogneisses from Ocoee Supergroup rocks, and the contact is nearly horizontal, parallel to the axial plane of the fold shown in the photo. Note hammer near the center of the photo for scale.

Figure 3.14. F_2 fold in the Elkmont Sandstone. Tight fold in kyanite mica schist of the Elkmont Sandstone where the foliation is parallel to the axial surface of the fold. Located 200 m southwest of Middle Top.

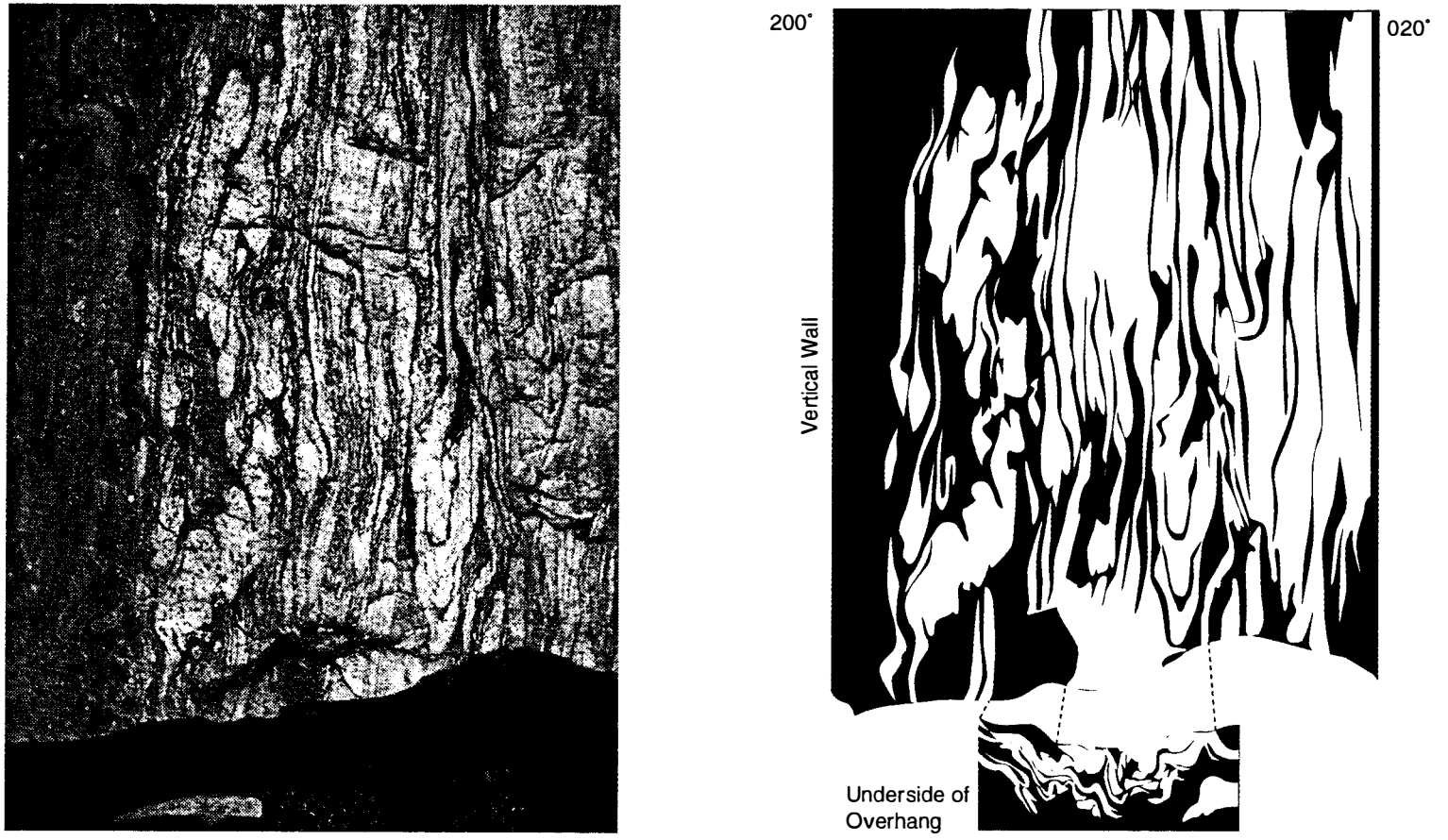

Figure 3.15. F_2 folding in biotite paragneiss. Disharmonic, noncylindrical folds in a quartz-feldspar-biotite paragneiss (Tallulah Falls Formation?). Located along Highway 276, 1.5 km south of the intersection with Interstate 40.

Figure 3.16. F_2 ptygmatic and isoclinal folding in biotite paragneiss. Biotite paragneiss (Tallulah Falls Formation?). Located along the road to Walker Bald 100 m above Hemphill Creek.

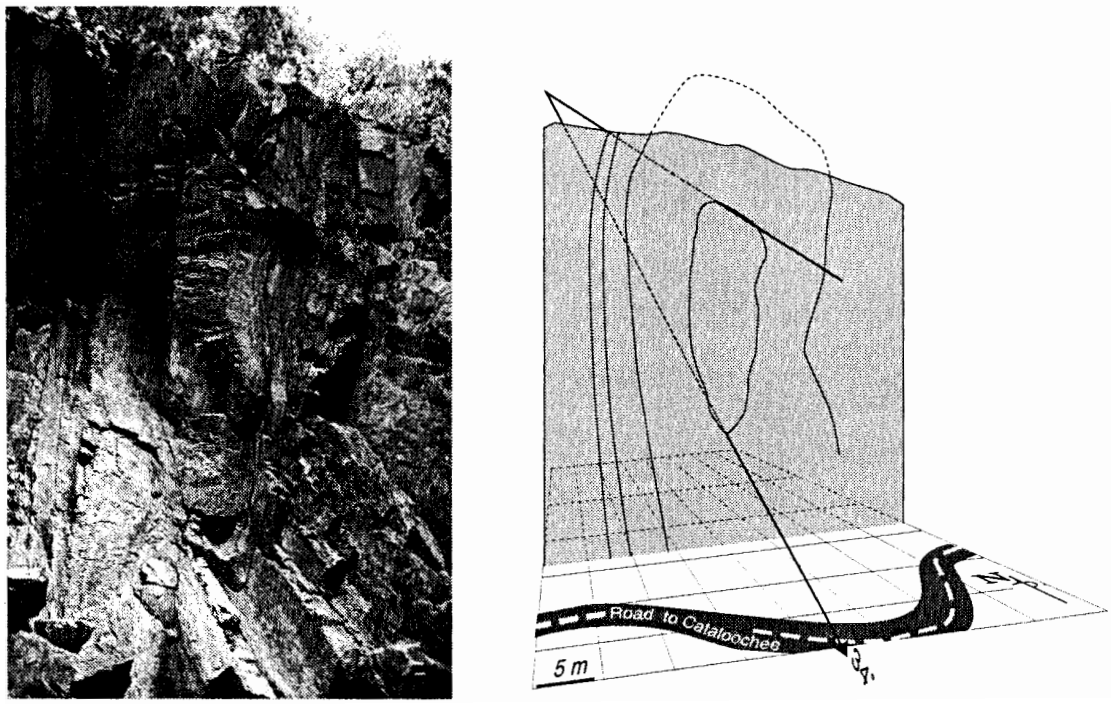

Figure 3.17. Mesoscopic F_2 sheath fold. Fold in a massive sandstone bed in the upper part of the Great Smoky Group, probably the Anakeesta Formation. Mineral lineation, parallel to the fold axis is 210°, 34°. Located along the road to Cataloochee, approximately 2 km northwest of Cove Creek Church.

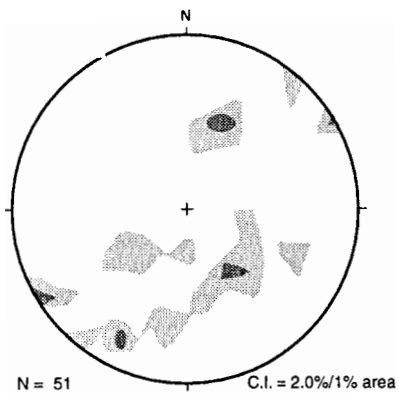

(a)

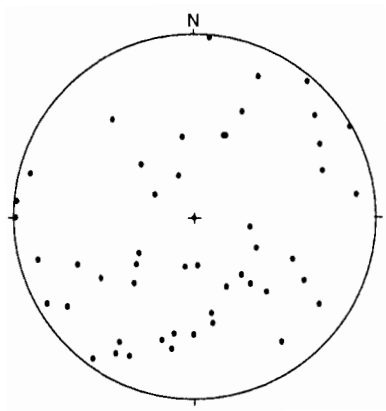

(b)

(c)

Figure 3.18. Veins and joints in the study area.
(a) Contoured lower-hemisphere equal-area plot of poles to joints in the area mapped.
(b) Lower-hemisphere equal-area plot of 51 poles to joints in the area mapped.
(c) Undeformed pegmatite vein cutting a retrograde mylonite foliation in the Thunderhead Sandstone. Located approximately 500 ENE of North Eaglenest Mountain.

deformed along with the country rock. Also, pegmatites occur as veins as thin as 10 cm and dikes up to 3 m wide. Pegmatites are composed of very coarse-grained muscovite, quartz, and feldspar (oligoclase and perthite), and occasional minor biotite, kyanite, and magnetite.

F_3 folds

F_3 folds consist of first-order, steeply inclined, gently plunging folds; second-order similar class 2 and 3 folds; and third-order crenulations. First-order folds from west to east are: the Cataloochee Divide syncline, Fie Creek anticline, Buck Mountain syncline, Campbell Creek anticline, and Walker Bald syncline (Fig. 3.1). These folds trend 030 to 040, have axial surfaces dipping 50° to 70° E (Plate II), often have overturned flanks facing northwest, and have variable plunge magnitudes to the NE and SW. Cataloochee Divide syncline plunges gently NNE; Buck Mountain syncline plunges gently SSW; and Walker Bald syncline and Campbell Creek anticline are gently to moderately doubly plunging folds. Other first-order folds were mapped within the Ocoee Supergroup between the Cataloochee Divide syncline and the Fie Creek anticline; these are here called the Double Gap anticline and the Hemphill Bald syncline (Fig. 3.1); otherwise, the fold names of Hadley and Goldsmith (1963) were employed. The nearly straight map trace (Plate I and Fig. 3.1) of the first-order folds axial planes indicates that these are near-planar folds that have not been refolded, and the consistent plunge direction of each fold suggests that these folds are nearly cylindrical.

Because bedding (Fig. 3.19a) and foliation (Fig. 3.19b) are parallel throughout the area mapped, an equal-area projection of poles to bedding and foliation (Fig. 3.20) is useful to constrain the geometry of first-order folds, and the locus of first-order F_3 fold axes. A bimodal distribution with a maximum at 044, 56° E, and a less pronounced cluster at 196, 36° W (Fig. 3.20b) suggests F_3 folding is asymmetric, with SE-inclined axial planes, and narrow hinges. A π-diagram (Fig. 3.20b) reveals that the overall plunge of the F_3, first-order fold axes is 215, 13°.

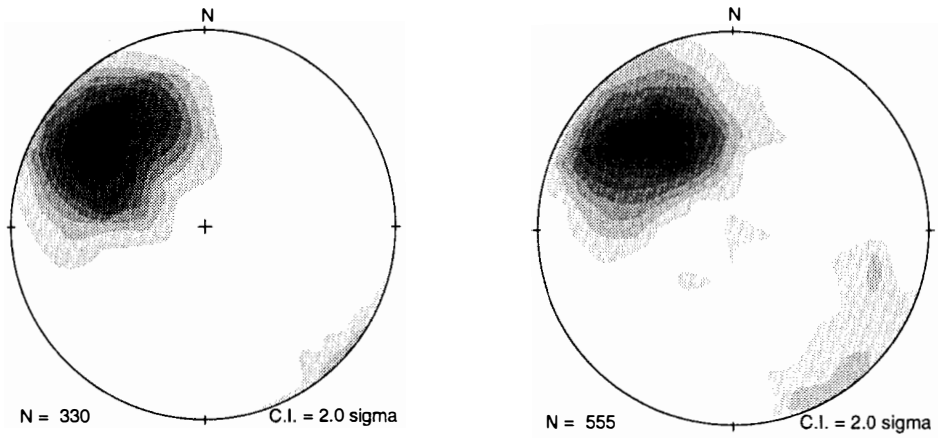

(a) (b)

Figure 3.19. Kamb contoured diagrams of poles to foliation and bedding in the study area.
(a) Lower-hemisphere equal-area plot of poles to bedding.
(b) Lower-hemisphere equal-area plot of poles to foliation.

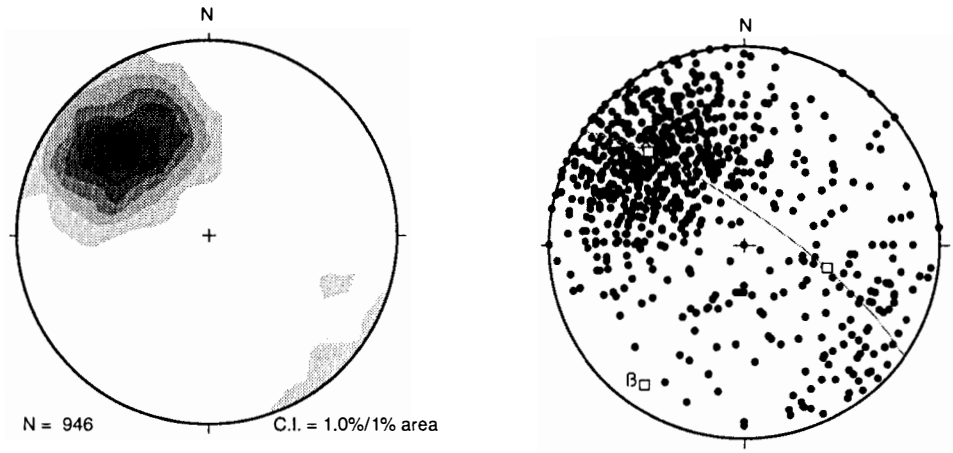

(a) (b)

Figure 3.20. Fabric diagrams of bedding and foliation in the area mapped.
(a) Lower-hemisphere equal-area plot of poles to bedding and foliation.
(b) Lower-hemisphere equal-area projection of 946 poles to bedding and foliation. Since bedding and foliation are consistently parallel throughout the area mapped, a ∏ equal-area plot was constructed to show the trend and plunge of the ß pole (215, 13°). This line represents the locus of fold axes of macroscopic folds. The value of the best fit great circle is 305, 77°N. The bimodal distribution, biased toward one maximum, is characteristic of asymmetric folding with inclined axial planes.

Second-order F3 folds more commonly are similar, harmonic, asymmetric, class 2 and 3, flexural-flow folds (Fig. 3.21). The axial planes of these folds are not highlighted by axial-planar cleavage, and the limbs do not show traces of flexural slip. Wavy parallel and chevron folds also occur but are not as common. Ptygmatic folding locally occurs where a strong rheologic contrast exists, e.g., between orthoquartzite and schist of the Longarm Quartzite (Fig. 3.22). The interlimb angle for the second-order folds greatly varies, as well as the plunge and trend (Fig. 3.23a), even though the trends are mostly NE-SW (Fig. 3.23b). An equal-area projection reveals that the distribution of mesoscopic fold axes fit a great circle, suggesting that they are parasitic folds to a planar feature striking 35°, and dipping 56°E (Fig. 3.23c). That plane contains the mean fold axis determined for the first-order folds (215, 13°, Fig. 3.22b), and is approximately coplanar with the overall attitude of mesoscopic fold axial surfaces (027, 45°E; Fig. 3.24). The spatial relations among first- and second-order folds as inferred from the fabric diagrams are explained in Figure 3.25. Third-order folds are crenulation folds (Fig. 3.26) usually developed as crinkling of schistosity planes along the hinges of second-order folds. In a few localities this folding shows a weak crenulation cleavage.

Fold interference patterns

F_3 folds not only deform original bedding (S_0) and the principal foliation (S_2), but also fold preexisting structures such as isoclinal, passive-flow folds (F_2 folds) and premetamorphic faults. The fold interference patterns resulting from the overprinting of the early F_2 folds are more easily recognized in outcrops of the Thunderhead Sandstone and the biotite paragneiss of the Tallulah Falls Formation because the lithologic contrast between individual layers highlight the structure. The style of interference approximates the type 3 and type 2 interference patterns (Ramsay, 1967) produced by overprinting originally reclined to recumbent isoclines (F_2), gently E and NE-plunging, by steeply SE-dipping, NNE-trending, and gently plunging (F_3) second-order folds. The examples of mesoscopic interference patterns in the field

Figure 3.21. Dip-isogon analysis of two folds in the area mapped.
(a) Class 3 flexural-flow fold from the Thunderhead Sandstone showing slightly divergent isogons, interlimb angles between 50° and 70°, and moderate hinge zone thickening, characteristic of this set of folds. Note the cuspate-lobate folds developed in the hinge of this fold probably related to a rheological contrast between the fine- and the medium-grained sandstone. Sample from near the top of the North Eaglenest Mountain. The isogon interval is 10°.
(b) Class 2 similar passive-flow fold in the Longarm Quartzite showing nearly parallel isogons and thickening of the hinge zone. Located approximately 500 m north of Moody Top along the hinge of the Buck Mountain syncline. The isogon interval was changed to better show the variations in shape.

(a)

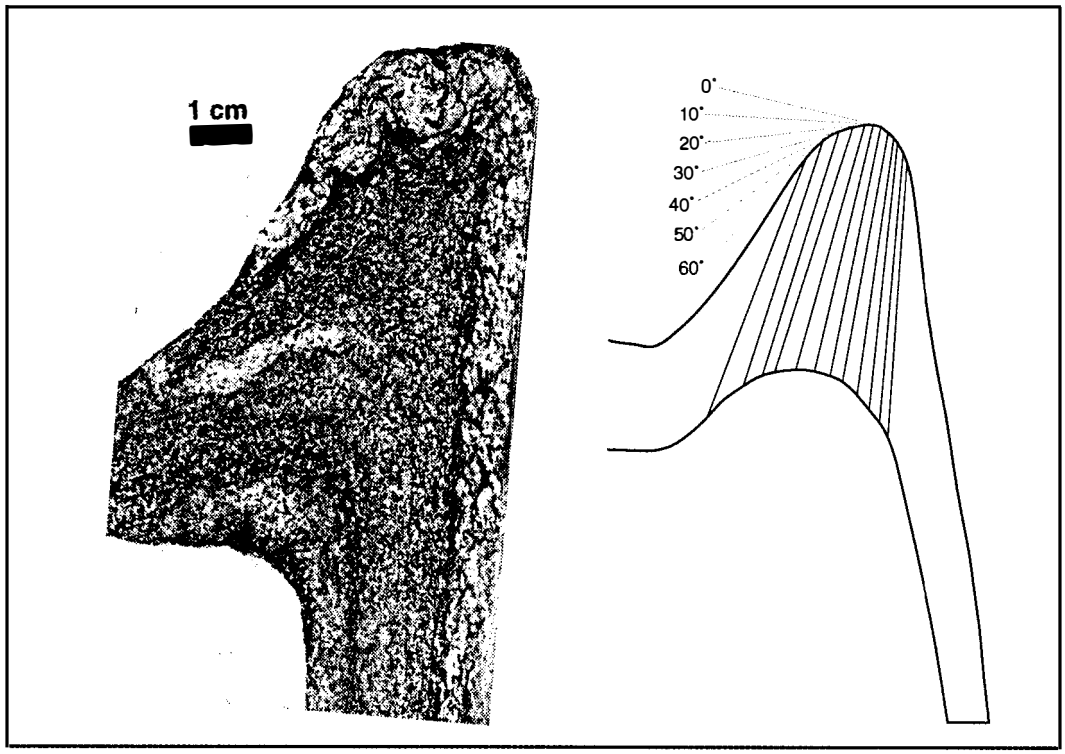

(b)

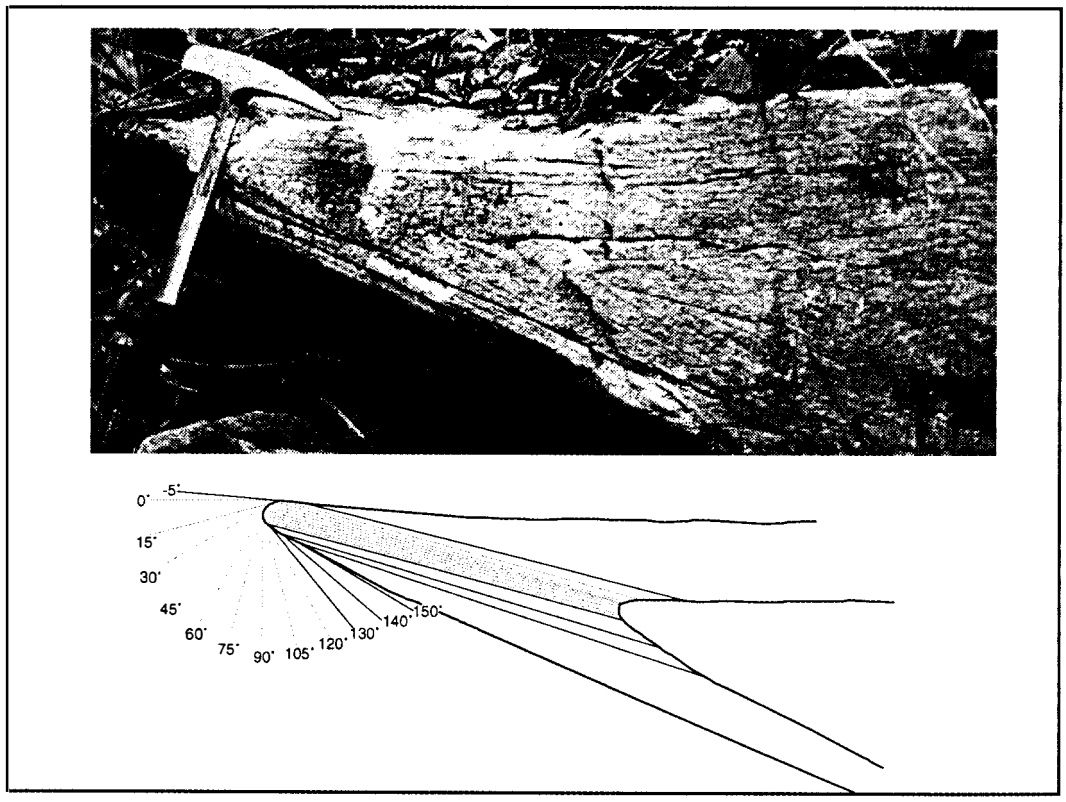

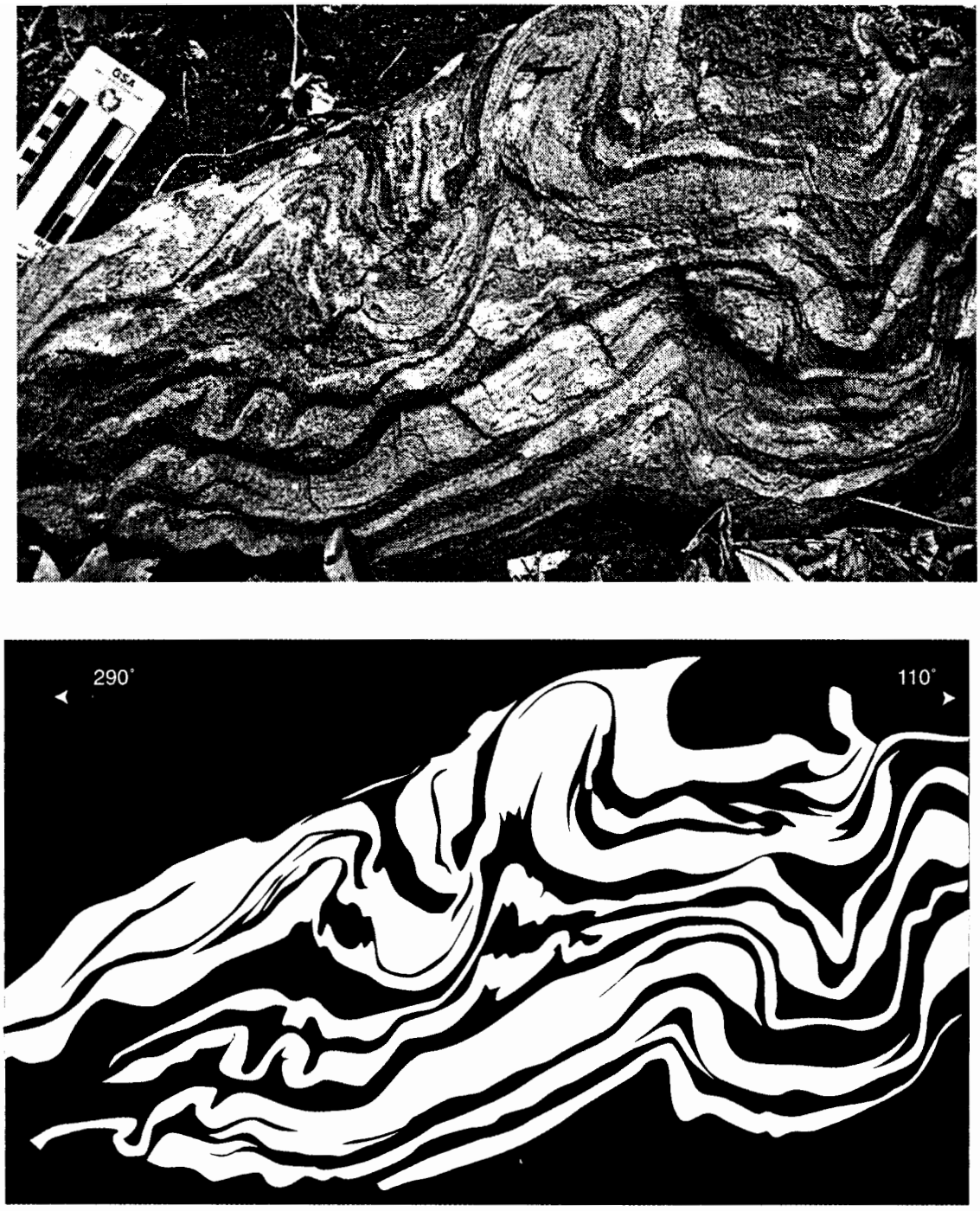

Figure 3.22. Folding in Longarm Quartzite. Ptygmatic disharmonic folds in interlayered orthoquartzite and schist. Crenulations develop in the schist layers near the hinges of folds. Located approximately 1 km south of Little Bald Knob.

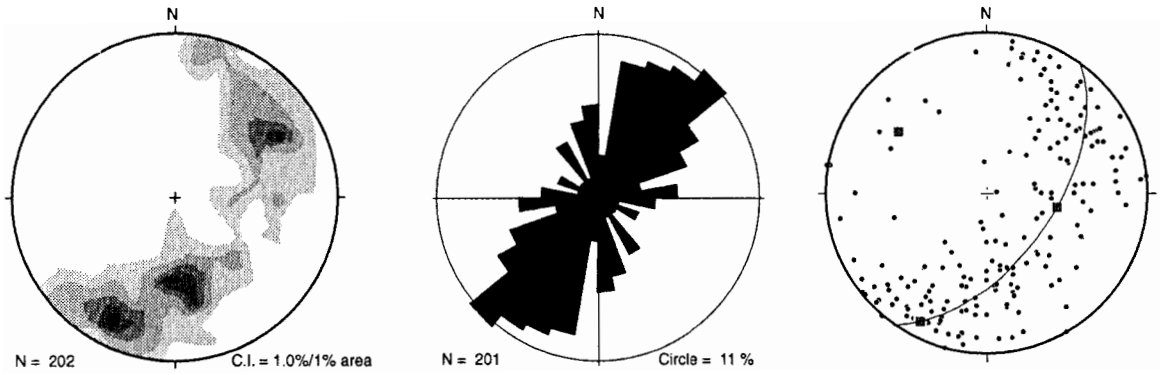

(a) (b) (c)

Figure 3.23. Fabric diagrams of fold axes in the area mapped
(a) Contoured lower-hemisphere equal-area plot of mesoscopic F_3 fold axes. The distribution of the folds axes adjusts to a great circle.
(b) Rose diagram of trends of mesoscopic F_3 fold axes.
(c) Lower-hemisphere equal-area projection of 202 mesoscopic F_3 fold axes. A great circle (35, 56°E) describes the distribution of the mesoscopic fold hinges.

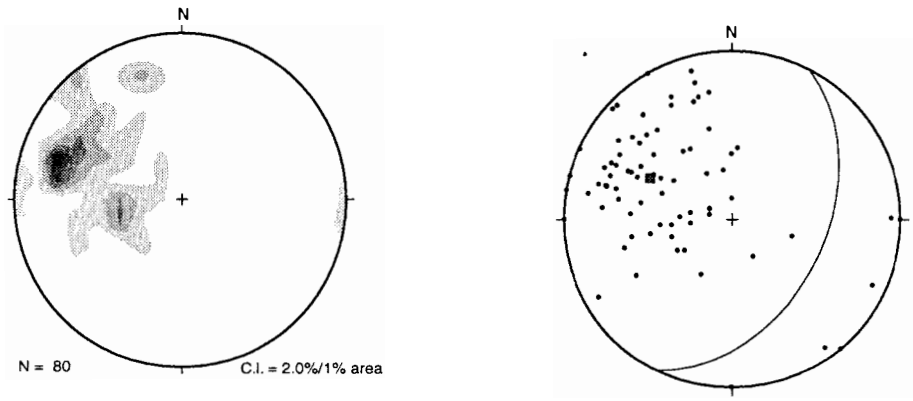

(a) (b)

Figure 3.24. Fabric diagrams of fold axial surfaces in the area mapped.
(a) Contoured lower-hemisphere, equal-area plot of poles to mesoscopic F_3 axial planes.
(b) Lower-hemisphere, equal-area projection of 80 poles to mesoscopic F_3 axial planes. The value of the best-fit great circle is 027, 45°E indicating the average attitude of these planes.

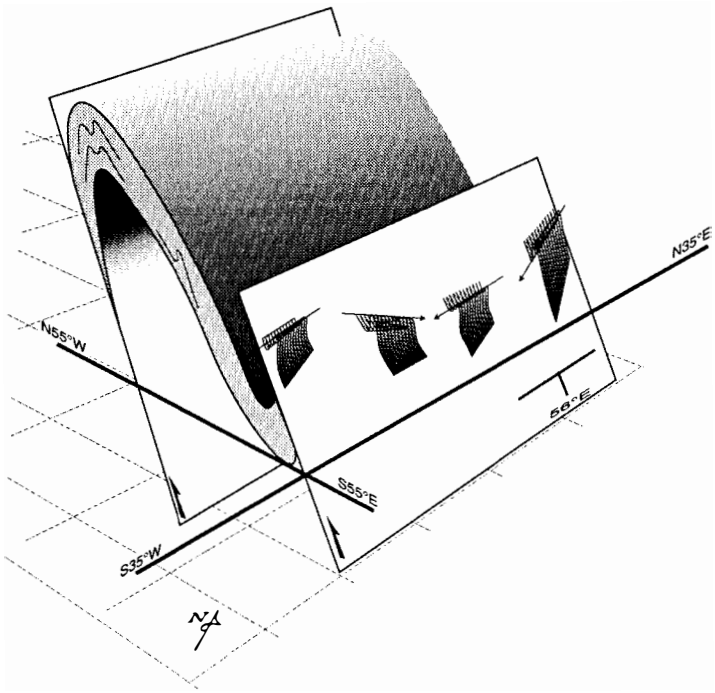

Figure 3.25. Spatial relationships among different postmetamorphic fabric elements in the area mapped. Large anticline represents the first-order, gently plunging, northwest-verging folds. The plane striking 035 and dipping 56° E is defined by the distribution of mesoscopic F_3 folds axes along a great circle, and by the first order, F_3 fold axes (205, 13°). This plane also has similar orientation to the postmetamorphic faults in the area mapped (030° and 060°).

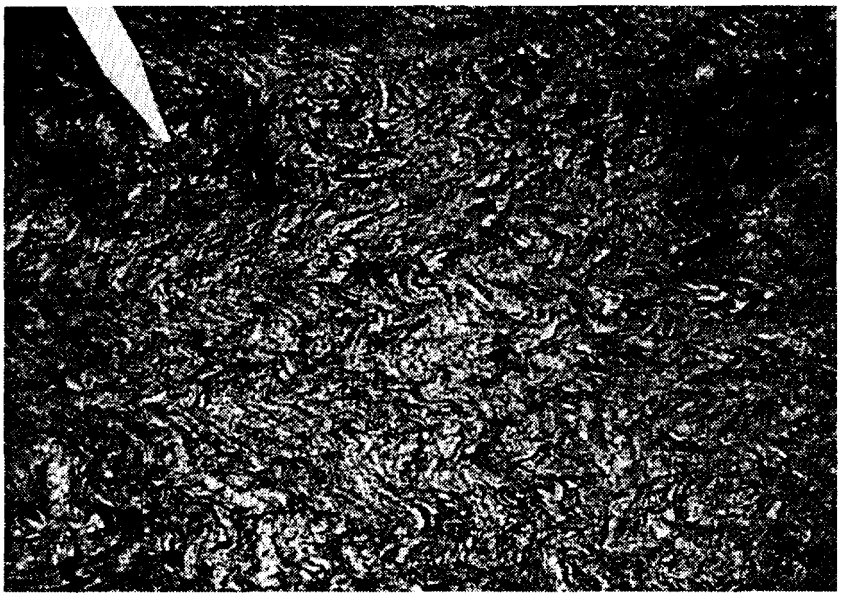

Figure 3.26. Crenulations in mylonitic basement orthogneiss. Located approximately 300 m north of Nick Gap.

shown in Figures 3.27 through 3.30 illustrate the geometry of these patterns, where the axial planes of both folding sets are often at a high angle to one another, but the fold axes are nearly coaxial. In map scale type-2 and -3 interference patterns were deciphered by analyzing the changes in the facing directions in graded conglomerate sandstone beds at the Thunderhead Sandstone. Between the Buck Mountain syncline and the Walker Bald syncline (Plates I and II) map-scale complex folding was initially inferred from the observation of abundant mesoscopic refolded folds, and map pattern was resolved by tracking graded conglomeratic-sandstone beds of the base of the Thunderhead Sandstone (Plates I and II). Map-scale fold-interference patterns can also be inferred from the observation of the contacts drawn by Hadley and Goldsmith (1963, Plate 2) in the valley of Hemphill Creek, where the contact between ortho- and paragneisses (the Hayesville fault) exhibits a characteristic hook shape, probably related to the type-2 interference patterns observed immediately south of Hemphill Creek between the Buck Mountain syncline and Walker Bald syncline in the turbidites of the Thunderhead Sandstone.

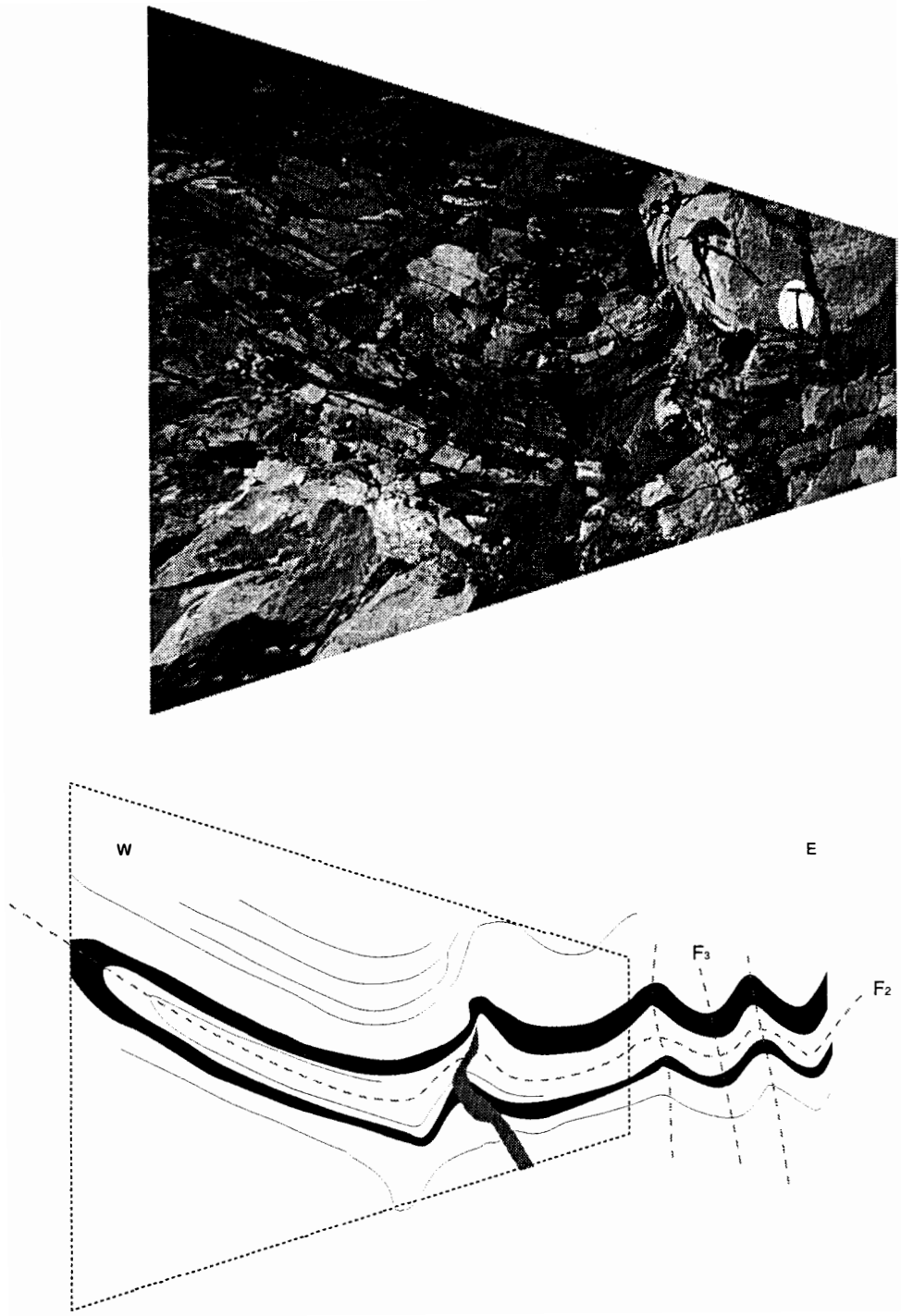

Figure 3.27. Type 3 interference pattern in the Thunderhead Sandstone. The photograph was skewed to partially correct for perspective since the outcrop is not perpendicular to the fold axis. An undeformed pegmatite vein was intruded almost parallel to the F_3 fold axes. Highlighted hammer in the upper-right quarter of the photo for scale. Located approximately 100 m southwest of Leatherwood Top.

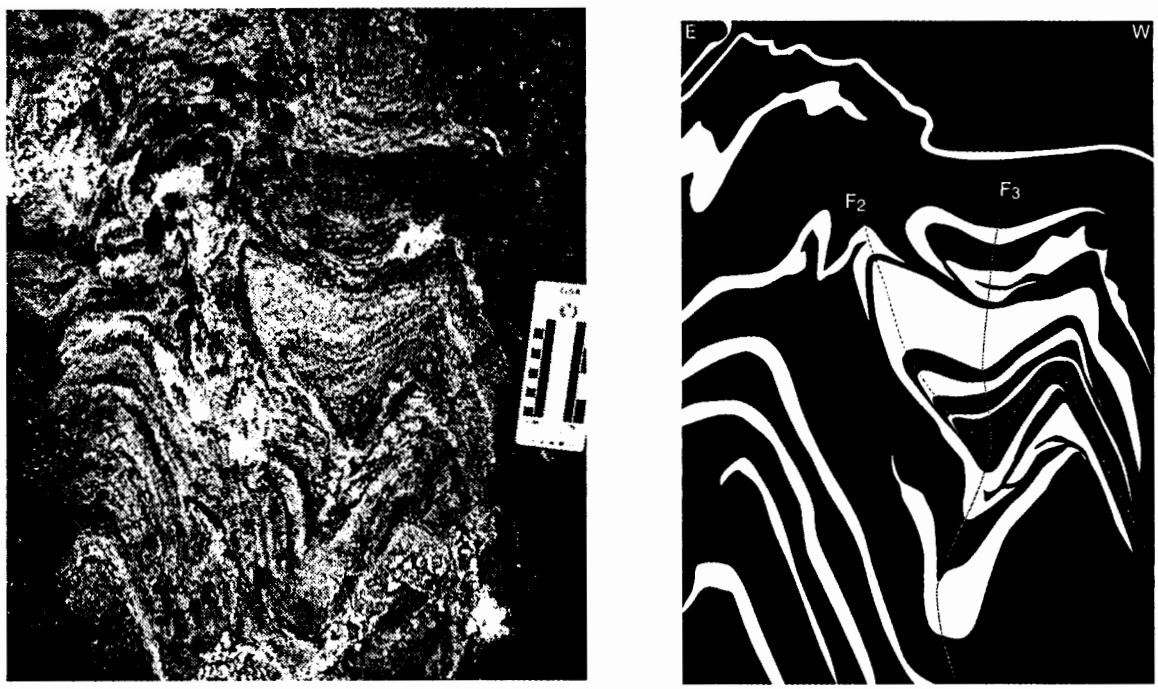

Figure 3.28. Type 2 interference pattern in Thunderhead Sandstone. A pegmatite vein is near the bottom of the photo. Located approximately 1 km north of Walker Bald.

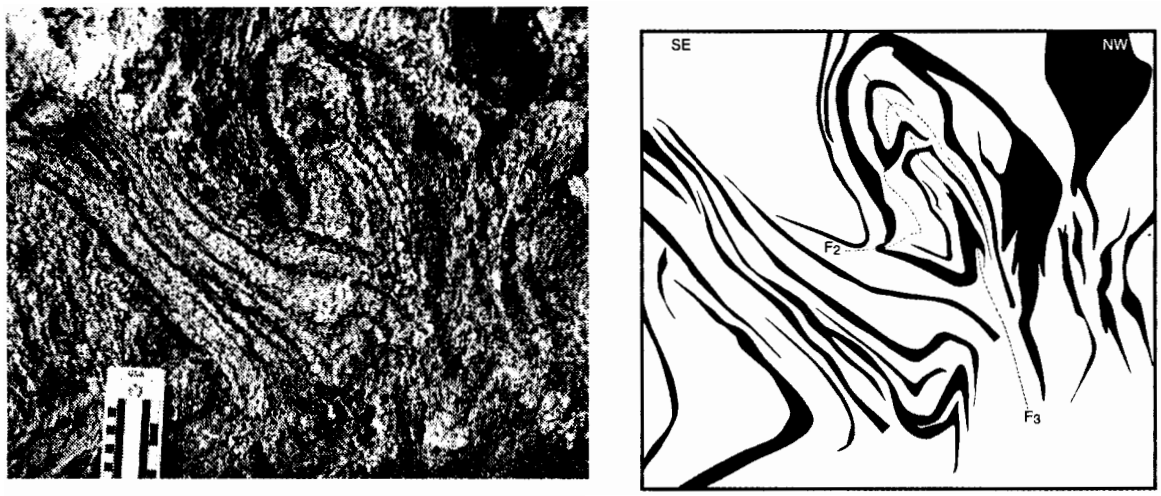

Figure 3.29. Modified type 2 interference pattern in the Thunderhead Sandstone. Located 200 m southeast of Ghost Town amusement park.

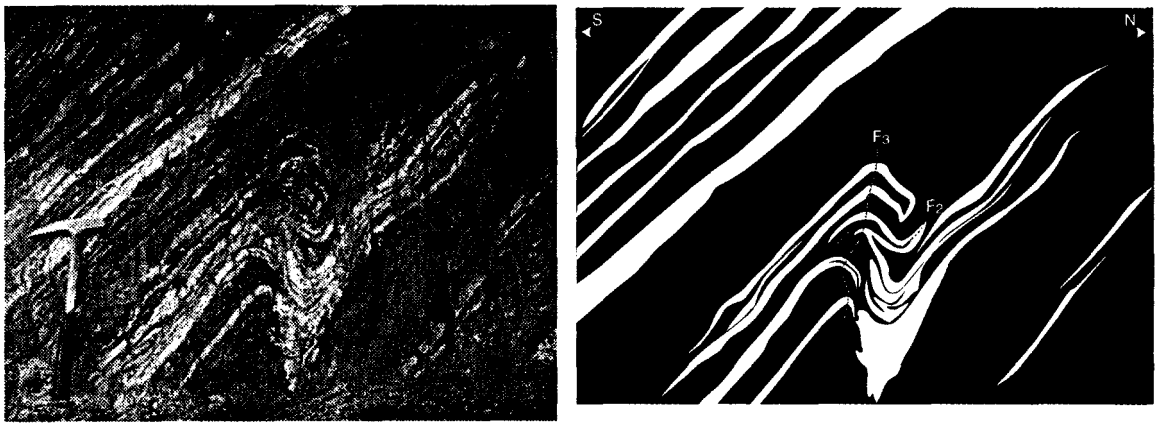

Figure 3.30. Type 3 interference pattern in biotite paragneiss.
Located 1 km ENE of Campbell Lick.

Postmetamorphic faults

Postmetamorphic faults in the study area transect the metamorphic foliation, offset metamorphic isograds, have nearly straight traces trending 030 and 060 (Plate I), dip steeply SE, and often contain retrograde mylonitic rocks along their traces. Chlorite was occasionally found as a retrograde mineral along shear zones. Two distinct belts of postmetamorphic faults exist within the boundaries of the area mapped: a 030 trending belt, located northwest of the Cataloochee Divide syncline, and a 060 trending belt located southeast of the Walker Bald syncline (Plate I and Fig. 3.1).

The Caldwell Creek (named here) and Cold Springs faults are the most prominent faults in the northwestern belt of postmetamorphic faults. In the Great Smoky Mountains National Park, Caldwell Creek drains NNE along a nearly straight, narrow valley that separates the Cataloochee Divide to the southeast from Big Fork Ridge to the northwest. Along Caldwell Creek, a thick sequence of Longarm Quartzite and Roaring Fork Sandstone exposed along Big Fork Ridge is progressively in contact to the northeast with older rocks exposed in the northwestern flank of the Cataloochee Divide syncline (Fig. 3.1). From southeast to northwest the sequence in contact with the thick sequence of Longarm Quartzite and Roaring Fork Sandstone is the upper

half of the Elkmont Sandstone, a thin sequence of Snowbird Group rocks, and granodioritic basement. This clearly faulted contact was interpreted as the southeastern continuation of the premetamorphic Greenbrier fault by Hadley and Goldsmith (1963) despite the changes in the stratigraphic packages in contact and in the style of the fault. North of the confluence between Caldwell Creek and Snake Branch this fault was traced following topographic breaks in otherwise steep ridges on the northwestern flank of Cataloochee Divide. As discussed later in this chapter, my mapping shows that this fault is not the premetamorphic Greenbrier fault, but a postmetamorphic fault that was most likely reactivated following the trace of a Late Proterozoic growth fault (Chapter II), because its trace coincides with important thickness and facies changes that occur in the Longarm Quartzite. This postmetamorphic fault is here named Caldwell Creek fault. Exposures of this fault along the road to Cataloochee (Fig. 2.4 in Chapter II), as well as geomorphic features such as deep, straight valleys and breaks in the slope, indicate that this fault is postmetamorphic. Southward, this fault crosses the Cataloochee Divide near Garrets Gap, and is well exposed again along the old road to the Masonic Monument (Fig. 2.6, in Chapter II), where it locally thrust mylonitic orthogneiss and Wading Branch Formation on top of Wading Branch Formation rocks, deleting the Longarm Quartzite. This stratigraphic separation indicates that the dip slip along this fault is more than the local thickness of the Longarm Quartzite (approximately 100m). Further south this fault branches, placing a 200-m thick horse of mylonitic orthogneiss in Longarm Quartzite rocks in Smoky Falls (2 km NNW of Soco Gap off State Highway 19).

The easternmost outcrops of the Ocoee Supergroup in the Blue Ridge in western North Carolina occur in a belt bounded by postmetamorphic faults that trend 060° and dip steeply southeast (Plate I, Fig. 3.1). This belt extends in the area mapped from the Hornbuckle Valley overlook on the Blue Ridge Parkway to State Highway 19 east of Dellwood, along the steep northern flank of Eaglenest and Hard Ridges. The belt is made up of Ocoee Supergroup rocks, mostly Thunderhead Sandstone, at kyanite and sillimanite grade, and a horst of mylonitic orthogneiss (between Mine Branch and Pine Tree Cove, Plate I). Discrete faults were mapped in this belt by

tracing retrograde mylonitic zones (usually less than 50 m thick) along strike. These zones have nearly straight traces striking 060° and contain retrograde mylonites (Fig. 3.31). An approximately 20-m thick fault zone could be followed from the bottom of the valley of Gaddis Branch to the top of Hard Ridge (200 m of relief) to the east. The fault zone strikes 065 and dips 85° SE. The character of these fault zones is clearly retrograde (3.31c) because the quartz grains have not recrystallized after deformation took place.

CROSS SECTION CONSTRUCTION AND INTERPRETATION

Four cross sections (Plate II) show the relationships among major structures, and the interpreted structural geometry of the area mapped derived from field observations and analysis of map patterns.

Cross section construction (Plate II) relied on down-plunge projection of geologic map data (Plate I). The continuity of rock units, the nearly cylindrical, first-order F_3 folds, and the nearly straight traces of postmetamorphic faults in the northwestern half of the area mapped (mostly in Ocoee Supergroup units), permit the use of this kind of projection. Dip data were corrected for apparent dip, and projected to the section line along or perpendicular to the strike where projection along strike does not cross the section line. Dips measured near first-order folds and major faults were projected along the trend of these structures to the section line where no data points could be located near it. Care was taken not to project dip data across major structures. In places where too many data stations converge into a particular part of the cross section, data were averaged (if showing similar attitudes) for consistency.

Three cross sections (A-A', B-B', and C-C') were constructed approximately perpendicular (NW-SE) to the trends of first-order F_3 folds, and postmetamorphic faults, and thus reflect the approximate cross section geometry of these structures. Even though first-order F_3 folds plunge, the cross sections were drawn along vertical planes because some folds plunge northeastward, others southwestward, and some

Figure 3.31. Retrograde mylonite in the Great Smoky Group.
(a) Sawed section of a retrograde mylonite disrupting bedding in a sandstone bed located along the Blue Ridge Parkway, approximately 1 km south of Hornbuckle Valley overlook.
(b) Feldspathic sandstone within the Ocoee Supergroup showing grain-size reduction near the top of the sample. Also note the band of crystalline quartz running across the bottom of the sample. Located along Gaddis Branch approximately 1 km northeast of North Eaglenest Mountain.
(c) Quartz ribbons showing unrecovered deformation in the band of crystalline quartz mentioned above. Crossed nicols; the long edge of the photomicrograph is 4 mm.

(a)

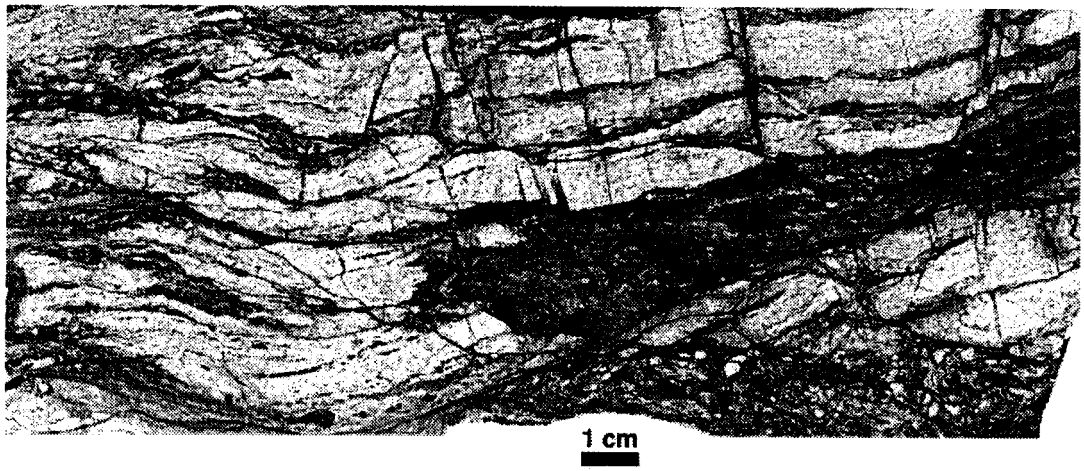

(b)

(c)

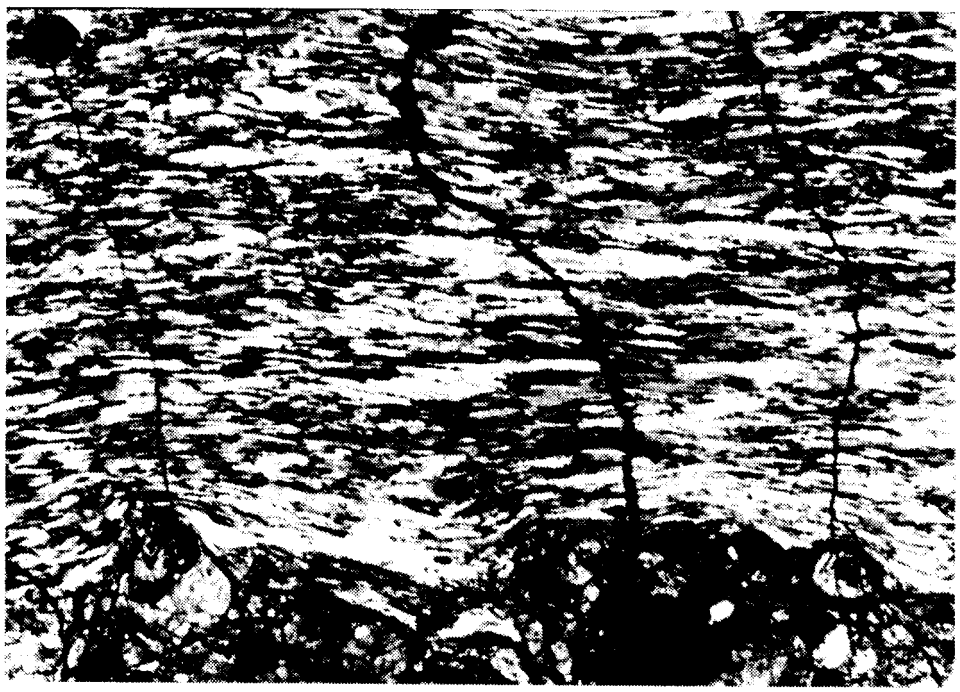

are doubly plunging folds. A fourth cross section (D-D') was constructed parallel (NE-SW) to the trends of first-order F_3 folds, and postmetamorphic faults, to better display the geometry of F_2 folds, and to portray the relationships among thrust sheets across the area mapped.

Section A-A'

The Caldwell Creek fault, an overturned portion of the Greenbrier fault, and the Hayesville fault are portrayed in this cross section.

The Caldwell Creek fault, previously interpreted as the Greenbrier fault by Hadley and Goldsmith (1963), separates a characteristically thick section of Snowbird Group (approximately 1,000 m; Chapter II) from the Elkmont Sandstone, and northward along the strike, from a thinner section (approximately 100 m; Chapter II) of Snowbird Group unconformably resting on basement orthogneiss. A southwestern-plunging postmetamorphic anticline brings this thinner section of Snowbird Group to the surface in the footwall of Greenbrier fault west of Cove Creek Gap. This anticline projects southward into cross sections A-A' and B-B'.

The Greenbrier fault in this cross section was deformed by this anticline and by the synclinorium defined by other first-order postmetamorphic folds (Cataloochee Divide syncline, Double Gap anticline, and Hemphill Bald syncline). The southeastern flank of this synclinorium is overturned, and so is the segment of Greenbrier fault exposed along the southeastern slope of the Cataloochee Divide. The Greenbrier fault along this segment separates orthogneiss and steeply SE-dipping Snowbird Group rocks from Elkmont Sandstone, Thunderhead Sandstone, and Anakeesta Formation. These cutoffs define a south-dipping hanging wall ramp (present coordinates), because the Greenbrier fault cuts progressively younger units from south to north along the southeastern slope of the Cataloochee Divide. The fault surface in this region ramped from the upper part of the Elkmont Sandstone to the Anakeesta Formation or higher in the Great Smoky Group.

Multiple folding of the Hayesville fault in the valley of Hemphill Creek makes difficult the distinction between hanging wall and footwall rocks. In this region of the map area, isoclinal synmetamorphic folds deforming the contrast between ortho- and paragneisses are overprinted by tight postmetamorphic folds. Northeast of High Top, and southwest of Purchase Knob, however, where the intensity of folding is less pronounced, the hanging wall of this fault is composed of biotite- and hornblende-biotite paragneiss whereas the footwall consists of orthogneiss. This relationship, along with mesoscopic interference patterns studied in the field (Figs. 3.12, and 3.27 to 3.30), were used to help interpret the map patterns in Hemphill Creek valley. The synmetamorphic isoclines verge north, and therefore are better represented in section D-D'. Some of the postmetamorphic folds deforming the Hayesville fault in Hemphill Creek valley can be traced southwards to connect with first-order postmetamorphic folds between the Buck Mountain the Walker Bald synclines.

Section B-B'

Some features discussed in the previous section also appear in this cross section: the overturned segment of Greenbrier fault along the southeastern slope of Cataloochee Divide, and the postmetamorphic anticline that north of section A-A' brings the footwall of Greenbrier fault to the surface. In this cross section, however, the postmetamorphic folds that define a synclinorium to the north are larger, and a splay of Greenbrier fault duplicates the upper part of the Elkmont Sandstone making the Greenbrier fault appear deeper in this section. The Caldwell Creek fault also appears in this cross section separating a thick section of the Snowbird Group from the Elkmont Sandstone, but immediately south of the cross section line the trend of this fault changes from NE-SW to almost N-S, offsetting the Greenbrier fault just north of section C-C'. Near the southeastern end of this cross section a belt of postmetamorphic faults exposes Great Smoky Group rocks surrounded by biotite paragneiss.

The footwall of Greenbrier fault in this cross section reflects the southeastward thinning of the Longarm Quartzite described in Chapter II, as well as small footwall ramps where Snowbird Group rocks are often missing and the orthogneiss is in contact with Great Smoky Group rocks. West of Cataloochee Divide the Greenbrier fault follows the Longarm Quartzite; in the Fie Creek anticline the orthogneiss is exposed immediately beneath Great Smoky Group rocks; in the Buck Mountain syncline the Greenbrier fault climbs up to the Roaring Fork Formation; and near Walker Bald syncline the orthogneiss and an even thinner Longarm Quartzite section are exposed underneath Great Smoky Group rocks.

Whether the Greenbrier fault steps into the basement southeast of Walker Bald syncline is still open to question. In this cross section, the Greenbrier fault is interpreted to be folded by a sheath fold wrapping around Middle Top. This interpretation is consistent with the absence of biotite paragneiss in contact with Great Smoky Group rocks. If the Greenbrier fault stepped into the basement immediately southeast of Walker Bald syncline, biotite paragneiss should be found on top of Great Smoky Group rocks. First-order, isoclinal synmetamorphic folds, uncommon elsewhere in Great Smoky Group rocks were mapped in the region around Middle Top and may indicate that the Greenbrier fault was more intensely folded in this region, as shown in cross sections B-B' and D-D'. An often thin body of orthogneiss separates the overturned Greenbrier thrust sheet from the Hayesville thrust sheet; my mapping and Hadley and Goldsmith's (1963) indicate that both the biotite paragneiss and the Great Smoky Group rest on top of this orthogneiss. The folding style suggested above and shown in cross sections B-B' and D-D' may help explain these relationships.

Section C-C'

This cross section displays the southern extension of the postmetamorphic Caldwell Creek fault offsetting the overturned segment of Greenbrier fault along the

southeastern slope of the Cataloochee Divide. The footwall of Greenbrier fault in this cross section also shows changes in the units in underneath Great Smoky Group rocks from Longarm Quartzite (NW) to orthogneiss (SE) most likely due to stratigraphic thinning (Chapter II).

The trace of postmetamorphic faults shown near the southeastern end of the section was constrained by mapping retrograde mylonite zones. Vergence of postmetamorphic faults was derived from the dip of retrograde mylonites zones mapped in the field, and from early studies showing similar attitudes in postmetamorphic faults in and around the study area (Hadley and Goldsmith, 1963).

In Campbell Creek valley, biotite paragneiss is exposed beneath mylonitic augen gneiss and granodioritic orthogneiss. The tectonostratigraphic position of this paragneiss in Campbell Creek valley is puzzling because it is indistinguishable from similar biotite paragneiss in the hanging wall of Hayesville fault near Hemphill Creek (cross sections A-A' and B-B') and from rocks correlated with the Tallulah Falls Formation near Sylva, North Carolina (Quinn, 1991) also in the hanging wall of Hayesville fault. The geometry of folding used to explain map pattern in sections A-A' and B-B' cannot explain the position of this paragneiss as part of the Hayesville fault hanging wall.

Section D-D'

The geometry of first-order synmetamorphic folds is better represented in this cross section because it was drawn approximately N-S, which is close to the trend of synmetamorphic folds observed in the field. This cross section also connects the interpreted geometry of contacts among different units and structures across the area mapped.

The lowermost unit found in the area mapped is the biotite paragneiss exposed in the core of the Campbell Creek syncline (Plate II, sections B-B', C-C', and D-D').

Immediately above is the granodioritic orthogneiss; it is mostly augen mylonitic orthogneiss near the contact with the biotite paragneiss, but the finer-grained variety of mylonitic orthogneiss is absent. The granodioritic orthogneiss is unconformably overlain by Snowbird Group rocks, and faulted along the Greenbrier fault with Great Smoky Group units. In Hemphill Creek valley the granodioritic orthogneiss is separated along the Hayesville fault from biotite paragneisses above. The role of the orthogneiss as apparent footwall for both the Hayesville and the Greenbrier thrust sheets may be explained by overturning the Greenbrier thrust sheet (Sections B-B' and D-D'), or alternatively by out-of-sequence movement of the Hayesville fault that emplaced granodioritic basement in between Great Smoky Group and biotite paragneiss. The exposures of Great Smoky Group rocks in the center of the area terminate south of the valley of Hemphill Creek. An overturned fold may also help to explain the termination of these rocks in the center of the area mapped.

INTERPRETATION

Greenbrier fault

The main contribution of this work is to demonstrate that the Greenbrier fault extends into the southeastern Great Smoky Mountains in central-western North Carolina. Consequently, the Snowbird Group is everywhere separated from the Great Smoky Group by the Greenbrier fault (Fig. 3.32a), and the stratigraphic hierarchy of the western Blue Ridge needs to be revised accordingly (Fig. 3.32b).

The results of this work can be compared with previous attempts (Woodward et al., 1991; Connelly and Woodward, 1992) to reconstruct the geometry and evolution of faults in this part of the Blue Ridge. The relationships of faults to hanging wall and footwall strata were used north and northwest of the area mapped to reconstruct the shapes of the Greenbrier and Dunn Creek thrust sheets in the western Blue Ridge of Tennessee and westernmost North Carolina (Fig. 3.33). In my study area, the Greenbrier fault follows bedding in the Snowbird Group (footwall), commonly

(a)

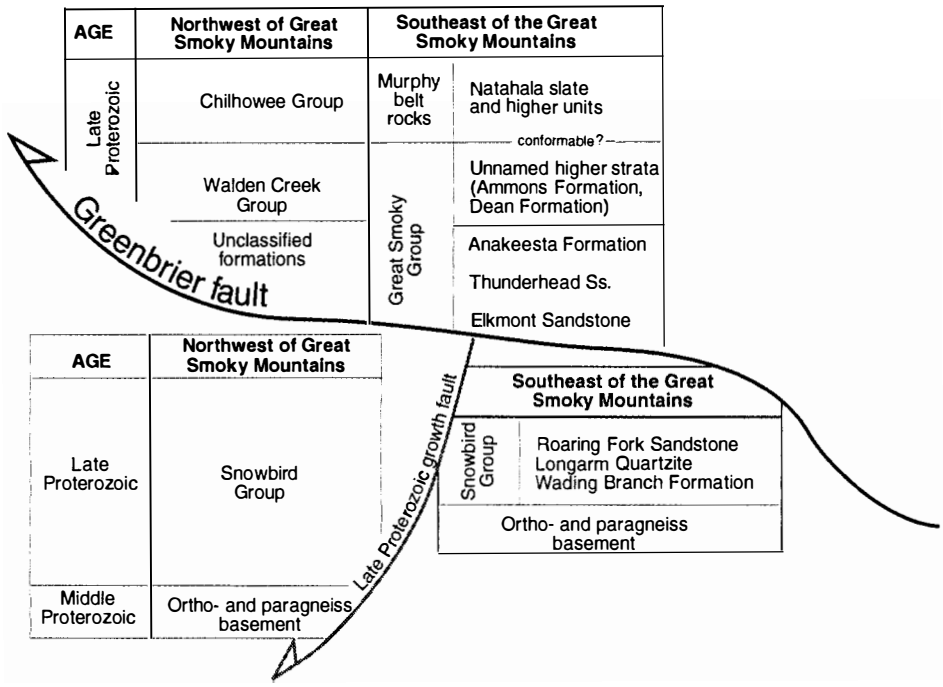

(b)

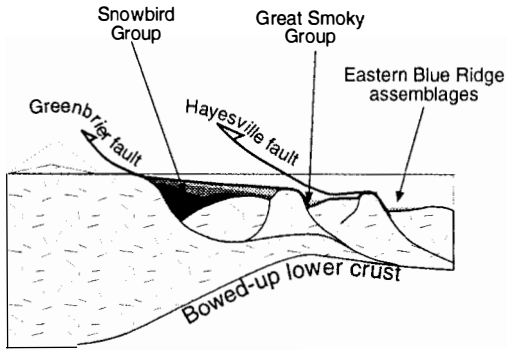

Figure 3.32 . Revision to stratigraphic nomenclature.
(a) Stratigraphic nomenclature of the Ocoee Supergroup modified from King *et al.*, 1958, and Carter *et al.*, 1995, to account for the new trace of the Greenbrier fault in central-western North Carolina.
(b) Stratigraphic section showing the relationship between Ocoee Supergroup units. The Snowbird Group and Great Smoky Group may be facies-equivalent strata accumulated in adjacent rift basins.

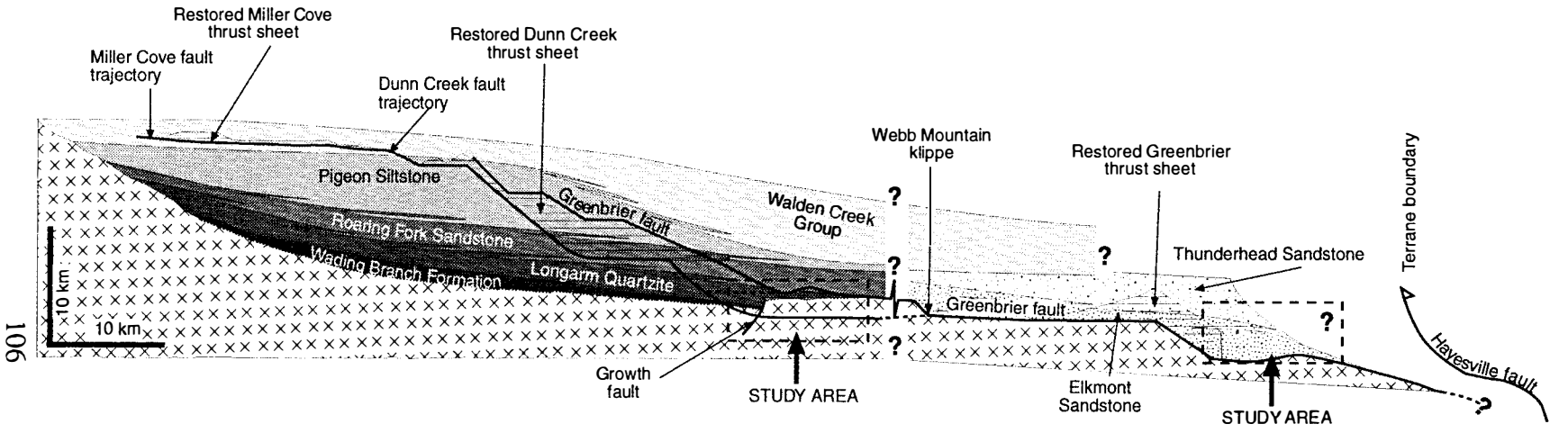

Figure 3.33. Schematic restored cross section of the Ocoee basin prior to Taconic deformation. Fault trajectories (thick lines), and thrust sheets (horizontal lines), restored by Woodward and Connelly, (1991) are shown along with changes suggested in my work. My work shows that the Greenbrier fault does not ramp from the basement, and the displacement of this fault increases to a minimum of 40 km. The Dunn Creek fault may ramp from the basement as suggested by Woodward and Connelly, (1991), to form the mylonitic zones in the basement. Another possibility is that it joins the Greenbrier fault.

within the Longarm Quartzite or the Roaring Fork Sandstone, and occasionally on top of the basement. Truncation of bedding by the Greenbrier fault more often occurs in the hanging wall, cutting across Thunderhead Sandstone. In terms of ramp-flat thrust geometries these relationships may approximate a footwall flat along the top of the Snowbird Group, and a hanging wall ramp cutting across Thunderhead Sandstone.

Near the Tennessee-North Carolina border, the steeply dipping overturned southeastern flank of the Alum Cave syncline was interpreted as a hanging wall ramp (Woodward et al., 1991; Connelly and Woodward, 1992) where the Greenbrier thrust sheet climbs from the basement. They supported this interpretation by citing truncation of bedding in the Great Smoky Group along the Greenbrier fault near Mt. Sterling (section B-B', Plate I in Hadley and Goldsmith, 1963). My mapping shows that basement is nowhere exposed in the hanging wall of this fault; thus the Greenbrier fault does not ramp from the basement immediately east of the Alum Cave syncline as suggested by Woodward et al., (1991), and Connelly and Woodward, (1992), but instead the Greenbrier fault follows the top of the Snowbird Group at least to the Walker Bald syncline (Plate II) in the study area. This also implies that the correlation of the Greenbrier fault to the north with the Devils Fork fault (Hadley and Nelson, 1971; Drake et al., 1989) may be incorrect. In addition, estimates of the displacement of Greenbrier fault made by calculating the minimum displacement on restored cross sections (Woodward et al., 1991; Connelly and Woodward, 1992), and on the basis of stratigraphic criteria (Hadley and Goldsmith 1963), increase from 23 km to a minimum of 40 km. This new estimate is based on the horizontal distance from the westernmost exposures of the hanging wall (west of the Tennessee-North Carolina border) to the easternmost exposures of the footwall in the study area near Dellwood.

Connelly and Woodward (1992) suggested that the Dunn Creek fault may ramp down into basement southeast of the Alum Cave syncline (Fig. 3.33). The projection of the Dunn Creek fault into western Blue Ridge basement may correspond to shear zones within the orthogneiss described in this chapter. The annealed mylonitic

shear zones within the orthogneiss are in the correct stratigraphic position to be the extension of the Dunn Creek fault. Alternatively, the Dunn Creek could also be an abandoned segment of the Greenbrier fault (Hatcher, personal communication, 1996) that was broken through after the toe of the thrust sheet locked.

Hayesville fault

The study of the contrast between eastern and western Blue Ridge affinity assemblages did not yield conclusive results regarding the evolution and character of the Hayesville fault partially because of incomplete stratigraphic controls in rocks of eastern Blue Ridge affinity. In particular, eastern Blue Ridge affinity rocks in the area mapped occupy two different tectonostratigraphic positions: above and below Greenbrier thrust sheet (Plate II). The biotite gneiss exposed above the Greenbrier thrust sheet can be correlated to similar rock types exposed south and southeast of the area mapped (Quinn, 1991) and correlated to the Tallulah Falls Formation. On the other hand, the biotite gneiss exposed in the core of the Campbell Creek anticline (below the Greenbrier thrust sheet) is indistinguishable from eastern Blue Ridge rocks exposed in the hanging wall of Hayesville fault, and cannot be linked to the Hayesville thrust sheet because in this case the footwall block is made up of biotite paragneiss.

Pressure and temperature estimates in rocks of the Tallulah Falls Formation southeast of the area mapped suggest that this unit was subjected to higher P-T conditions during peak metamorphism than the units across the premetamorphic Hayesville and Soque River faults (Quinn, 1991; Davidson, 1995; Brumback, 1990). This would indicate that both faults are postmetamorphic structures that telescoped the metamorphic isograds. Alternatively, the higher grade assemblages may be relict of an earlier metamorphism (Grenville?). Geochronologic work (Quinn and Wright, 1993; Miller et al., in press) carried out in this area suggests that rocks of eastern Blue Ridge affinity contain Middle Proterozoic 1.1 Ga Grenville rocks; whether or not these ages are representative of the entire terrane requires additional mapping and radiometric dating.

Timing of deformation

Growth faults probably related to the Late Proterozoic rifting of the eastern margin of Laurentia represent the earliest deformation in this area of the Blue Ridge. Whether or not fabrics in biotite paragneiss of eastern Blue Ridge affinity may correspond to the Grenville orogeny remains unresolved. The emplacement of the Greenbrier and Hayesville thrust sheets predated Taconic metamorphic peak, and synmetamorphic folding, most likely during the Penobscottian phase of the Taconic orogeny. During the Taconic metamorphic peak mylonite fabrics were annealed, faults were folded, and bedding surfaces rotated and transposed parallel to the foliation. Nearly intact stratigraphic sequences are preserved in the area studied probably because shearing during metamorphism locally took place subparallel to bedding emphasizing the compositional differences while maintaining some sedimentary structures such as graded bedding. Postmetamorphic (Alleghanian) folds and faults further modified the tectonostratigraphic assemblage in this part of the Blue Ridge, nonetheless, the effects of this events are more easily quantified because deformation was localized along discrete fault planes containing distinctive retrograde mylonites. Alleghanian folding was less pervasive, and facilitated the observation of refolded premetamorphic structures repeated along the flanks of first-order folds.

CONCLUSIONS

1) The Greenbrier fault in the easternmost western Blue Ridge is a premetamorphic fault separating the Great Smoky Group from the Snowbird Group. The minimum displacement of this fault is 40 km.

2) The Caldwell Creek, formerly mapped as the easternmost extension of Greenbrier fault, is a postmetamorphic fault that reactivated a Late Proterozoic growth fault. Contrasting facies of the Longarm Quartzite roughly delineate the trace of this growth

fault, and those changes coincide with the trace of Caldwell Creek fault.

3) The Hayesville fault is a premetamorphic fault separating mylonitic orthogneisses in the footwall from biotite paragneisses in the hanging wall. The tectonostratigraphic position of biotite paragneisses below the Greenbrier fault remains uncertain. Greenbrier and Hayesville thrust sheets were emplaced before the metamorphic peak, but the precise chronology among these two structures could not be resolved.

4) First-order, F_3 folds in the area mapped from west to east are the Cataloochee Divide syncline, Double Gap anticline, Hemphill Bald syncline, Fie Creek anticline, Buck Mountain syncline, Campbell Creek anticline, and Walker Bald syncline. Postmetamorphic faults mapped in this area from west to east are the Cold Springs fault, Caldwell Creek fault, and an unnamed belt of faults south of Dellwood, in the northern flank of the Eaglenest ridge.

CHAPTER IV
SUMMARY OF CONCLUSIONS

1) The relationship of the Longarm Quartzite to the nonconformity below is a distal downlap with a clastic provenance located to the northwest, and with an original depositional dip to the southeast.

2) The granitic rocks immediately beneath the Ocoee Supergroup in the eastern part of the western Blue Ridge did not contribute significantly to the sediment budget of the Late Proterozoic rifted margin of Laurentia.

3) A growth fault, active during the accumulation of the Longarm Quartzite, acted as a sedimentary trap. To the northwest subsidence kept pace with accumulation so that this unit accumulated over 1,000 m of arkose in the absence of a deep basin. To the southeast only a thin sequence of pelitic orthoquartzite accumulated, because most clastics were trapped to the northwest.

4) The Thunderhead Sandstone is a retrogradational turbiditic sequence with northwestern provenance.

5) The Greenbrier fault in the easternmost western Blue Ridge is a premetamorphic fault separating the Great Smoky Group from the Snowbird Group. The minimum displacement of this fault is 40 km.

6) The Caldwell Creek, formerly mapped as the easternmost extension of Greenbrier fault, is a postmetamorphic fault that reactivated a Late Proterozoic growth fault. Contrasting facies of the Longarm Quartzite roughly delineate the trace of this growth fault, and those changes coincide with the trace of Caldwell Creek fault.

7) The Hayesville fault is a premetamorphic fault separating mylonitic orthogneisses in the footwall from biotite paragneisses in the hanging wall. The tectonostratigraphic

position of biotite paragneisses below the Greenbrier fault remains uncertain. Greenbrier and Hayesville thrust sheets were emplaced before the metamorphic peak, but the precise chronology among these two structures could not be resolved.

8) First-order, F_3 folds in the area mapped from west to east are the Cataloochee Divide syncline, Double Gap anticline, Hemphill Bald syncline, Fie Creek anticline, Buck Mountain syncline, Campbell Creek anticline, and Walker Bald syncline. Postmetamorphic faults mapped in this area from west to east are the Cold Springs fault, Caldwell Creek fault, and an unnamed belt of faults south of Dellwood, in the northern flank of the Eaglenest ridge.

REFERENCES CITED

Absher, B. S., and McSween, H. Y., 1985, Granulites at Winding Stair Gap, North Carolina: The thermal axis of Paleozoic metamorphism in the southern Appalachians: Geological Society of America Bulletin, v. 96, p. 588-599.

Bartholomew, M. J., and Lewis, S. E., 1984, Evolution of Grenville massifs in the Blue Ridge geological province, southern and central Appalachians, in Bartholomew, M. J., ed., The Grenville event in the Appalachians and related topics: Geological Society of America Special Paper 194, p. 229-254.

Brumback, V. J., 1990, A metamorphic and structural transect in the central Blue Ridge, Jackson and Macon Counties, North Carolina [unpublished M.S. thesis]: Knoxville, University of Tennessee, 103 p.

Carpenter, R. H., 1970, Metamorphic history of the Blue Ridge province of Tennessee and North Carolina: Geological Society of America Bulletin, v. 81, p. 749-762.

Carter, M. W., Geddes, D. J., Hatcher, R. D., Jr., and Martin, S. L., 1995, Stratigraphic and structural relationships in the western Blue Ridge foothills of southeastern Tennessee: Guidebook for field trip excursions Southeastern Section, Geological Society of America: Knoxville, University of Tennessee, Department of Geological Sciences Studies in Geology, v. 24, p. 91-128.

Connelly, J. B., and Dallmeyer, R. D., 1993, Polymetamorphic evolution of the western Blue Ridge: Evidence from $^{40}Ar/^{39}Ar$ whole-rock slate/ phyllite and muscovite ages: American Journal of Science, v. 293, p. 322-359.

Connelly, J. B., and Woodward, N. B., 1992, Taconian foreland-style thrust system in the Great Smoky Mountains, Tennessee: Geology, v. 20, p. 177-180.

Dallmeyer, R. D., 1988, Late Paleozoic tectonothermal evolution of the western Piedmont and eastern Blue Ridge, Georgia: Controls on the geochronology of terrane accretion and transport in the southern Appalachian orogen: Geological Society of America Bulletin, v.100, p. 702-713.

Davidson, G. L., 1995, The tectono-metamorphic history of a portion of the eastern Blue Ridge, Jackson County, North Carolina [unpublished M.S. thesis]: Knoxville, University of Tennessee, 157 p.

Davis, R. A., Jr., 1992, Depositional systems: An introduction to sedimentology and stratigraphy: 2nd ed., Englewood Cliffs, New. Jersey, Prentice-Hall, 604 p.

De Windt, J. T., 1975, Geology of the Great Smoky Mountains, Tennessee and North Carolina, with road log for field excursion, Knoxville-Clingman's Dome-Maryville: Compass, v. 52, p. 73-129.

Dickinson, W. R., 1984, Interpreting provenance relations from detrital modes of sandstones, in Zuffa, G. G., ed., Provenance of Arenites: NATO Advanced Study Institute on Reading Provenance of Arenites, series C, v. 148, p. 333-363, Coanza, Italy, D. Riedel Pub. Co.

Drake, A. A., Jr., Sinha, A. K., Laird, J., and Guy, R. E., 1989, The Taconic orogen, in Hatcher, R. D., Jr., Thomas, W. A., and Viele, G. W., eds., The Appalachian-Ouachita orogen in the United States: Boulder, Colorado, Geological Society of America, The geology of North America, v. F-2, p. 101-177.

Eckert, J. O., Hatcher, R. D., Jr., and Mohr, D. W., 1989, The Wayah granulite-facies metamorphic core, southwestern North Carolina: High grade culmination of Taconic metamorphism in the southern Blue Ridge: Geological Society of America, v. 101, p. 1434-1447.

Folk, R. L., 1974, Petrology of sedimentary rocks: Austin Texas, Hemphill Publishing, 162 p.

Force, E. R., 1976, Metamorphic source rocks of Titanium placer deposits - a geochemical cycle: U.S. Geological Survey Professional Paper 959-B, 16 p.

Hadley, J. B., 1970, The Ocoee Series and its possible correlatives, in Fisher, G. W., Pettijohn, F. J., Reed, J. C., and Weaver, K. N., eds., Studies of Appalachian geology: Central and southern: New York, Interscience Publishers, p. 247-259.

Hadley, J. B., and Goldsmith, R, 1963, Geology of the eastern Great Smoky Mountains, North Carolina and Tennessee: U.S. Geological Survey Professional Paper 349-B, 118 p.

Hadley, J. B., and Nelson, A. E., 1971, Geologic map of the Knoxville quadrangle, North Carolina, Tennessee, and South Carolina: U. S. Geological Survey Miscellaneous Investigations, Map I-654, scale 1:250,000.

Hatcher, R. D., Jr., 1971, Geology of Rabun and Habersham Counties, Georgia: A reconnaissance study: Georgia Geological Survey Bulletin, 83, 43 p.

Hatcher, R. D., Jr., 1978, Tectonics of the western Piedmont and Blue Ridge, southern Appalachians: Review and speculation: American Journal of Science, v. 278, p. 276-304.

Hatcher, R. D., Jr., 1987, Tectonics of the southern and central Appalachians internides: Annual Reviews of Earth and Planetary Science Letters, v. 5, p. 337-362.

Hatcher, R. D., Jr., 1989, Tectonic synthesis of the U.S. Appalachians, in Hatcher, R. D., Jr., Thomas, W. A., and Viele, G. W., eds., The Appalachian-Ouachita orogen in the United States: Boulder, Colorado, Geological Society of America, The geology of North America, v. F-2, p. 511-535.

Hatcher, R. D., Jr., and Butler, J. R., 1979, Guidebook for southern Appalachian field trip in the Carolinas, Tennessee and northeastern Georgia: International Geological Correlation Program: Caledonides project 27, University of North Carolina, Chapel Hill 117 p.

Hatcher, R. D., Jr., and Goldberg, S. A., 1991, The Blue Ridge geologic province, in Horton, J. W., Jr., and Zullo, V. A., eds., The geology of the Carolinas-Carolina Geological Society 50th Anniversary Volume: Knoxville, TN, The University of Tennessee Press, p. 11-35.

Hatcher, R. D., Jr., Merschat, C.E., Wiener, L. S., and Quinn, M. J., 1991, Basement-cover relationships in the Carolinas and Georgia Blue Ridge: Problems with contacts and correlations: Geological Society of America Abstracts with Programs, v. 23, p. 43.

Hatcher, R. D., Jr., Thomas, W. A., Geiser, P. A., Snoke, A. W., Mosher, S., and Wiltschko, D. V., 1989, Alleghanian orogen, in Hatcher, R. D., Jr., Thomas, W. A., and Viele, G. W., eds, The Appalachian-Ouachita orogen in the United States: Boulder, Colorado, Geological Society of America, The Geology of North America, v. F-2, p. 233-318.

Hatcher, R., D., Jr., Acker, L. L., Bryan, J. G., and Godfrey, S. C., 1979, The Hayesville thrust of the central Blue Ridge of North Carolina and nearby Georgia: A pre-metamorphic, polydeformed thrust and cryptic suture within the Blue Ridge thrust sheet: Geological Society of America Abstracts with Programs, v. 11, p. 181.

Hess, H. H., 1955, Serpentines, orogeny, and epirogeny: Geological Society of America Special Paper 62, p. 391-408.

Hopson, J. L., Hatcher, R. D., Jr., and Stieve, A. L., 1989, Geology of the eastern Blue Ridge, northeastern Georgia and the adjacent Carolinas: Georgia Geological Society Guidebook, v. 9, p. 1-40.

Hurlbut, C. S., 1971, Dana's manual of mineralogy: New York, John Wiley & Sons, 579 p.

Ingersoll, R. V., and Busby, C. J., 1995, Tectonics of sedimentary basins, in Busby, C. J., and Ingersoll, R. V., eds., Tectonics of Sedimentary Basins: Cambridge, MA, Blackwell Science, p. 1-52.

Keith, A., 1904, Description of the Asheville quadrangle (Tennessee and North Carolina): U.S. Geological Survey Atlas, Folio 116, 10 p.

Keller, F. B., 1980, Late Precambrian stratigraphy, depositional history, and structural chronology of part of the Tennessee Blue Ridge: [unpublished Ph. D. thesis], Yale University, 351 p.

Keller, G. R., Lidiak, E. G., Hinze, W. J., and Braile, L. W., 1983, The role of rifting in the tectonic development of the midcontinent, U.S.A.: Tectonophysics, v. 94, p. 391-412.

King, P. B., Hadley, J. B., Neuman, R. B., and Hamilton, W., 1958, Stratigraphy of Ocoee Series, Great Smoky Mountains, Tennessee and North Carolina: Geological Society of America Bulletin, v. 69, p. 947-966.

King, P. B., 1963, Geology of the central Great Smoky Mountains: U. S. Geological Survey Professional Paper 349-C,

Kittleson, R., 1988, The amphibolite-to-granulite facies transition in the Franklin and Corbin Knob quadrangles, North Carolina Blue Ridge: [unpublished M.S. thesis]: Knoxville, University of Tennessee, 111 p.

Larrabee, D. M., 1966, Map showing distribution of ultramafic and intrusive mafic rocks from northern New Jersey to eastern Alabama: USGS, Miscellaneous geologic investigations, Map I-476, Sheet 1, scale 1:500.000.

Leeder, M. R., 1995, Continental and proto-oceanic rift troughs, in Busby, C. J., and Ingersoll, R. V., eds., Tectonics of sedimentary basins: Cambridge, MA, Blackwell Science, p. 120-148.

Lewis, D. W., and McConchie, D., 1994, Practical sedimentology: New York, Chapman & Hall, 220 p.

Lister, G. S., Etheridge, M. A., and Symonds, P. A., 1986, Detachment faulting and the evolution of passive continental margins: Geology, v. 14, p. 246-250.

Lister, G. S., Etheridge, M. A., and Symonds, P. A., 1991, Detachment models for the formation of passive margins: Tectonics, v. 10, p. 1038-1064.

McClellan, E. A., 1988, Geologic history of a portion of the eastern Blue Ridge, southern Appalachians: Tray Mountain and Macedonia 7 1/2' quadrangles, Georgia: [unpublished M.S. thesis], University of Tennessee, Knoxville, 179 p.

Miller, C.J., Hatcher, R. D., Jr., Gorish, E. B, Harrison, T. M., and Coath, C., in press, Ages of plutonism, granulite facies metamorphism, and oldest basement in the southern appalachian orogen, SW North Carolina - NE Georgia: high resolution ion probe dating of zircon and monazite: Geological Society of America Abstracts with Programs.

Milton, D. J., 1983, Garnet-biotite geothermometry confirms the premetamorphic age of the Greenbrier fault, Great Smoky Mountains, North Carolina: Geological Society of America Abstracts with Programs, v. 15, p. 90.

Misra, K. C., and McSween, H. Y., Jr., 1984, Mafic rocks of the southern Appalachians: A review: American journal of Science, v. 284, p. 294-318.

Misra, K., C., and Keller, F. B., 1978, Ultramafic bodies in the southern Appalachians: A review: American Journal of Science, v. 278, p. 389-418.

Normark, W. R., Posamentier, H., and Mutti, E., 1993, Turbidite systems: State of the art and future directions: Reviews of Geophysics, v. 31, p. 91-116.

North Carolina Geological Survey, 1985, Geologic map of North Carolina: North Carolina Department of Natural Resources and Community Development, Division of Land Resources, scale 1:500,000.

Odom, A. L., and Fullgar, P. D., 1984, Rb-Sr whole-rock and inherited zircon ages of the plutonic suite of the Crossnore Complex, southern Appalachians, and their implications regarding the time of opening of the Iapetus Ocean, in Bartholomew, M. J., ed., The Grenville event in the Appalachians and related topics: Geological Society of America Special Paper 194, p. 255-262.

Ori, G. G, 1989, Geologic history of the extensional basin of the Gulf of Corinth (?Miocene-Pliocene), Greece: Geology, v. 17, p. 918-921.

Quinn, M. J., 1991, Two lithotectonic boundaries in western North Carolina: Geologic interpretation of a region surrounding Sylva, Jackson County [unpublished M.S. thesis]: Knoxville, University of Tennessee, 223 p.

Quinn, M. J., and Wright, J. E., 1993, Extension of Middle Proterozoic (Grenville) basement into the eastern Blue Ridge of southwestern North Carolina: Results from U-Pb geochronology: Geological Society of America Abstracts with Programs, v. 25, p. A483.

Ramsay, J. G., 1967, Folding and fracturing of rocks: New York, McGraw-Hill, 568 p.

Rankin, D. W., 1975, The continental margin of eastern North America in the southern Appalachians: The opening and closing of the Proto-Atlantic Ocean: American Journal of Science, v. 275-A, p. 298-336.

Rankin, D. W., Drake, A. A., Jr., Glover, L., III, Goldsmith, R., Hall, L. M., Muray, D. P., Ratcliff, N. M., Read, J. F., Secor, D. T., Jr., and Stanley, R. S., 1989, Pre-orogenic terranes, in Hatcher, R. D., Jr., Thomas, W. A., and Viele, G. W., eds., The Appalachian-Ouachita orogen in the United States: Boulder, Colorado, Geological Society of America, The geology of North America, v. F-2, p. 7-100.

Rankin, D. W., Espenshade, G. H., and Shaw, K. W., 1973, Stratigraphy and structure of the metamorphic belt in northwestern North Carolina and southwestern Virginia: A study from the Blue Ridge across the Brevard fault zone to the Sauratown Mountains anticlinorium: American Journal of Science, Cooper v. 273-A, p. 1-40.

Rast, N., and Kohles, K. M., 1986, The origin of the Ocoee Supergroup: American Journal of Science, v. 286, p. 593-616.

Rodgers, J., 1972, Latest Precambrian (Post-Grenville) rocks of the Appalachian

region: American Journal of Science, v. 272, p. 507-520.

Schoch, R. M., 1989, Stratigraphy, principles and methods: New York, Van Nostrand Reinhold, 375 p.

Shanmugam, G., Damuth, J. E., and Moiola, R. J., 1985, Is the turbidite facies association scheme valid for interpreting ancient submarine fan environments?: Geology, v. 13, p. 234-237.

Simpson, C., and Kalaghan, T., 1989, Late Precambrian crustal extension preserved in Fries fault zone mylonites, southern Appalachians: Geology, v. 17, p. 148-151.

Stow, D. A. V., Howell, D. G., and Nelson, C. H., 1985, Sedimentary, tectonic, and sea-level controls in submarine fans and related turbidite systems, in Bouma, A. H., Normark, W. R., and Barnes, eds., Frontiers in sedimentary geology: New York, Springer-Verlag, p. 15-22.

Thomas, W. A., 1991, The Appalachian-Ouachita rifted margin of southeastern North America: Geological Society of America Bulletin, v. 103, p. 415-431.

Wagoner, J. C., Van, 1995, Overview of sequence stratigraphy of foreland basin deposits: Terminology, summary of papers, and glossary of sequence stratigraphy, in Wagoner, J. C. Van, and Bertram, G. T., Sequence stratigraphy of foreland deposits: American Association of Petroleoum Geologists Memoir 64, p. ix-xxi.

Wehr, F., and Glover, L., III, 1985, Stratigraphy and tectonics of the Virginia-North Carolina Blue Ridge: Evolution of a late Proterozoic-early Paleozoic hinge zone: Geological Society of America Bulletin, v. 96, p. 285-295

Wernicke, B., 1985, Uniform-sense normal simple shear of the continental lithosphere: Canadian Journal of Earth Sciences, v. 22, p. 108-125.

Wernicke, B., and Axen, G. J., 1988, On the role of isostasy in the evolution of normal fault systems: Geology, v. 16, p. 848-851.

Williams, H., and Hiscott, R. N., 1987, Definition of the Iapetus rift-drift transition in western Newfoundland: Geology, v. 15, p. 1044-1047.

Woodward, N. B., Connelly, J. B., Walters, R. R., and Lewis, J. C., 1991, Tectonic evolution of the Great Smoky Mountains: Studies of Precambrian and Paleozoic stratigraphy in the western Blue Ridge, in, Kish, S. A., ed.: Carolina Geological Society field trip guide, p. 57- 68.

APPENDICES

APPENDIX A: MODAL ANALYSES

Table A..1. Modal analyses percentages, and percentages for the Q-F-M diagrams. Fsp: feldspar. Plag: plagioclase. Mu: muscovite. B: biotite. G: garnet. St: staurolite. Ky: kyanite. Si: sillimanite. Q: quartz. F: feldspar content. M: mica-clay content.

Sample and unit	Location	n	Quartz	K-Fsp	Plag.	Fsp	Mu.	B.	G.	St.	Ky.	Si.	Total	Q	F	M
6.2.1a Thunderhead Ss.	83°4'54" W 35°30'56"N	801	48	0	0	35	0	17	0	0	0	0	100	48	35	17
25.4.9 Longarm Qzte	83°5'16"W, 35°30'28"N	1069	79	0	0	6	14	0	0	0	0	0	100	79	6	14
25.1.5 Longarm Qzte	83°6'12"W 35°33'4"N	1845	72	3	19	0	3	1	0	0	0	0	99	72	23	5
1.2.6 Thunderhead Ss.	83°4'46"W 35°31'44"N	798	52	0	32	0	8	7	0	0	0	0	100	52	32	15
31.7.8 Thunderhead Ss.	83°7'44"W 35°28'43"N	1000	52	0	0	30	3	15	0	0	0	0	100	52	30	18
6.2.6 Longarm Qzte.	83°4'49"W 35°31'12"N	3520	73	0	5	0	20	1	0	0	0	0	100	73	5	21
29.12.4 Thunderhead Ss.	83°3'21"W 35°29'55"N	518	58	0	0	23	19	0	0	0	0	0	100	58	23	19
26.7.8 Longarm Qzte.	83°9'19"W 35°30'51"N	999	86	0	0	5	9	0	0	0	0	0	100	86	5	9
21.6.13 Thunderhead Ss.	83°9'15"W 35°29'41"N	1000	55	0	0	35	0	10	0	0	0	0	100	55	35	10
15.4.13 Longarm Qzte.	83°4'18"W 35°33'6"N	649	86	0	0	8	4	2	0	0	0	0	100	86	8	6
3.5.4b Longarm Qzte.	83°6'11"W 35°32'9"N	833	76	1	17	0	2	3	0	0	0	0	99	76	18	5
19.4.2d Thunderhead Ss.	83°1'57"W 35°30'33"N	1029	23	0	7	0	14	35	17	5	0	0	100	23	7	71
1.2.4 Thunderhead Ss.	83°5'2"W 35°31'44"N	1051	34	5	10	0	21	21	3	4	2	0	100	34	15	51
22.2.11 Thunderhead Ss.	83°4'46"W 35°31'59"N	1080	23	4	10	0	31	25	7	0	0	0	100	23	14	63
19.4.10 Thunderhead Ss.	83°2'12"W 35°30'17"N	870	12	0	0	0	63	13	11	0	0	0	100	12	0	88
Elkmont Elkmont Ss.	83°2'41"W 35°37'57"N	522	45	0	0	0	20	33	1	0	0	0	100	45	0	55
26.1.1 Elkmont Ss.	83°4'58"W 35°33'2"N	1033	34	9	7	0	31	10	8	0	1	0	100	34	16	50

APPENDIX B: STRUCTURAL DATA

Station	Bedding	Foliation	Joints	Axial planes	Lineation	Hinges	Crenulation axis
9.8.1		42 80 E					
9.8.2		40 87 E	50 40 W		57 220		
9.8.3						45 180	40 192
9.8.4		46 36 S				35 295	
11.8.1		160 39 W					
11.8.2		122 40 S					
11.8.3		40 85 N				55 210	
11.8.4		50 90					
11.8.5		70 50 S				39 220	
11.8.6						62 160	
11.8.7							
12.8.2		210 77 E					
12.8.3		50 75 S					
12.8.4		45 68 S				50 180	
12.8.5	46 78 S		100 23 N		41 195		
16.8.1		205 50 E			9 195		
16.8.2		10 44 E	90 55 N				
17.8.1		185 51 E					
17.8.2		N-S 55W			40 240		
18.8.1		142 70 S			5 142		
18.8.2		170 60 E					
18.8.3		15 60 W					
18.8.4		145 46 W	260 50 N				
20 8.1		55 55 S	65 35 N				
20.8.2		46 65 E					50 90
20.8.3		41 45 S				6 225	
20.8.4		85 50 N					
20.8.5		225 75 E					
22.8.1		130 35 N			39 70		
22.8.2			50 60 S				
22.8.3							
22.8.4				165 30 E		22 60	
22.8.5		30 65 S					
23.8.1						25 65	
23.8.2		35 65 N	30 20 E				
27.12.1				50 85 S			
27.12.2				45 85 S			
27.12.3		50 65 S					
27.12.4		65 90					
27.12.5		65 90		75 72 S		67 120	
27.12.6						45 55	
29.12.1		50 90					
29.12.2		50 87 S					
29.12.3		56 85 N					
29.12.4		70 78 N					
29.12.6							
31.12.1		45 70 S	86 22 N		10 51		

Station	Bedding	Foliation	Joints	Axial planes	Lineation	Hinges	Crenulation axis
31.12.2		45 75 S		25 55 S	26 50	40 55	
31.12.3		70 77 N					
31.12.4		65 72 S					
2.1.1		75 80 N					
2.1.2		70 86 S			34 80		
2.1.3		70 70 S	55 45 S				
2.1.4		130 90		90 90		85 82	
2.1.5		90 65 S		72 62 S			
13.1.1							
13.1.2		250 60 S					
13.1.3		90 75 S					
13.1.4					40 100		
13.1.5		100 70 S					
13.1.6		55 S					
16.1.1	30 62 E				40 187		
16.1.2		45 80			55 199		
16.1.3		23 80 E			40 195		
16.1.4		45 50 E			44 170		
16.1.5	150 54 W				25 170		
17.1.1		45 50 E					
17.1.2		20 62 E					
17.1.3		15 65 E					
17.1.4					60 205	40 40	
18.1.1					52 350		
18.1.2		27 71 W			55 230		
18.1.3		5 72 E					
18.1.4		5 80 E					
18.1.5		10 55 E					
19.1.1		35 70 E					
23.1.1	40 61 N						
23.1.2	50 25 S						
23.1.3	80 74 S						
23.1.4	45 60 S						
23.1.5		34 65 N			20 210		
23.1.6		30 65 S					
23.1.7		30 62 S					
24.1.1		46 80 S					
24.1.3	25 55 W				25 215		
24.1.4	65 70 S		100 63 N				
24.1.5	25 42 E						
24.1.6						26 225	
24.1.7		53 86 S					
24.1.8	50 80 S						
25.1.1		30 85 E					
25.1.2	50 55 S				20 220		
25.1.3	40 75 S						
25.1.4	40 55 S						

Station	Bedding	Foliation	Joints	Axial planes	Lineation	Hinges	Crenulation axis
25 1.5	45 75 S						
25.1.6	40 67 S						
25.1.7							
25.1.8		55 60 S					
25.1.9					20 210		
26.1.1		40 74 S		43 85 S		15 220	
26.1.2	75 50 S		150 72 W				
26.1.3		20 70 E					
26.1.4		25 40 E					
26.1.5		28 90					
26.1.6		60 60 S	50 60 S				
31.1.1		45 40 S					
31.1.2		60 45 S			15 55		
31.1.3		50 50 S			30 190		
31.1.4		15 50 W					
31.1.5		125 35 N					
31.1.6		155 32 N		25 80 W		25 35	
31.1.7		50 35 S					
31.1.8		60 80 S					
31.1.9		45 70 N		0 90		72 185	
1.2.1		95 20 N					
1.2.2		15 60 W					
1.2.3		40 70 W	120 84 S		35 235		
1.2.4		35 90		45 90		15 25	45 90
1.2.5				5 66 E		12 15	
1.2.6	20 47 E						
3.2.1		5 47 W			54 244		
3.2.2				30 44 S		52 42	
3.2.3				25 67 E		10 30	
3.2.4		0 6 W		45 60 S		10 200	
3.2.5		25 60 W			30 210		
3.2.6						22 235	
6.2.1		45 42 S					
6.2.2	20 50 E						
6.2.3	25 45 E						
6.2.4	30 52 S	30 52 S		30 52 S		10 10	
6.2.5		25 50 S					
6.2.6							
9.2.1		56 80 S					
9.2.2	5 65 W	0 30 W					
9.2.3	50 60 N						
9.2.4		35 65 N					
9.2.5	10 30 N						
9.2.6							
9.2.7		14 70 E		15 60 E		48 40	
14.2.1		20 60 W					
14.2.2		46 80 N					

Station	Bedding	Foliation	Joints	Axial planes	Lineation	Hinges	Crenulation axis
14.2.3		25 80 E					
14.2.4		20 70 E					
14.2.5		30 80 E					
18.2.1		26 70 S					
18.2.2		30 70 S					
18.2.3		30 70 S					
18.2.4	35 65 S						
18.2.5	6 70 E						
18.2.6	36 70 S						
18.2.7	20 67 S		50 45 N				
18.2.8							
18.2.9	20 80 E						
18.2.11		20 55 E					
18.2.12	25 80 E						
18.2.13	20 45 E						
18.2.14	0 65 E						
18.2.15	50 60 S						
18.2.16	34 57 S						
18.2.17		40 75 S					
18.2.18		40 67 S					
18.2.19		30 75 E			50 190		
19.2.1		35 62 S					
19.2.2		50 55 S					
19.2.3	40 65 S				40 210	57 95	
19.2.4		20 70 E					
19.2.5	355 60 E						
19.2.6	20 60 W						
19.2.7		70 55 S		15 66 E			65 100
19.2.8	25 70 E						
19.2.9	20 50 S						
19.2.10	35 65 S						
19.2.11		27 70 E					
19.2.12		50 75 S					
19.2.13		54 90					
21.2.1		70 89 S					
21.2.2		70 50 S					
21.2.4							45 70
22.2.2							75 190
21.2.3		70 55 S			50 205		
21.2.4		10 50 E		150 30 E			45 70
22.2.1		10 55 S					
22.2.2		100 62 S					75 190
22.2.3		90 35 S					
22.2.4		130 60 S					
22.2.5		30 55 S					
22.2.6		75 75 S					
22.2.7		50 50 S					

Station	Bedding	Foliation	Joints	Axial planes	Lineation	Hinges	Crenulation axis
22.2.8	15 50 E						
22.2.9		12 54 E					
22.2.10		40 75 S					
22.2.11		150 45 E		20 65 E		50 55	
22.2.12		15 40 E		62 65 S			
22.2.13		35 52 E					
22.2.14	5 50 E						
22.2.15	15 45 E						
23.2.1		35 80 S		60 40 S			18 227
23.2.2		40 75 S					
23.2.3		55 80 S					
23.2.4		90 55 S		15 70 E			50 140
23.2.5		105 35 S					
23.2.6		50 25 S					
23.2.7		125 44 S					
23.2.8	60 25 N					150 0	
23.2.9		140 50 W					
23.2.10		65 30 S					
23.2.11	165 80 E						
23.2.12		5 65 E					
23.2.13		50 60 S					
23.2.14		15 78 W					
23.2.15		170 65 E		0 90		50 180	
23.2.16	30 20 E			40 65 E		10 40	
25.2.1	50 55 S				35 204		
25.2.2		50 65 S					
25.2.3		50 75 N					
25.2.4	40 75 S						
25.2.5		50 72 N					
25.2.6	30 60 S						
25.2.7	40 75 S		100 55 N		35 202		
25.2.8		50 80 S			50 205		
25.2.9		25 75 S					
25.2.10		15 90					
25.2.11	50 65 S						
25.2.12	30 80 N						
25.2.13		120 45 S					
25.2.14					30 205		
25.2.15					25 200		
2.3.1	39 65 S						
2.3.2		37 75 E					
2.3.3	20 60 S						
2.3.4	30 50 S						
2.3.5	50 55 S						
2.3.7		65 60 S			55 155		
12.3.1		50 65 S					
12.3.2		51 55 S			50 175		

Station	Bedding	Foliation	Joints	Axial planes	Lineation	Hinges	Crenulation axis
12.3.3		40 50 S			40 180		
12.3.4	45 40S						
12.3.5	45 45 S						
12.3.6		50 35 S					
12.3.7		30 74 S					
12.3.8		25 90					
12.3.9		40 65 S		25 90		35 186	
12.3.10		5 50 E					
12.3.11		35 50 S					
12.3.13		35 55 S					
12.3.14		40 58 S					
12.3.15		20 75 E					
12.3.16		25 77 S					
12.3.17		35 65 S					
12.3.18		20 65 S					
13.3.1		45 50S			39 175		
13.3.2	35 55 S				24 195		
13.3.3		50 45 S					
13.3.4		35 65 S					
13.3.5	50 50 S						
13.3.6		30 65 S					
13.3.7	20 65 S						
13.3.8		20 65 S					
13.3.9		50 55 S					
13.3.10		50 85 S					
13.3.11		30 80 E					
13.3.12		41 54 S					
13.3.13		60 60 S					
13.3.14		50 70 S					
13.3.15		40 65 S					30 210
13.3.16		35 53 S					
13.3.17		50 55 S					
13.3.18		30 55 S					
14.3.1		110 60 S			20 225		
14.3.2		30 30 N					25 300
14.3.3	55 57 S						
14.3.4		105 50 S			40 200		
14.3.5		345 40		75 64 S		20 80	30 35
14.3.6		0 65 W			44 210		
14.3.7		340 45 W			52 225		
14.3.8		60 55 S					
14.3.9							
14.3.10		265 50 S			50 200		
14.3.11					55 200		
14.3.12		0 90					
15.3.1	50 55 S						
15.3.2	50 55 S				20 210		

Station	Bedding	Foliation	Joints	Axial planes	Lineation	Hinges	Crenulation axis
15.3.3		40 80 S					
15.3.4		60 80 S					
15.3.5		20 70 W					
15.3.6		45 70 S					
15.3.7	60 46 S						
15.3.8	45 30 S						
15.3.9	65 40 S						
15.3.10	60 55 S				17 215		
15.3.11		115 55 S					
15.3.12		35 55					
15.3.13	27 57 S				10 35		
15.3.14	50 60 S		150 90		40 205		
15.3.15	45 55 S		145 75 E		40 195		
15.3.16	45 60 S				19 200		
15.3.17		350 70 W				40 195	
15.3.18					45 210		
19.3.1		80 40 S			25 210		
19.3.2		50 52 S	70 25 N		45 180		
19.3.5							
19.3.6		70 57 S			70 155		
19.3.7		45 50 S			40 165		
19.3.8		55 45 S	36 75 N		45 180		
19.3.9		60 65 S					
19.3.10		70 35 S					
19.3.11		70 50 S					
19.3.13		90 30 S					
19.3.14		80 40 S			33 170		
21.3.2		57 80 S					
21.3.3		30 65 S					
21.3.4		54 49 S	5 90		56 170		
21.3.5		36 45 S			35 174		
21.3.6		40 75 S					
21.3.7		45 65 S					
21.3.8		38 60 S					
21.3.9		38 62 S			30 195		
21.3.10	25 36 S						
21.3.11		10 90					
21.3.12	15 70 W				20 205		
21.3.13					15 200		
22.3.1		45 60 S			42 195		
22.3.2					60 190		
22.3.3					40 190		
22.3.4		40 60 S	135 70 S		55 170		
22.3.5		10 50 E					
22.3.6		24 75 S					
22.3.7		40 55 N					
22.3.8		75 30 N					

Station	Bedding	Foliation	Joints	Axial planes	Lineation	Hinges	Crenulation axis
22.3.9		60 64 S			30 215		
22.3.10		10 80 E					
22.3.11		15 75 E					
28.3.1		65 44 S			24 90		
28.3.2		40 55 S		20 36S		25 50	
28.3.3				54 82 N		25 60	
28.3.4		75 40 N		60 90		20 60	
28.3.5		56 72 N					
28.3.6		50 52 N					
28.3.7		68 80 N			27 70		
28.3.8		85 80 S			30 90		
28.3.10		60 77 S			45 80		
28.3.11		55 85 S			60 50		
28.3.12		75 80 S					
28.3.13		65 40 S					
28.3.14		72 75 S		76 46 S		15 75	
28.3.15		100 80 S					
28.3.16	50 64 S						
28.3.17		45 80 N					
28.3.18		65 70 N					
28.3.20		130 40 N		50 90			25 50
28.3.21		95 42 S					40 220
1.4.1	45 70 S						
1.4.2	40 65 S				45 165		
1.4.3	45 55 S				50 190		
1.4.4		40 65 S					
1.4.5		20 70 S					
1.4.6		40 90			3 40		
1.4.7							18 15
1.4.8		44 77 S					
1.4.9		25 26 S		10 45 E		5 10	
1.4.10		30 35 S			10 170		
1.4.11	0 50 E						40 95
1.4.12		55 41 S		55 41 S		36 165	
1.4.13		60 52 S			60 180		
1.4.14	55 66 S						
1.4.15		55 50 S					
1.4.16		95 50 S			35 165		
1.4.17		35 40 S			35 150		
1.4.18		60 45 S					
1.4.19	45 40 S			110 50 S		30 140	
3.4.1		24 58 S					
3.4.2				165 55 S			65 85
3.4.3	47 62 S						
3.4.4		45 53 S					
3.4.5				147 27 E		30 55	
3.4.6	12 55 S	15 47 S		80 65 S			

Station	Bedding	Foliation	Joints	Axial planes	Lineation	Hinges	Crenulation axis
3.4.7				24 51 E		40 110	
3.4.9	50 65 S						
3.4.10	90 65 S						
3.4.12	45 64 S						
3.4.13	65 70 S						
3.4.14		35 58 S					
3.4.15	60 75 S						
3.4.16		45 70 N					
3.4.17		25 80 S					
3.4.18		40 60 S					
3.4.19		40 90					
3.4.20	45 57 S						
11.4.1		56 56 S					
11.4.2		25 65 S					35 50
11.4.3		40 57 S					
11.4.4		45 35 S			45 225		19 200
11.4.5		10 25 N					
11.4.6		20 70 S					
11.4.7		30 84 S					
11.4.8	45 58 S						
11.4.9				90 10 S	25 230		7 235
13.4.2		60 72 S					
13.4.3	25 45 S						
13.4.4		30 33 S					
13.4.5		115 70 S					
13.4.6		0 42 E			15 10		
13.4.7		45 40 S					
13.4.8		40 50 S			40 350		
13.4.9		10 45 W					
13.4.10		0 60 W					30 200
13.4.11	40 85 S						
13.4.12		35 35 S					
13.4.13	35 30 N						
13.4.14	45 55 S						
14.4.1		35 76 S					
14.4.2	40 55 S						
14.4.3	30 60 S						
14.4.5		15 65 W		95 35 S			45 210
14.4.6		20 70 W					
14.4.7		24 44 N					
14.4.8	20 20 W						
14.4.9		35 90					
14.4.10		10 65 W					
14.4.11		80 25 S					
14.4.12		60 68 N					
14.2.13		50 65 S					
15.4.1		15 65 E			38 165		

Station	Bedding	Foliation	Joints	Axial planes	Lineation	Hinges	Crenulation axis
15.4.2	90 45 S			22 70 E		50 180	45 195
15.4.3		80 40 S					60 175
15.4.4		65 45 S					48 150
15.4.5		55 55 S					
15.4.6							45 190
15.4.7		70 50 S		10 75 E			50 180
15.4.8	40 50 S						
15.4.9		350 75 N					
15.4.10		100 60 S					55 175
15.4.11	120 90						
15.4.12	65 45 S						41 165
15.4.13	145 40 S						
15.4.14							
19.4.1		110 75 N		330 55		41 330	
19.4.2	65 90				13 60		
19.4.3		70 90					
19.4.4		25 50 E		210 65E		65 170	
19.4.5		55 74 S					
19.4.6		55 75 S					30 60
19.4.7		85 90					
19.4.8		65 90					
19.4.9		75 80 S	170 65 W			29 200	
19.4.10		30 90					
19.4.11		150 70 W					
19.4.12		55 65 S					
19.4.13		65 55 E					
19.4.14	90 60 S						
20.4.1		75 60 S					50 125
20.4.2		40 45 S					44 85
20.4.3		80 40 S					48 65
20.4.4		75 40 S					
20.4.5		55 55 S					
20.4.6		64 64 S			57 200		
20.4.7		65 70 S					
20.4.8		90 42 S					
20.4.9		80 24 S		80 24 S			34 165
20.4.10	138 51 W		80 45 N	35 70 E			50 164
20.4.11		0 90					30 185
20.4.12		60 47 S			45 140		
20.4.13		25 64 S		25 64 S			52 170
20.4.14	30 60 S						
20.4.15		60 46 S					
20.4.16		40 50 S					
20.4.17		55 30 S					
22.4.1		10 70 W					
22.4.2		10 70 W			9 180		
22.4.3		25 55 W		40 90		25 207	

Station	Bedding	Foliation	Joints	Axial planes	Lineation	Hinges	Crenulation axis
22.4.4	0 50 N						
22.4.5	0 65 W						
22.4.6	0 65 W						
22.4.7		0 90					
22.4.8				0 85 W			17 200
22.4.9	60 35 N						
22.4.10		95 45 S		62 25 E		30 190	32 191
22.4.11		125 26 S					25 185
22.4.12		35 55 E					
22.4.13	21 47 S						25 180
22.4.14	130 40 S						
24.4.1	86 25 S						
24.4.3	112 29 N						
24.4.4		54 52 S					
24.4.5	50 65 S						
24.4.6	40 90						
24.4.7	45 80 S						
24.4.8	0 54 E						
24.4.9		40 51 S					60 140
24.4.10							45 30
24.4.11	60 70 S						
24.4.12	50 80 S						
25.4.1		80 21 N			15 50		
25.4.2		100 20 N					
25.4.3		40 65 S					
25.4.4		155 60 W					
25.4.5		120 55 N					
25.4.6		137 65 N					17 314
25.4.7	5 76 E						
25.4.8	21 65 E						
25.4.9	0 61 E						
25.4.10		60 90					
1.5.1		27 90			80 310		
1.5.2		25 80 W					
1.5.3	15 26W						
1.5.4		16 44 W		175 20 E		14 15	
1.5.5		0 75 W					29 170
1.5.6	50 40 N						
1.5.7	10 35 E						10 220
1.5.8		15 50 E					
2.5.1		90 20 S					
2.5.2		165 35 W					
2.5.3		0 0					10 170
2.5.4		10 15 W		15 65 E			206 205
2.5.5		15 30 W				21 210	
2.5.6		60 46 N		45 85 E			4 225
2.5.7		70 32 S					15 215

Station	Bedding	Foliation	Joints	Axial planes	Lineation	Hinges	Crenulation axis
2.5.8		120 31 N	95 90				
2.5.9		60 75 S					50 200
3.5.1		25 85 E			49 210		
3.5.2		44 60 E					
3.5.3		90 65 S					
3.5.4	50 60 S	45 52 E					
3.5.5		30 70 S					
3.5.6		40 75 E					
3.5.7						14 52	26 210
5.5.1		80 26 S		15 70 E			13 190
5.5.2		75 36 S					10 195
5.5.3		58.36 S					
5.5.4		46 55 S					
5.5.5	87 36 S						
5.5.6		0 50 E					
5.5.7		70 44 S					
5.5.8		50 26 N					
5.5.9		45 55 S					
5.5.10		20 62 E					11 184
5.5.11		0 0					24 165
5.5.12		14 40 E					30 170
5.5.13		24 62 E					
5.5.14		35 62 E					
5.5.15		18 69 W		120 30 N			8 20
5.5.16	30 40 W						
5.5.17	30 90						
5.5.18		0 60 W					
5.5.19		20 90					
5.5.20		160 60 E					
5.5.21		10 80 W					
5.5.22		160 77 W		90 32 S			38 162
5.5.23		170 64 E					
5.5.24		165 90					76 145
5.5.25		140 90					
5.5.26		140 90					50 165
5.5.27		110 50 S					
5.5.28		140 77 S					
5.5.29		145 74 W					
5.5.30		70 90					
8.5.1		52 85 S					
8.5.2	20 40 W						
8.5.3		65 80 S			27 245		
8.5.4		90 80 N					
8.5.6		70 85 N			0 0		
8.5.7		55 76 S					
8.5.8		70 75 N					
10.5.1		66 60 S			46 200		

Station	Bedding	Foliation	Joints	Axial planes	Lineation	Hinges	Crenulation axis
10.5.2	40 45 N						
10.5.3	50 80 N						
10.5.4	40 65 N				42 245		
10.5.5	40 70 S		130 70 S		40 208		
10.5.6	40 80 S						
10.5.7	40 75 N						
10.5.8	55 82 N	50 80 N					
10.5.9		36 77 W		170 40 E			19 10
10.5.10				175 35 E			21 30
10.5.11	120 70 N			10 57 E			45 90
10.5.12	37 68 S						
10.5.13				25 57 E			13 20
10.5.14		45 61 N					60 110
10.5.15				40 60 S			40 85
10.5.16		20 70 E					
11.5.1	45 60 S						
11.5.2	35 65 S				45 190		
11.5.3		25 90					
11.5.5		35 70 S					24 200
11.5.6	40 66 S			165 30 S	31 202		
11.5.8		50 55 S					
11.5.9		62 60 S			60 115		
11.5.10				165 55 E		1 84	15 145
11.5.11	100 25 S						
1.6.1	20 44 E						
1.6.2	15 50 E		112 40 S				
1.6.3	15 70 E						
1.6.4	15 44 E		0 90				
1.6.5	35 80 E						
1.6.6	34 40 E						
1.6.7	30 70 E		152 40 W				
1.6.8	30 45 E						
1.6.9	40 75 S						
1.6.10	35 84 S		30 60 N				30 202
1.6.11	15 69 E						
1.6.12	0 33 E		110 40 S	10 20 E		12 165	
1.6.13	352 19 E		115 54 S				
3.6.1	32 50 E						
3.6.2	30 25 E		82 37 S				
3.6.3	15 20 E						
3.6.4	30 80 E						
3.6.6		65 88 S					
3.6.7	14 80 E						
3.6.8	14 70 E						
3.6.9	0 70 E						
4.6.1	12 55 E						
4.6.2	20 67 E						

Station	Bedding	Foliation	Joints	Axial planes	Lineation	Hinges	Crenulation axis
4.6.4		70 61 S					
4.6.5		70 90					
4.6.6		26 64 E					
4.6.7		10 71 E					
4.6.8		65 54 S					
4.6.9	50 50 S				37 100		
4.6.10	30 46 S				44 114		
4.6.11	60 46 S				40 110		
4.6.12	74 41 S						
4.6.14	20 26 E						
4.6.15		50 34 S					
4.6.16	41 44 S						
4.6.17		105 58 N					
4.6.18		55 45 S					
4.6.19		155 25 N					
5.6.1		75 77 S					
5.6.2	127 21 S						
5.6.4	95 50						
5.6.6	80 65 S						44 135
5.6.7	65 34 S						
5.6.8	87 55 S						
5.6.9		15 60 E					
5.6.10	80 50 S						
5.6.11	60 40 E						
5.6.12		65 70 S					
5.6.13		165 76 E					26 60
5.6.14	85 61 S			30 40 S		34 210	
6.6.1	40 69 S						
6.6.2	20 40 S						
6.6.3	10 68 E						
6.6.4		44 45 S					
6.6.5	40 61 S						
6.6.6	70 46 S				37 185		
7.6.1		70 45 S					
7.6.2		55 55 S					
7.6.3		60 45 S					
7.6.4						30 219	
7.6.5		142 70 S					
9.6.1	350 40 E						
9.6.2	30 31 S						
9.6.3	42 50 S						
9.6.5	45 72 S						
9.6.6		80 70 S					
9.6.7		85 26 S					
9.6.8		50 44 S					
9.6.9	20 45 S						
9.6.10	30 47 S						

Station	Bedding	Foliation	Joints	Axial planes	Lineation	Hinges	Crenulation axis
9.6.11	30 70 S						
9.6.12	35 55 S						
9.6.13	34 52 S				51 110		
9.6.15	37 57 S		45 34 S				
10.6.1	60 80 S						
10.6.2		120 26 N		170 50 E			27 17
10.6.3	40 70 S						
10.6.4	50 35 S						
10.6.5	30 58 S						
10.6.6	35 50 S						
10.6.7	30 80 S						
10.6.8	20 90						
10.6.9	28 82 S						
10.6.10		34 65 S					
10.6.11	45 75 S						
10.6.12	160 55 N						
10.6.13		20 80 W					
10.6.14	35 65 S						
10.6.15		70 35 S					
11.6.1	353 60 E						
11.6.2	20 82 E						
11.6.3	35 45 S						
11.6.4		40 45 S					10 205
11.6.5		0 44 E					
11.6.6	75 26 S						
11.6.7	55 43 S						
11.6.8	52 38 S						27 190
11.6.9		62 20 S		150 80		15 95	42 175
11.6.10		65 38 S					
11.6.11	60 67 S						20 60
11.6.12	25 50 S						
11.6.13		50 80 N					
16.6.1	43 90		27 32 W				
16.6.2	30 30 S						
16.6.3	15 27 E						
16.6.5	130 20 W						
16.6.6		86 40 S					
16.6.7	0 45 E						
16.6.8	20 75 E		160 65 S				
16.6.9	39 90						
17.6.1	34 78 S						
17.6.2		21 62 S					16 25
17.6.4		25 45 S					
17.6.5		42 39 S					
17.6.6	163 50 E						
17.6.7		56 65 S	126 87 N				
17.6.8		30 35 S					

Station	Bedding	Foliation	Joints	Axial planes	Lineation	Hinges	Crenulation axis
17.6.9	25 33 E						
17.6.10		70 34 S					
17.6.11		45 35 S					
17.6.12		20 27 E					
17.6.13	25 61 W						
17.6.14		105 25 N					
17.6.15		0 0	158 60 E				
17.6.16	18 40 E						
17.6.17	0 0					14 40	7 25
17.6.18		31 80 N					10 213
18.6.1	30 20 S		165 80 E				10 191
18.6.2	90 17 N						
18.6.3	25 65 N						
18.6.4	43 70 N				30 225		
18.6.5		37 80 S					
18.6.6		70 45 S		5 85			
18.6.7	21 90						11 210
18.6.8		14 25 W					
18.6.9		120 24 N					
18.6.10		11 35 E					
18.6.11		40 25 S	55 74 N		17 195		
19.6.1		30 49 S			15 196		
19.6.2		10 25 E	147 52 E				
19.6.3		57 37 S			31 192		
19.6.4		0 46 E	150 70 W				
19.6.5		100 65 N					
20.6.1		90 65 S					
20.6.2	60 55 S						
20.6.3		54 66 S					
20.6.4		55 54 S					
20.6.6		65 70 S			22 80		
20.6.7		35 72 S					
20.6.8	50 77 S						
20.6.9		74 42 S					10 72
20.6.10		49 60 S					
20.6.11		45 71 S					
20.6.13	60 75 S						
22.6.1		80 77 S					
22.6.2		64 33 S					
22.6.3		20 90					
22.6.4		37 65 S					
22.6.5	80 62 S	66 40 S					
22.6.6		31 40 S					
22.6.8		49 65 S					
22.6.9	40 86 S						
22.6.10		50 90					
22.6.11		17 47 E					

Station	Bedding	Foliation	Joints	Axial planes	Lineation	Hinges	Crenulation axis
22.6.12	27 42 E						
22.6.13				45 60 S		10 205	
22.6.14		20 48 E					
22.6.15	70 55 S						
22.6.16	30 65 S						
22.6.17		105 45 N					
22.6.18		34 80 W					
22.6.19	55 70 S						
22.6.20	50 90						
23.6.1	70 70 S				16 245		
23.6.2	66 71 S		132 41 N		39 229		
23.6.3	69 65 S						
23.6.4		47 41 S					
23.6.5		65 35 S					
23.6.6	20 54 E						
23.6.7		25 80 S					
23.6.8	40 71 S						
23.6.9						16 225	
23.6.10		86 35 S	50 34 N				
23.6.11		75 40 S					
23.6.12		72 36 S					
23.6.13	95 30 S						
23.6.14	75 35 S		46 48 N				
23.6.15	100 35 S						
23.6.16	73 50 S						
23.6.17	64 67 S						
24.6.1	61 56 S						
24.6.2	81 64 S						
24.6.3				175 90		25 85	
24.6.4	70 71 S						
24.6.5		75 90				20 270	
24.6.6	42 37 S						
24.6.7		40 75 S					
26.6.1		107 36 S					
27.6.1		0 35 E					
27.6.2		71 70 S					
27.6.3		52 40 S					
27.6.4		70 74 S					
27.6.5		60 10 S					
27.6.6		85 45 S					
27.6.8		90 86 S					9 260
27.6.9		64 61 N					
27.6.10		77 61 N					
27.6.11		80 76 S			29 250		
27.6.12		69 90				41 255	
27.6.13					4 232		
27.6.15		55 80 S					2 231

Station	Bedding	Foliation	Joints	Axial planes	Lineation	Hinges	Crenulation axis
28.6.1		84 44 S					
28.6.2	68 60 S						
28.6.3	70 51 S						
28.6.4	60 58 S						20 74
28.6.5		65 56 S			24 80	35 115	
28.6.6		65 85 S					
28.6.7	60 71 S						
28.6.8	74 70 S						
28.6.9	65 80 S						
3.7.1		25 55 S					
3.7.2	30 44 S						
3.7.3	25 69 S				36 139		
3.7.4	62 51 S						
3.7.5		50 51 S					46 162
3.7.6		10 60 E					
3.7.7	30 40S						
3.7.8	30 54 S						
3.7.9	30 50 S						
3.7.10	30 54 S						
3.7.11	5 51 S						
3.7.12		56 61 S					
3.7.13	56 45 S						
3.7.14	50 50 S						65 80
5.7.1		92 85 S					
5.7.2	68 42 S						
5.7.4		50 50 S					36 115
5.7.5		74 59 S					
5.7.6	30 45 S						
5.7.7	34 61 S						
5.7.8	50 62 S						
5.7.9		40 46 S					
5.7.10	57 60 S						
5.7.11		60 46 E					
5.7.12	77 55 S						
5.7.13		68 52 S					61 117
5.7.14	52 57 S						
5.7.15		55 54 S					62 90
5.7.16		50 35 S					35 100
5.7.17		30 44 S			50 125		
5.7.18		20 31 s			50 115		
17.7.1	60 59 S				54 178		
17.7.2	70 56 S						
17.7.5	50 56 S						
17.7.7	42 39 S						
18.7.1	170 79 E						
20.7.1		27 70 S			35 45		35 45
20.7.2	49 75 S						

Station	Bedding	Foliation	Joints	Axial planes	Lineation	Hinges	Crenulation axis
20.7.3	65 90						
20.7.4		60 77 N					34 34
20.7.5		55 90					
20.7.6		42 65 S			46 86		
20.7.7		0 55 E					
20.7.8		50 62 S				49 140	
20.7.9		65 49 S			40 180		
20.7.10		75 60 S					
20.7.11		62 55 S					
20.7.12		75 61 S					
20.7.13	75 60 S						
20.7.14		102 90		3 50 E		57 90	
24.7.1		62 71 N					32 40
24.7.2	56 84 N						62 47
24.7.3		45 86 N					66 30
24.7.5		54 59 N					22 42
24.7.6		105 38 S					
24.7.7		122 66 S					
24.7.8					20 100	2 280	20 10
25.7.1	75 75 S		147 30 N				
25.7.2	160 65 E						
25.7.3	25 25 S						
25.7.4	175 64 E						
25.7.5	64 55 S		121 70		45 195		
25.7.6		160 60 E					
25.7.7		45 5 N					
25.7.8		20 48 E					
25.7.9		65 85 N					
25.7.10		70 45 N					32 327
25.7.11		74 41 N					
25.7.12	66 60 S						
25.7.13	80 49 S						
25.7.14	24 75 S		140 34 N				
25.7.15	40 64 S		10 26 W				
25.7.16	10 85 W						
25.7.17	44 70 S						
25.7.18	2 25 E			2 25 E			
26.7.1		120 42 N					
26.7.2		55 64 N					
26.7.3		70 70 S					
26.7.4		65 67 S					
26.7.6		65 90	15 84 E				
26.7.7	22 49 S		140 72 S				
26.7.8	36 55 E		115 75 S		15 215		
26.7.9		151 25 N					
29.7.1		65 40 S					
29.7.2		38 50 S					

Station	Bedding	Foliation	Joints	Axial planes	Lineation	Hinges	Crenulation axis
29.7.3		60 45 S					
29.7.4	85 31 S				16 235		
29.7.5		30 26 S				2 230	
29.7.6		55 44 S					
29.7.7		48 30 S					
29.7.8		25 42 S					
29.7.9		80 29 S					
29.7.10		34 32 S					
29.7.11		70 50 S					
29.7.12		40 56 S					
29.7.13		80 55 S				49 160	
29.7.14	80 37 S						
29.7.15	70 50 S						
29.7.16	30 45 S						
31.7.1		32 62 S					
31.7.2	65 38 S						
31.7.3	73 64 S				48 210	25 220	
31.7.4	64 70 S						
31.7.5	105 40 S						
31.7.6	69 37 S						
31.7.7	74 56 S						9 243
31.7.8	78 62 S						
31.7.9	75 60 S						
31.7.10		50 35 S					
31.7.11		75 49 S					
2.8.1		85 50 S					
2.8.2		52 64 S			41 22		45 68
2.8.3	75 43 S						
2.8.4	52 24 S				23 130		
2.8.5		74 50 S					
2.8.6		70 54 S					42 174
2.8.7	66 37 S						
2.8.8	62 41 S						
2.8.9		70 56 S					
2.8.10	80 10 S						
2.8.11		65 42 S					
2.8.13		70 35 S					
2.8.14	90 45 S				30 181		
4.8.1		0 69 E					
4.8.2		17 50 E					
4.8.3		55 35 S					
4.8.4	43 32 S						
4.8.5	25 60 S		120 76 N				
4.8.6	156 25 E						
4.8.7		20 7 W					
4.8.8		140 84 S					
4.8.9		175 50 E					

Station	Bedding	Foliation	Joints	Axial planes	Lineation	Hinges	Crenulation axis
4.8.10		150 62 E					34 85
9.8.1		25 49 S					9 207
9.8.2	90 80 S						
9.8.3		140 31 S					
9.8.4		175 86 E					74 355
9.8.5		0 65 E					
9.8.6		5 55 E					
9.8.7	22 60 S						
9.8.8		110 24 S					
9.8.9		20 50 W					
9.8.10		15 66 W					
9.8.11	0 0						
9.8.12		50 25 S	115 74 N				
9.8.13	10 25 E					5 60	
9.8.14		15 47 E					
9.8.15		32 40 S	105 60 N				41 141
10.8.1	20 55 E						
10.8.2		15 64 W		175 29 E			1 195
10.8.3	40 51 S						
10.8.4		45 40 S		15 30 W			14 214
10.8.5		34 42 S					13 204
10.8.6		46 44 S					
10.8.7		16 52 E					6 189
10.8.8		72 70 N		34 34 S			29 66
10.8.9	130 9 N						
10.8.10	39 76 S	15 36					
10.8.11	150 50 N						
10.8.12	25 44 S			40 50 S		20 49	
10.8.13	22 41 S						
BB1	30 90						
BB2	124 31 N						
BB3	0 0						
BB4		54 50 S					
BB5	76 29 N						
BB6	14 65 S						
BB7		7 40 E					
BB8	10 44 E						
BB9	65 72 S		150 85 N				
BB10	50 75 N			30 65 E		25 32	
BB11	50 60 S						
BB12		36 26 S					
BB13		175 50 E					
BB14	6 30 E						
BB15				12 11 E		10 230	
BB16	71 90			64 69 S		33 55	

VITA

Camilo Montes was born in Santafé de Bogotá, Colombia on April 29, 1967. His love for the great Andean outdoors, and his aversion for desk-based disciplines and for wearing ties, made him follow geology as his major in the Universidad Nacional de Colombia. He received his degree in Geology in 1992 from this institution. During this time, continued exploration of the high Andes made him realize that there was so much more to know and study beyond the Bachelor's degree. He joined the Master's program at the University of Tennessee, in fall 1993, officially receiving the Master's degree in May 1997, while working in his Ph. D. at the same institution.

Plate I
Geologic Map of Part of the Eastern Great Smoky Mountains, Western North Carolina

Camilo Montes, 1996

Explanation

Stratigraphic contact, solid where exactly located, dashed where approximately located, dotted where inferred.

Premetamorphic fault, solid where exactly located, long dashes where approximately located, dotted where concealed. Open teeth on hangingwall block.

Postmetamorphic fault, solid where exactly located, long dashes where approximately located, dotted where concealed. Solid teeth on hangingwall block.

Trace of postmetamorphic anticline (simple dash), double dashed where approximately located, dotted where inferred. Overturned.

Trace of postmetamorphic syncline (simple dash), double dashed where approximately located, dotted where inferred. Overturned.

Strike and dip of bedding

Horizontal bedding

Strike and dip of overturned bedding

Strike and dip of isoclinally folded beds

Strike and dip of vertical beds

Strike and dip of foliation

Strike and dip of vertical foliation

Horizontal foliation

Plunge of mineral lineation

Plunge of axes of minor folds

Isograds:
- -Garnet
- -Staurolite
- -Staurolite-kyanite
- -Kyanite
- -Sillimanite

Stratigraphic scheme

NW

Great Smoky Group
- Thunderhead Sandstone
  - p€a Anakeesta fm.
  - p€tp pelites
  - p€ts graded psammites
  - p€t undifferentiated
  - p€tr graded rudites
- p€gs Great Smoky Group undifferentiated
- p€e Elkmont Sandstone

Greenbrier fault

Snowbird Group
- Roaring Fk. Sandstone
  - p€rp pelites
  - p€r undifferentiated
  - p€rs psammites
- p€lq Longarm Quartzite
- p€w Wading Branch fm.

Hayesville fault

Eastern Blue Ridge Units
- p€b Biotite gneiss
- p€h Hornblende-biotite gneiss

p€lq

p€w

Middle Proterozoic granodioritic basement
- p€gm Mylonitic orthogneiss
- p€ga Mylonitic augen orthogneiss
- p€go Granodioritic orthogneiss

Eastern Blue Ridge Units ?
- p€b? Biotite gneiss.
- p€h? Hornblende-biotite gneiss.

Recommended colors:
Anakeesta Fm. (740,5); Anakeesta Fm. (751); Thunderhead SS: pelite (738,5); graded psammite (739); undifferentiated (738); graded rudite (730,5).
Great Smoky Group undiff. (737,5); Elkmont Sandstone: pelite (756); graded rudite (743); Roaring Fork Sandstone: pelite (757); undiff. (736); psammite (755)
Longarm Quartzite (735); Wading Branch Fm. (759); Mylonitic orthogneiss (748,5); Mylonitic augen orthogneiss (752); Granodioritic orthogneiss (743)
Biotite gneiss (754); Hornblende-biotite gneiss (740); Amphibolite ( )

Index to mapping:

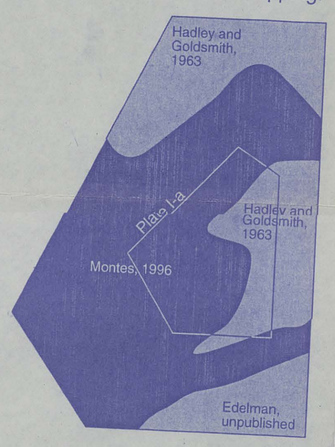

A
A'
B
B'
C
C'
D
D'

35°37'30"
35°30'00"
83°7'30"

1 0 1 MILE
1000 0 1000 2000 3000 4000 5000 6000 7000 FEET
1 0 1 KILOMETER

Scale: 1:24,000

Plate I-a

Geologic Map of Part of the Eastern Great Smoky Mountains, Western North Carolina (enlargement)

Camilo Montes, 1996

Explanation

Stratigraphic contact, solid where exactly located, dashed where approximately located, dotted where inferred.

Premetamorphic fault, solid where exactly located, long dashes where approximately located, dotted where concealed. Open teeth on hangingwall block.

Postmetamorphic fault, solid where exactly located, long dashes where approximately located, dotted where concealed. Solid teeth on hangingwall block.

Trace of postmetamorphic anticline (simple dash), double dashed where approximately located, dotted where inferred. Overturned.

Trace of postmetamorphic syncline (simple dash), double dashed where approximately located, dotted where inferred. Overturned.

Strike and dip of bedding

Horizontal bedding

Strike and dip of overturned bedding

Strike and dip of isoclinally folded beds

Strike and dip of vertical beds

Strike and dip of foliation

Strike and dip of vertical foliation

Horizontal foliation

Plunge of mineral lineation

Plunge of axes of minor folds

0 500 m 1,000 m

Scale: 1:12,000

Index to mapping:

Stratigraphic scheme

NW

Great Smoky Group
- p€a Anakeesta fm.
- Thunderhead Sandstone: p€tp pelites; p€ts graded psammites; p€t undifferentiated; p€tr graded rudites
- p€gs Great Smoky Group undifferentiated
- p€e Elkmont Sandstone

Snowbird Group
- Roaring Fk. Sandstone: p€rp pelites; p€r undifferentiated; p€rs psammites
- p€lq Longarm Quartzite
- p€w Wading Branch fm.

Eastern Blue Ridge Units
- p€b Biotite gneiss
- p€h Hornblende-biotite gneiss

Greenbrier fault

Hayesville fault

Middle Proterozoic granodioritic basement
- p€gm Mylonitic orthogneiss
- p€ga Mylonitic augen orthogneiss
- p€go Granodioritic orthogneiss

Eastern Blue Ridge Units ?
- p€b? Biotite gneiss.
- p€h? Hornblende-biotite gneiss.

Recommended colors:
Ammons Fm. (740,5). Anakeesta Fm. (751). Thunderhead SS: pelite (738,5); graded psammite (739); undifferentiated (758); graded rudite (739,5).
Great Smoky Group undiff. (737,5). Elkmont Sandstone: pelite (758); graded rudite (740). Roaring Fork Sandstone: pelite (757); undiff. (736), psammite (755).
Longarm Quartzite (735), Wading Branch Fm. (750). Mylonitic orthogneiss (746,5); Mylonitic augen orthogneiss (752); Granodioritic orthogneiss (743).
Biotite gneiss (754). Hornblende-biotite gneiss (748). Amphibolite ( )

Plate II. Cross sections across part of the eastern Great Smoky Mountains, western North Carolina. Montes, 1997.

Plate II
Cross sections across part of the eastern Great Smoky Mountains, western North Carolina.

Stratigraphic scheme

NW

Great Smoky Group
- p€a Anakeesta fm.
- p€tp pelites (Thunderhead Sandstone)
- p€ts graded psammites (Thunderhead Sandstone)
- p€t undifferentiated
- p€tr graded rudites
- p€gs Great Smoky Group undifferentiated
- p€e Elkmont Sandstone

Greenbrier fault

Snowbird Group
- Roaring Fk. Sandstone
- p€rp pelites
- p€r undifferentiated
- p€rs psammites
- p€lq Longarm Quartzite
- p€w Wading Branch fm.

Eastern Blue Ridge Units
- p€b Biotite gneiss
- p€h Hornblende-biotite gneiss

Hayesville fault

p€lq

p€w

Middle Proterozoic granodioritic basement
- p€gm Mylonitic gneiss
- p€ga Medium-grained mylonitic augen gneiss
- p€go Coarse grained mylonitic augen gneiss

Eastern Blue Ridge Units ?
- p€b? Biotite gneiss.
- p€h? Hornblende-biotite gneiss.

Explanation

- Foliation
- Bedding
- Overturned bedding
- Trace of postmetamorphic faults
- Trace of premetamorphic faults
- Trace of postmetamorphic fold axes
- Trace of synmetamorphic fold axes

Scale 1:24,000

No vertical exaggeration

0 6,000 ft

0 3,000 m

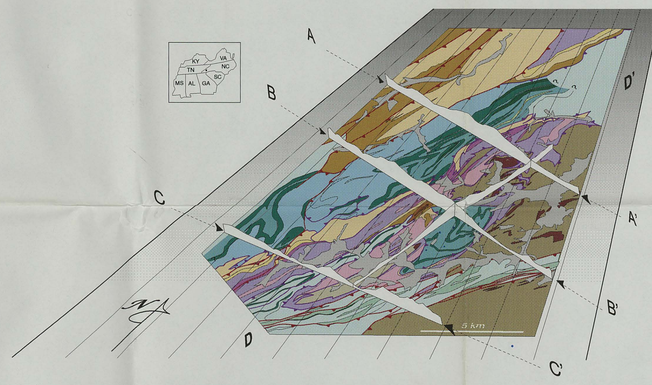

Location of the cross sections relative to the Geologic Map (Plate I)

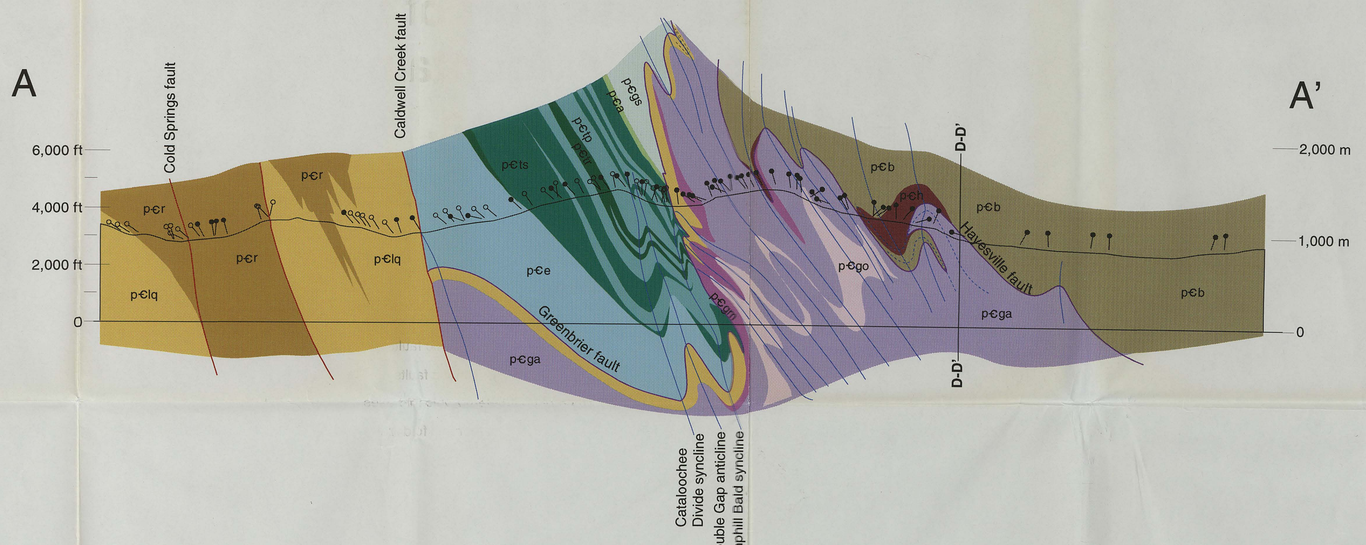

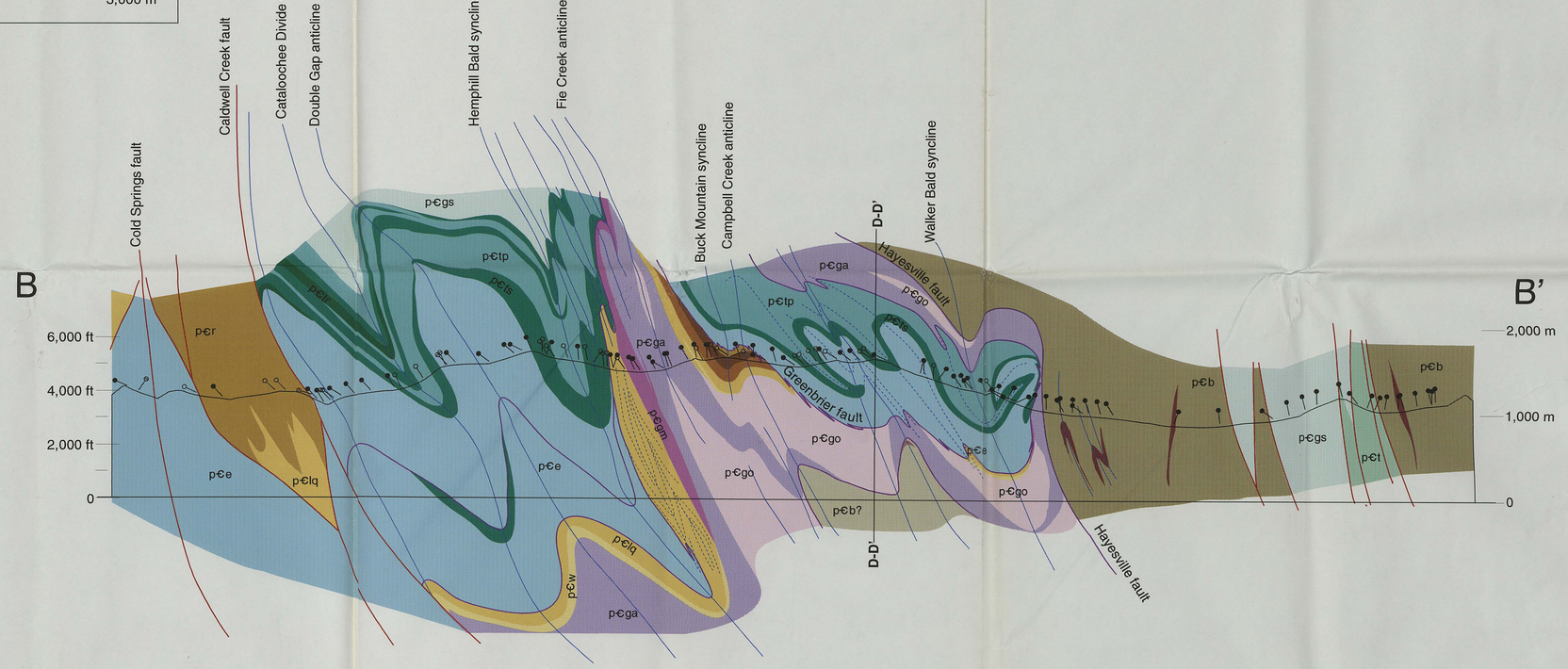

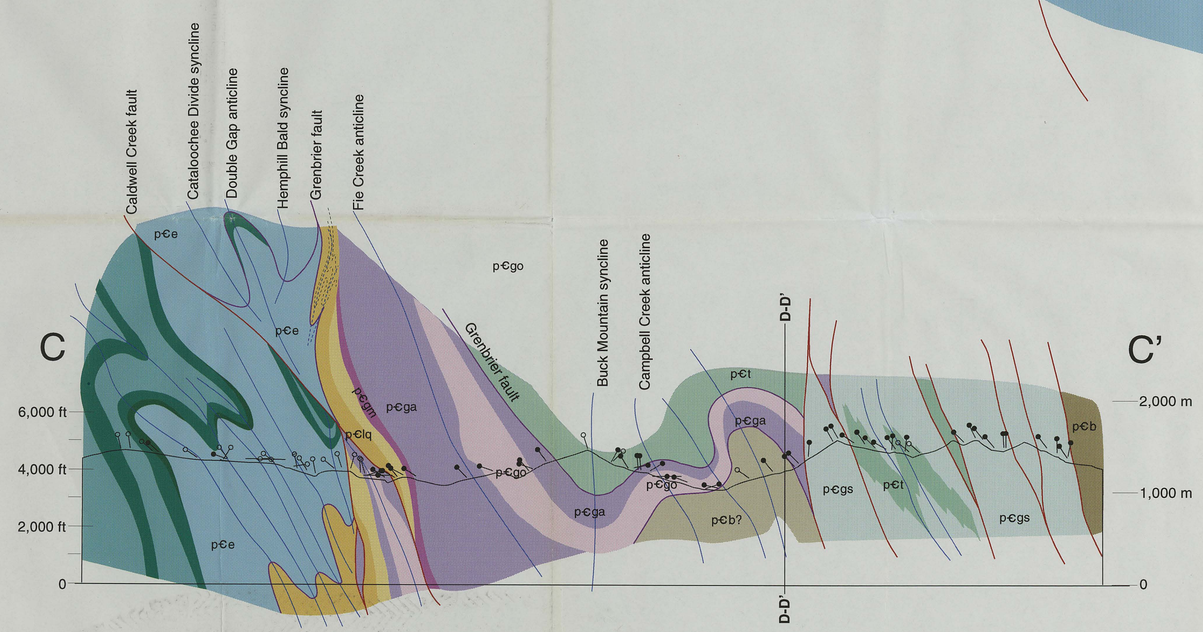

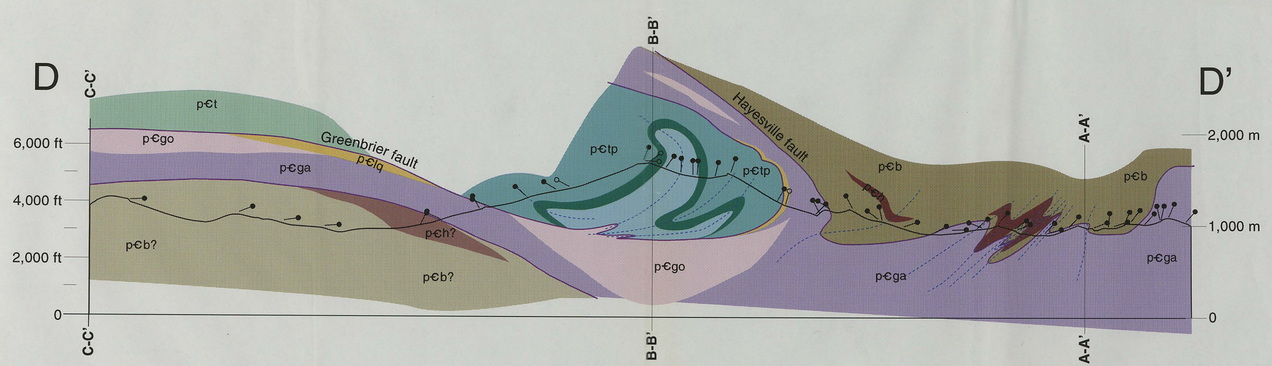

Plate III
Station map.
Great Smoky Mountains, Western North Carolina

Camilo Montes, 1996